

BRNO UNIVERSITY OF TECHNOLOGY  
VYSOKÉ UČENÍ TECHNICKÉ V BRNĚ

FACULTY OF ELECTRICAL ENGINEERING AND COMMUNICATION  
ÚSTAV TELEKOMUNIKACÍ

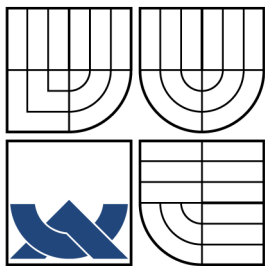
FAKULTA ELEKTROTECHNIKY A KOMUNIKAČNÍCH TECHNOLOGIÍ  
DEPARTMENT OF TELECOMMUNICATIONS

LOCALIZATION IN WIRELESS ENERGY-CONSTRAINED  
NETWORKS

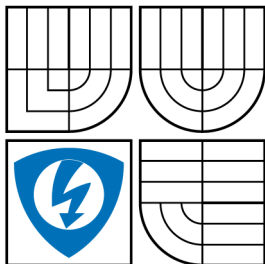
DOCTORAL THESIS  
DIZERTAČNÍ PRÁCE

AUTHOR  
AUTOR PRÁCE

Ing. et Ing. PATRIK MORÁVEK



BRNO UNIVERSITY OF TECHNOLOGY  
VYSOKÉ UČENÍ TECHNICKÉ V BRNĚ



FACULTY OF ELECTRICAL ENGINEERING AND  
COMMUNICATION  
ÚSTAV TELEKOMUNIKACÍ



FAKULTA ELEKTROTECHNIKY A KOMUNIKAČNÍCH  
TECHNOLOGIÍ  
DEPARTMENT OF TELECOMMUNICATIONS

## LOCALIZATION IN WIRELESS ENERGY-CONSTRAINED NETWORKS

LOKALIZACE V BEZDRÁTOVÝCH SÍTÍCH S OMEZENÝMI ENERGETICKÝMI  
ZDROJI

DOCTORAL THESIS  
DIZERTAČNÍ PRÁCE

AUTHOR  
AUTOR PRÁCE

Ing. et Ing. PATRIK MORÁVEK

SUPERVISOR  
VEDOUCÍ PRÁCE

doc. Ing. DAN KOMOSNÝ, PhD.

BRNO 2012

## ABSTRACT

The doctoral thesis is devoted to localization in wireless networks, and particularly, to distance estimation. Localization is an important process in many wireless networks with both static and mobile nodes since it provides a position knowledge which can be further exploited during the application lifetime. The thesis presents a novel method for distance estimation based on received signal strength measurement. The method respects both the application accuracy requirements and dynamic ambient radio conditions while performing with minimal energy costs.

Before the design of the novel method an experimental analysis of signal propagation for localization and energy consumption was performed. Based on the results of the analysis the novel Adaptive Energy-aware Distance Estimation method was proposed and subsequently evaluated in both simulator and experimental testbed under real conditions.

## KEYWORDS

Localization, Ad-hoc, wireless sensor networks, distance estimation, received signal strength.

## ABSTRAKT

Tato disertační práce se věnuje lokalizaci v bezdrátových sítích se zaměřením na odhad vzdálenosti. Lokalizace je v bezdrátových sítích s mobilními ale i statickými uzly důležitým procesem, neboť znalost pozice uzlů může být během provozu sítě dále s výhodou využita. V práci je prezentována nová metoda odhadu vzdálenosti na základě měření síly přijatého signálu. Navržená metoda je postavena tak, aby s co nejnižšími energetickými náklady dosáhla požadovaného stupně přesnosti i ve značně odlišných rádiových podmínkách.

Před návrhem vlastní metody byla provedena experimentální analýza spotřeby energie a šíření signálu s jeho využitím pro lokalizační účely. Na základě provedené analýzy byla navržena nová metoda (Adaptabilní energeticky nenáročná metoda odhadu vzdálenosti), která byla následně ověřena v simulátoru a experimentální síti za reálných podmínek.

## KLÍČOVÁ SLOVA

Lokalizace, Ad-hoc sítě, bezdrátové senzorové sítě, odhad vzdálenosti, přijatá síla signálu, spotřeba energie.

MORÁVEK, Patrik *Localization in wireless energy-constrained networks*: doctoral thesis. Brno: Brno University of Technology, Faculty of Electrical Engineering and Communication, Ústav telekomunikací, 2012. 122 p. Supervised by doc. Ing. Dan Komosný, PhD.

## DECLARATION

I declare that I have elaborated my doctoral thesis on the theme of “Localization in wireless energy-constrained networks” independently, under the supervision of the doctoral thesis supervisor and with the use of technical literature and other sources of information which are all quoted in the thesis and detailed in the list of literature at the end of the thesis.

As the author of the doctoral thesis I furthermore declare that, concerning the creation of this doctoral thesis, I have not infringed any copyright. In particular, I have not unlawfully encroached on anyone's personal copyright and I am fully aware of the consequences in the case of breaking Regulation § 11 and the following of the Copyright Act No 121/2000 Vol., including the possible consequences of criminal law resulted from Regulation § 152 of Criminal Act No 140/1961 Vol.

Brno .....

.....

(author's signature)

To my family,

friends, colleagues and supervisors supporting me during my studies.

# CONTENTS

<b>Introduction</b>	<b>11</b>
<b>1 State of art</b>	<b>14</b>
1.1 Localization in wireless networks . . . . .	14
1.1.1 Localization algorithms . . . . .	16
1.1.2 Evaluation of localization . . . . .	21
1.1.3 Overview of localization methods . . . . .	23
1.1.4 Received signal strength method (RSS) and radio signal prop- agation . . . . .	25
1.1.5 Ultrasonic ranging method . . . . .	31
1.2 Energy consumption . . . . .	33
1.3 Chapter summary . . . . .	36
<b>2 Objectives</b>	<b>37</b>
<b>3 Experimental analysis of localization</b>	<b>39</b>
3.1 Analysis of ranging methods . . . . .	39
3.1.1 Received signal strength method (RSS) . . . . .	39
3.1.2 RSS uncertainty . . . . .	48
3.1.3 Ultrasonic system . . . . .	51
3.2 Impact of ranging on position estimation . . . . .	54
3.2.1 Position estimation using lateration . . . . .	55
3.2.2 Experimental measurement focused on RSS uncertainty . . . . .	57
3.2.3 Anchor-Free Localization . . . . .	60
3.2.4 Frequency diversity for ranging optimization . . . . .	62
3.3 Chapter summary . . . . .	64
<b>4 Experimental analysis and simulation of energy consumption</b>	<b>67</b>
4.1 Energy consumption measurement . . . . .	67
4.2 Energy model definition . . . . .	73
4.3 Simulation of energy consumption . . . . .	75
4.4 Chapter summary . . . . .	76
<b>5 Proposal of novel distance estimation method</b>	<b>78</b>
5.1 Adaptable energy-aware distance estimation (AEDE) . . . . .	78
5.1.1 Format of localization packets . . . . .	81
5.1.2 Analysis of signal strength measurement . . . . .	83
5.2 Chapter summary . . . . .	88

<b>6</b>	<b>Evaluation of novel method in simulator</b>	<b>89</b>
6.1	Implementation and simulation results . . . . .	89
6.2	Chapter summary . . . . .	93
<b>7</b>	<b>Experimental evaluation of proposed method in real network</b>	<b>94</b>
<b>8</b>	<b>Conclusion</b>	<b>99</b>
	<b>Bibliography</b>	<b>101</b>
	<b>List of symbols, physical constants and abbreviations</b>	<b>114</b>
	<b>List of appendices</b>	<b>117</b>
<b>A</b>	<b>Appendix 1</b>	<b>118</b>
A.1	RSS lookup table . . . . .	118
<b>B</b>	<b>Appendix 2</b>	<b>120</b>
B.1	AEDE evaluation under real conditions – additional measurements .	120

# LIST OF FIGURES

1.1	Infrastructure of AFL algorithm. . . . .	18
1.2	Map-growing algorithm. . . . .	19
1.3	Two-ray ground signal propagation model. . . . .	27
1.4	Basic schema of a WSN node. . . . .	34
3.1	Scheme of the experimental testbed for RSS measurements. . . . .	40
3.2	The detailed scheme of the receiving part of the measurement testbed. . . . .	40
3.3	Received signal power measurement – indoors. . . . .	41
3.4	Measurement testbed. . . . .	42
3.5	Received signal power measurement – outdoors. . . . .	42
3.6	Simulated path loss as a function of distance at 2.45 GHz with different antenna heights. . . . .	43
3.7	Measured received power as a function of distance at 2.4 GHz and different antenna heights. . . . .	44
3.8	Comparison of simulated signal propagation with different frequencies. . . . .	45
3.9	Measured received power as a function of distance with different frequencies and antenna height 2 m. . . . .	45
3.10	Error of the distance estimation using RSS method in outdoor measurement. . . . .	46
3.11	Received signal strength indicated by receiver ( $P_t = 3.2$ dBm). . . . .	47
3.12	The power levels and standard deviation of RSS indoor measurements at different distances. The minimum (green +), maximum (red *) and average (blue o) value of each in-place measurement are depicted. . . . .	49
3.13	The power levels and standard deviation of RSS outdoor measurements. The minimum (green +), maximum (red *) and average (blue o) value of each in-place measurement are depicted in the left part of the figure. . . . .	50
3.14	Standard deviation of indoor measurement with IRIS nodes. . . . .	51
3.15	Estimated distance for both indoor and outdoor environment. . . . .	53
3.16	Standard deviation of both indoor and outdoor measurement (20 values measured at each point). . . . .	54
3.17	Mean absolute error of distance estimation. . . . .	54
3.18	Trilateration result with $\epsilon_r = 10$ % in a field 20 x 20 m. . . . .	56
3.19	Impact of ranging error $\epsilon_r$ on the trilateration. . . . .	56
3.20	Standard deviation of RSS measurements at 25 locations. . . . .	57



3.21	Example of three measurements at three different points. In the left column, there are determining multilateration circles and the right side is focused on position calculation using a different number of samples. All units are in meters. The red cross shows the real position of the sensor. . . . .	59
3.22	Overall position estimation as a function of the number of samples taken at each point. The total number of measurement points was 25. . . . .	60
3.23	Expended energy and mean of absolute error of estimated position with different number of samples. . . . .	61
3.24	Dependence of anchor-free localization error on the ranging error. . . . .	62
3.25	Localization error (expressed by color) of Centroid and Least Square (LS) algorithms employing single frequency measurement (upper part) and frequency diversity (lower part). . . . .	64
3.26	Cumulative distribution function of the error using the least square and weighted centroid algorithms for antenna heights of 0.5 m and 2 m, with single frequency and two frequencies. . . . .	65
4.1	Experimental testbed for measurement of energy consumption. . . . .	68
4.2	Current measurement with a shunt resistor and low pass filter (adapted from [95]). . . . .	69
4.3	Power consumption of IRIS node during RF communication. . . . .	70
4.4	Current drained during association and binding phase of ZigBee communication. . . . .	71
4.5	Consumption of data transmission process in ZigBee networks with an acknowledgment at the application layer. . . . .	73
4.6	Remaining energy resources of nodes after 160 rounds (left) and the rate of functional nodes during simulation rounds (right). . . . .	76
5.1	Time diagram of AEDE method. . . . .	79
5.2	Content of the RSS request packet. . . . .	82
5.3	RSS response data field. . . . .	82
5.4	RSS response Format field. . . . .	82
5.5	Mean error of the RSS estimation with various number of measurement samples and under various channel uncertainty $u$ . . . . .	84
5.6	Error of RSS estimation with 20 measurement samples. . . . .	85
5.7	Mean error of the RSS estimation with various number of measurement samples together with its standard deviation. Channel uncertainty $u = 9$ . . . . .	86
5.8	Average error of the RSS estimation with different number of measurement sets with 20 measurement samples. . . . .	86
6.1	Performance of the AEDE method together with the classical approach. . . . .	91

6.2 Performance of the AEDE for applications with high accuracy needs. 92

6.3 Example of three accuracy levels of AEDE and its performance. . . . 92

7.1 Experimental testbed schema. . . . . 94

7.2 Flow chart of the implementation of the AEDE method. . . . . 95

7.3 Evaluation of the AEDE with Waspnotes (detail). . . . . 96

7.4 Improvement of RSSI estimation and extra cost using AEDE. . . . . 97

B.1 AEDE evaluation in series of RSSI measurements. . . . . 120

# LIST OF TABLES

1.1	Categorization of localization algorithms. . . . .	16
1.2	Power consumption of some COTS sensors [83]. . . . .	34
5.1	Coordination class codes. . . . .	83
A.1a	RSS lookup table. . . . .	118
A.2a	RSS lookup table (continuing). . . . .	119

# INTRODUCTION

Wireless ad-hoc networks have become of great interest to both research and industry sectors in the last decade. Often, they are supposed to work autonomously for a long-term period which presents several challenges.

Due to a low-cost node design, autonomous function and network lifetime, several limitations have to be considered during network design. Besides small memory, computational limits and narrow bandwidth, the energy self-sufficiency is the most restrictive factor. In a lot of applications, after deployment, the nodes are supposed to work autonomously without any human assistance and with their only energy source being the one with which they were initially equipped (not considering scarce energy harvesting applications).

Despite the limitations mentioned, WSNs are in experts' opinion a very promising technology expected to be one of the leading technologies in the 21st century. According to the IDTechEx report [1], WSN has the potential to become multibillion dollar business in the next ten years. For instance, ZigBee/802.15.4 chipsets, leading WSN standard, doubled in the year 2010 and are predicted to increase by up to 800 % in the next five years and approach a revenue of \$1.7 billion in 2015 [2]. Similarly, governmental and public union's fundings cover billions spent on WSN research worldwide at public institutions such as universities according to research reports published in ONWorld's [3].

WSN technologies emerged, like many others, from military requirements. Nowadays, the WSNs have found their way into many civil fields like medicine, industry, agriculture, environment or surveillance and security. For example, smart structures with embedded WSN technologies can actively respond to earthquakes and make buildings or other constructions safer; precision agriculture can reduce costs and environmental impact by watering and fertilizing only in the case of real need in specific parts of a field; WSNs deployed for environmental monitoring of water, air or soil quality will sense data in a real time to find the source of pollution as soon as possible.

According to ONWorld's report based on a study of 102 research end-to-end projects in 2010 the most commonly studied areas are related to environment (37 %) and healthcare (30 %), followed by public safety, transportation, structural monitoring, and industrial applications [3].

Many of WSN applications require the knowledge of a node's position to ensure the proper functioning of a network (e.g. [4]–[6]). The obvious reason for localization is a provision of sensed data with a geographical meaning. In other words, to know the position of the data origin in the area of interest. Considering mobile nodes in a network (for example logistic applications), the position is the measure that is

transferred as the data value. As an additional motivation, the sensor's position can be used for a scalable geographical routing, data gathering, hierarchical aggregation, object tracking, remote management etc. This makes automatic localization the key enabling technology in WSNs. The same or similar benefits lie in the localization for other wireless networks such as 802.15.4/ZigBee, WiFi, DASH7, UWB, CSS too.

In some special cases general positioning systems such as GPS (Global Positioning System) can be used. However, only a small minority of applications can use GPS because GPS is restricted to outdoor environment and, more significantly, it has high energy demands. Considering a GPS receiver at each node, the lifetime of the application would decrease substantially which is undesirable in most of the applications and does not comply with the low-energy requirement. Moreover, the cost of the wireless nodes would also increase.

This thesis focuses on localization and distance estimation in wireless networks with energy limited resources. The 2.4 GHz ISM frequency band is considered which includes network technologies such as 802.11 Wifi, Cordless telephony, Bluetooth, RFID and 802.15.4. This work directly addresses the problem of energy efficient distance estimation while fulfilling application specific accuracy requirements. Distances among nodes in a network represent necessary input variables for many localization algorithms. This makes the result of the position estimation highly dependent on the quality of the provided distance estimations. There are several techniques for distance estimation varying in cost and accuracy of the estimation but none which primarily respects the accuracy requirements of an application and ambient radio conditions while keeping the energy consumption as low as possible. An estimation technique based on received signal strength measurement is a widespread technique used in wireless applications providing sufficient accuracy of results while requiring lower complexity of implementation which makes it favored in research and industry. Therefore, this work is aimed at the technique based on the received signal strength. It analyses the problem of energy efficient distance estimation in detail and presents a new method of achieving the goal of efficient distance estimation while providing the required accuracy.

Due to stochastic conditions in a radio channel each measurement contains a certain degree of uncertainty. To mitigate the level of uncertainty several measurements have to be conducted which increases the energy costs of distance estimation. Depending on the application, and thus, the required level of accuracy, the new method consumes just the minimal amount of precious energy while respecting the accuracy requirements which increases the lifetime of the entire application.

The benefits of the new estimation method are significant mostly in the area of applications deployed in unstable stochastic radio conditions, frequently running position estimation which is the case especially in networks with mobile nodes. The

more often the localization runs the more energy is saved by the new method. This method can be used in static wireless networks as well, however, the significant improvement is achieved with the repetitive localization process. In addition, the method can use the environment characteristic obtained from the previous localization to set the initial parameters in the most efficient way and save even more energy.

This work is organized as follows. After the state of the art section which discusses the latest and most important achievements in this area, the objectives of this thesis are stated. Then, the description of the experimental analysis conducted on localization will be lined out. This section focuses on the distance estimation based on the signal strength measurement and channel characteristic influencing the estimation. The following chapter is devoted to the experimental analysis of energy consumption related to localization on wireless devices. After the analysis of both areas the novel distance estimation method is presented in chapter 5. The next two chapters are devoted to the verification of the proposed method in simulations and experimental testbed with sensor nodes. The last chapter concludes the work and discusses its results and contributions.

# 1 STATE OF ART

This chapter gives an overview of work closely related to the topic of this thesis. It describes the most relevant localization approaches with the main focus on the issues further investigated in this work. The entire chapter section is devoted to energy consumption since it is a key aspect of the localization in energy constrained networks. Furthermore, it identifies an uncovered field of localization in wireless networks and points out the challenges of that field.

This chapter can also serve as an introduction and determine the terms used in this research area. Since there is a very active investigation of various aspects of WSNs and many publications presenting cutting edge results of the field occur everyday, the terms used in these publications can differ in meaning, which can be rather confusing. Therefore, the terms used in this work are presented in this chapter together with their meaning in order to avoid confusion. The intention is to use the meaning widely used and generally accepted although it could differ in particular publications.

## 1.1 Localization in wireless networks

Generally speaking, the term *localization* relates to searching a position of a certain object in a predefined area. Localization in WSNs can be accordingly defined as a process during which nodes obtain their position in the whole network or in a defined part of the network (not considering a manual setting of coordinates). The result of the localization process is the knowledge of a real or absolute position that a node obtains thanks to a certain localization algorithm. Localization can be performed for a single node, for example, when a new node is added to an existing network or for all nodes simultaneously (e.g. after network deployment or during periodic position update in the case of mobile nodes). Localization also means the process of finding a particular object in the area under a WSN surveillance. In this case the term localization is often associated with the term *tracking*. The difference is that the tracking means to follow the movement of an object (which is not a part of the network topology) along its trajectory. Subsequently, it is possible to draw its trajectory in a defined time and space. In this work, we focus on an active cooperation of nodes which are being localized, and thus, we refer only to the *localization* in the sense of autonomous active cooperation of wireless nodes.

Formally, in the graph theory, the localization of a node can be expressed as a process of determining coordinations of a node  $s_x$  in a graph  $G(V, E)$ .  $V$  is a vertex set and  $E$  is an edge set. Each node  $s_x$  (where  $x = 1, 2, ..N$  and  $N$  is a number of nodes) is represented by a vertex  $X \in V$  and each node pair  $(s_x, s_y)$ ,

which has a direct radio connection, corresponds to an edge  $(X, Y) \in E$ . The graph  $G(V, E)$  is called underlying graph of the network [7]. In most of the applications only a planar representation of a location is sufficient. Then, the representative graph has a mapping  $p : V \rightarrow R^2$  assigning a coordination in  $R^2$  to each vertex in  $V$ . In applications with three-dimensional location requirements the mapping is  $p : V \rightarrow R^3$  assigning each vertex in  $V$  with a coordination in  $R^3$ .

A location system can provide information about position either in physical or symbolic form [8]. Symbolic (explicit) form expresses coordinates of position (GPS coordinates for instance) while physical (implicit) form has mostly descriptive expression (i.e. in the room 222, next to the table, on a track approaching to Barcelona, etc.). Moreover, both forms can be linked and physical location can be translated according to database records to the symbolic form.

Coordinates can be expressed in different forms related to the reference coordinate system. Besides well known geographical, Cartesian, spherical coordinate systems, new synthetic coordinate systems were proposed to meet the real conditions in communication networks [9]–[11]. Thanks to the employment of these coordinate systems, it is possible to create a map of a network without measurements between each pair of nodes. However, the study of synthetic coordinate systems was devoted only to localization in IP networks so far. Although many coordinate systems are available, the vast majority of current research work uses the Cartesian coordinate system because of its practical use in real applications. However, virtual coordinates are used, for example, in geographical routing [12]–[14].

Objects and nodes in a network can be located either in an absolute coordination system or in a relative one. An absolute coordination system uses the same reference grid for all objects in the network. For example, longitude, latitude and altitude (or their equivalents such as Universal Transverse Mercator coordinates) are coordinates for all GPS receivers. And all GPS receivers will refer their position in shared reference grid. On the other side, relative coordinates are used by each node in its own frame of reference or in a certain network part (cluster). Relative coordinates of a particular node in a network have sense only with the respect to this node or network cluster but have no sense anywhere else [15]. The same meaning can be understood by terms *global* and *local* coordinates which refer to absolute respectively relative coordinates [16].

In a network certain nodes can be aware of their coordinates; either by manual setting or using different location system. These reference nodes form an infrastructure and are called *beacons*, *landmarks* or *anchors* in literature. The number of reference nodes  $R_x \in R \subset V$  is much smaller than the number of unlocalized nodes  $U_x \in U \subset V$ ;  $|R| \ll |U|$ .

Obtaining a location information is called a *localization process*. A localization



process can be either run next to other processes after a network deployment in the initial phase or periodically (in case of mobile nodes). Localization process can be also requested upon a particular event (before the transmission of sensed data). Generally, the localization process composes of two phases: i)collecting input information, ii)determining a position of the unlocalized node. The first phase is called *ranging* (or *localization method*) and the latter one referred as a *localization algorithm* [17]–[19]. *Localization protocol* can be used as a means of transmitting location related information.

### 1.1.1 Localization algorithms

The localization algorithm describes the way how the distance or other position indicating information is manipulated and how the localization system works from the whole network point of view. If the node already knows the localization parameters and its position in a certain coordinate system, the localization algorithm determines how this information is handled and distributed to other nodes to help them with their own position estimation. The localization algorithm can also optionally correct the errors in the estimation and refine the coordinates. The localization algorithms can have a lot of aspects, which can be used for their categorization or vice-versa to distinguish among them. Therefore, the following part goes through the main factors and explains their basic features and the way they influence the localization process.

Distinguishing feature	Category I	Category II
Given structure of reference nodes	Anchor-based	Anchor-free
Centralization of management	Centralized	Distributed (Decentralized)
Ranging	Range-based	Range-free
Coverage	Single-hop	Multi-hop

Tab. 1.1: Categorization of localization algorithms.

*Single-hop* or *multi-hop* communication schemes are the ways two nodes can communicate. A hop is a direct link between two nodes. If a localization algorithm uses only direct links for communication between two nodes, it is called one-hop or single-hop localization algorithm ([20]). This is the easier way that can be used only under specific conditions when two communicating nodes are in the radio range of each other. In certain cases, in environmental monitoring WSN application for example, natural obstacles, such as trees, rocks etc. impede the direct communication. Then, other interleaving nodes are used for delivery if there are some. This is

multi-hop communication, which requires more complex management. Unlike the single-hop system, the multi-hop one is much more scalable, e.g. [21], [22].

The range information, including distances and angles, is used to create a certain map of network nodes in a certain coordinate system. This is a natural way to treat localization called *range-based* localization [23]. However, there are certain localization methods that do not need the range information. Instead, they work with hops as a metric of distance estimation. Obviously, these *range-free* localization techniques do not reach the accuracy of range-based techniques but their accuracy is satisfactory in a lot of applications, which do not require high accuracy of position knowledge (AFL [24], DV-HOP [22], etc.).

The natural primary task of WSNs is to collect data and to accumulate them in one or more powerful servers where these data are processed. This fundamental process implies the centralized characteristic of the topology. During *centralized* localization, the process is managed from one place in the network. At this central point, all significant localization information is available for all nodes. This structure has a considerable advantage in the provided accuracy. On the other hand, centralized localization requires more long-distance multi-hop communication. Moreover, the nodes close to the central processing server consume more energy, which causes their energy depletion much sooner. The comparable energy consumption of all participating nodes during localization is ensured by distributed algorithms. *Distributed* techniques do not prefer any central point for storing localization information and each node uses only information provided by its neighbors. This means that the localization error increases while the estimated coordinates are distributed in a network and used in other node for position determination. The representatives of centralized algorithms are multidimensional scaling improvement (MDS-MAP) [25], simulated annealing localization [26] and RSSI based centralized localization [27]. Ad-hoc positioning system (APS) [22], anchor free algorithm (AFL)[24] or S-MRL [28] are examples of distributed localization algorithms.

The other type of categorization is devoted to the existence of anchor nodes. The *anchor-based* localization exploits the position knowledge of a certain fraction of nodes. The predetermined coordinates can be obtained from manual configuration or another localization system such as GPS as the most common. The other nodes then derive their own position based on the measurement and information obtained from the anchor neighbors (e.g. APS [22] or APITHE-[30]).

*Anchor-free* algorithms (such as AFL[24] or Map-growing [31]) work without predetermined information. The nodes determine their position in relative coordinates, and then subsequently this system can be embedded into another coordinate system (e.g. global coordinates). The anchor-free algorithms can be divided into two groups: *incremental* and *concurrent*. In the incremental ones, the nodes estimate

their coordinates one by one using the coordinates previously calculated. The incremental process implies higher error propagation, which causes poor overall accuracy. Unlike the incremental algorithms, the concurrent ones incorporate all participating nodes at the same time, in other words, the nodes calculate and refine their coordinates simultaneously. Description of certain algorithms in more detail will follow now.

### Anchor-free localization algorithm – AFL

Anchor free localization is applied in a network where no initial reference node structure is available. Therefore, it has to be created by AFL first. The objective of the phase building the reference structure is to determine a quadrilateral structure of reference nodes on the periphery of the network with a fifth reference node in the middle (Fig. 1.1).

The AFL progresses as follows and introduced in [24]. First, one node is randomly selected from the set of all the nodes ( $n_0$ ). It broadcasts a message searching for a node located furthest from it ( $n_1$ ). To find that node the hop counts are compared. When the node  $n_1$  receives an announcement that it was selected as the first node of the structure it subsequently runs the similar procedure to determine the node  $n_2$ . Then, two nodes ( $n_3$ ,  $n_4$ ) forming a perpendicular line approximately in the axis of the line  $n_1$ – $n_2$  are selected. At the end the central node is found complying the condition that it has roughly the same distance to all the peripheral reference nodes. The node  $n_5$  is then set as the central point of the new coordinate system.

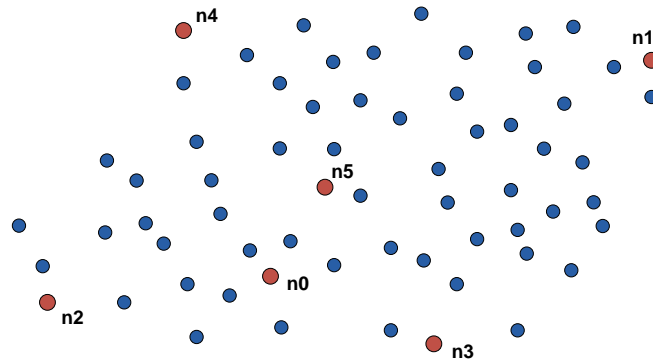


Fig. 1.1: Infrastructure of AFL algorithm.

When the initial AFL structure is established each node calculates its polar coordinates:

$$\rho = d_5 \times R, \quad (1.1)$$

$$\theta = \tan^{-1} \left( \frac{d_1 - d_2}{d_3 - d_4} \right). \quad (1.2)$$

$R$  is the radio range of the node, and  $d_i$  are distances to the particular reference node.

### Map-growing localization algorithm

The Map-growing localization algorithm ([31]) is a representative of the iterative anchor-free localization algorithms. At the very beginning one random node is selected to start the localization and create the initial local map. This node picks another two nodes to form a triangle provided that each of the inner angles is larger than 30 degrees (the algorithm performs more accurately then). The initial triangle is a basic element for the initial coordinate system. The center of the coordinate system is set to the location of the first node (n1 in Fig. 1.2). The node n2 has coordinates  $[0, d(n1, n2)]$ . The coordinates of the third node are  $[x, y]$  where

$$x = \frac{d(n1, n2)^2 + d(n1, n3)^2 - d(n2, n3)^2}{2d(n1, n2)}, \quad (1.3)$$

$$y = \pm \frac{\sqrt{4(d(n1, n2)^2 d(n2, n3)^2) - (d(n1, n2)^2 - d(n1, n3)^2 + d(n2, n3)^2)^2}}{2d(n1, n2)}. \quad (1.4)$$

The notation  $d(n_i, n_j)$  stands for the distance between nodes  $n_i$  and  $n_j$ .

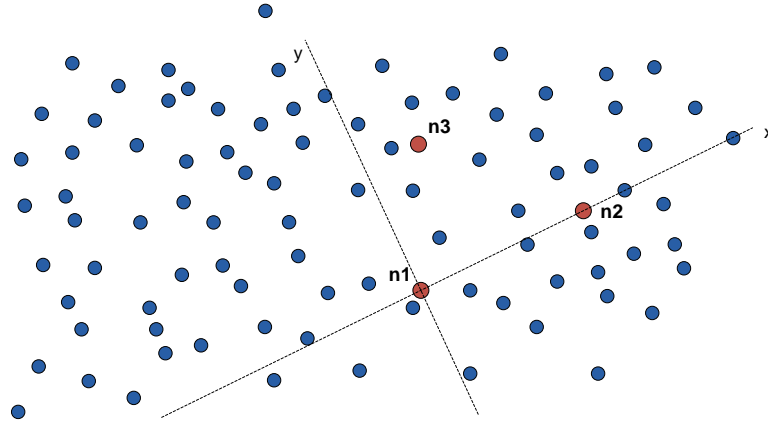


Fig. 1.2: Map-growing algorithm.

After the initial phase the first round of the map growing is performed. Each node of the initial triangle broadcasts its coordinates into the one-hop neighborhood. If an unlocalized node receives the coordinates from three reference nodes it runs

trilateration and calculates its own coordinates. Thus, the node becomes a reference node and broadcast its coordinates in the next round as well. In the second round more reference nodes are available and so there is a better chance for unlocalized nodes to obtain coordinates from at least three reference nodes. If there is more than three nodes with known coordinates in the one-hop neighborhood multilateration can be performed. For both trilateration and multilateration the distances to anchor nodes are necessary.

The basic formula to identify the distance between the reference node and an unlocalized node in Euclidian space is following:

$$d_i^2 = (x - x_i)^2 + (y - y_i)^2. \quad (1.5)$$

For each reference node included in lateration a corresponding equation is used. In the used notation unlocalized node coordinates are  $[x, y]$ , coordinates of  $i$ -th reference node are  $[x_i, y_i]$  and  $d_i$  stands for the distance between the unlocalized and the reference node. This set of quadratic equations can be solved by subtracting the last equation from the others one by one which gives a set of linear equations. Subsequently, LU decomposition or a certain iterative algorithm (e.g. Least Square Error) can be used for solving the set [32]. When assuming  $M$  suitable reference nodes, the equation set can be presented as

$$\mathbf{Ax} = \mathbf{b}, \quad (1.6)$$

where

$$\mathbf{A} = 2 \begin{bmatrix} x_1 - x_M & y_1 - y_M \\ x_2 - x_M & y_2 - y_M \\ \vdots & \vdots \\ x_{M-1} - x_M & y_{M-1} - y_M \end{bmatrix}, \quad (1.7)$$

$$\mathbf{b} = \begin{bmatrix} x_1^2 - x_M^2 + y_1^2 - y_M^2 - y_M^2 - d_1^2 - d_M^2 \\ x_2^2 - x_M^2 + y_2^2 - y_M^2 - y_M^2 - d_2^2 - d_M^2 \\ \vdots \\ x_{M-1}^2 - x_M^2 + y_{M-1}^2 - y_M^2 - y_M^2 - d_{M-1}^2 + d_M^2 \end{bmatrix} \quad (1.8)$$

and vector of unknown coordinates

$$\mathbf{x} = [x \ y]^T. \quad (1.9)$$

### Least Square and Weighted Centroid localization algorithms

The Least square method belongs to the range-based algorithms which means that it uses a distances between nodes to estimate the positions of the unknown

nodes. Distances can be obtained from several measurements methods presented in the next section. The Least square method is based on the hyperbolic positioning algorithm [33], which reduces the positioning problem to a linear least-square problem. Once the distances between the unknown node and the anchor nodes have been estimated, the position of the unknown node can be calculated using the algorithm.

Weighted centroid localization algorithm is a representative of the second class known also as approximated algorithms [34]. In contrast with algorithms based on the Least squared method, these algorithms avoid determining distance in their approach. Regarding the energy constraints in sensor networks, these approximated algorithms consume less power but their position estimates can contain higher localization errors.

### 1.1.2 Evaluation of localization

When talking about localization process, accuracy and precision always have to be considered. It is often the most important criterion when choosing a localization algorithm for a specific application. *Accuracy* means the largest difference between estimated and real position. *Precision* denotes the ratio with which the accuracy is reached over the number of estimates. Therefore, these values should be always considered together.

The errors in position estimations are mainly caused by ranging error. The more erroneous the input data (distances, angles), the higher the inaccuracy resulting from a localization algorithm. Therefore, the elimination of a ranging error was addressed by many research groups with partial achievement but the full elimination or significant reduction of this error could not be achieved until now [35].

The best accuracy of various localization methods in real conditions differs significantly. Apart from quality and theoretical expectations of the methods, the accuracy depends on surrounding conditions and robustness of the methods. But even in very adverse conditions an average accuracy 0.2 m can be reached with a special testbed setting [36].

There are lower limits on localization covariance achievable by any unbiased location estimator given by following:

- number of known-position and unknown-position nodes,
- sensor geometry,
- two or three dimension system,
- measurement type (based on signal strength, time or angle – details provided in following section),
- channel parameters,
- in-network connectivity,

- nuisance (unknown) parameters that must be also estimated [37].

The Cramér-Rao Bound (CRB) provides the tool how to calculate the lower bound on the covariance [38]. CRB can be calculated without any knowledge of location estimation method just considering statistical model of random measurements  $f(X|\theta)$ , where  $X$  is the random measurement and  $\theta$  stands for the parameter that is going to be estimated. The smallest variance of any unbiased estimator  $\hat{\theta}$  is given by inverse of the Fisher information  $I(\theta)$

$$\text{var}(\hat{\theta}) \geq \frac{1}{I(\theta)}, \quad (1.10)$$

where the Fisher information  $I(\theta)$  is defined by

$$I(\theta) = \text{E} \left[ \left( \frac{\partial l(x; \theta)}{\partial \theta} \right)^2 \right], \quad (1.11)$$

with  $l(x; \theta) = \ln f(x; \theta)$ , natural logarithm of likelihood function  $f$  and  $\text{E}$  expresses the expected value. CRB can be very useful for researchers testing localization algorithms. If their algorithm accuracy is close the theoretical lower bound there is little reason to continue with its optimization. Several papers were published with results of CRB for different types of measurement [37], [39]–[42] which gives analysis of CRB under different conditions.

Other accuracy metrics for a network with  $n$  nodes presented in [43] include:

- Mean Absolute Error (MAE):

$$MAE = \frac{\sum_{i=1}^n \sqrt{(x_i - \hat{x}_i)^2 + (y_i - \hat{y}_i)^2 + (z_i - \hat{z}_i)^2}}{n}, \quad (1.12)$$

- Frobenius (FROB):

$$FROB = \sqrt{\frac{1}{n^2} \sum_{i=1}^n \sum_{j=1}^n (d_{ij} - \hat{d}_{ij})^2}, \quad (1.13)$$

- Global Energy Ratio (GER):

$$GER = \frac{1}{n(n-1)/2} \sqrt{\sum_{i=1}^n \sum_{j=i+1}^n \left( \frac{d_{ij} - \hat{d}_{ij}}{d_{ij}} \right)^2}, \quad (1.14)$$

- Global Distance Error (GDE):

$$GDE = \frac{1}{R} \sqrt{\frac{\sum_{i=1}^n \sum_{j=i+1}^n \left( \frac{d_{ij} - \hat{d}_{ij}}{d_{ij}} \right)^2}{n(n-1)/2}}. \quad (1.15)$$

The node's estimated position is labeled as  $[\hat{x}_i, \hat{y}_i, \hat{z}_i]$  and its actual true position as  $[x_i, y_i, z_i]$ ,  $\hat{d}_{ij}$  and  $d_{ij}$  represent estimated and true distance between nodes  $i$  and  $j$ .  $R$  stands for the average radio range.

Those metrics are related only to the error of position estimation, however, there are other aspects of the localization algorithms which should be considered during evaluation. More general evaluation includes: scalability, coverage, costs, etc. The metrics can be also combined resulting in hybrid metrics.

When a new algorithm is presented it can be evaluated by generally used metrics or by specific metric presented together with the algorithm (e.g. [44],[45]). Probably the most complex metric which uses accuracy and energy cost to express energy efficiency is proposed in [46] and commented also in [47]. This metric is derived from CRB (Cramér-Rao Bound), is objective, bounded and proportional.

### 1.1.3 Overview of localization methods

Localization algorithms require certain input information for position determination. They work with information including hops, maps, distances or angles. Hops are used in range-free localization and the number of hops between two nodes is derived from the Time-to-Live value decremented at each node forwarding the packet. When using the fingerprint approach maps are used as a pattern with which a current observation is compared in order to estimate the position. For many algorithms distances or angles are the basic crucial information needed for the estimation. To obtain these input values, specific measurement techniques are used. These techniques can be categorized into three main classes based on [48]:

- Time of Arrival (ToA),
- Angle of Arrival (AoA),
- Received Signal Strength (RSS).

Time of Arrival (or Time of Light) [48] is a method based on the known speed of signal propagation, which serves for distance calculation. For small distances, the time of flight is very small and high accuracy and precise time synchronization is required. To overcome this inconveniences, round-trip delay (RTT) can be calculated. The difference between sending and arrival time is measured at the same node, and thus, the synchronization is not necessary. However, the delay related to processing of the received packet (packet reception, decoding, transmitting the response) at the other node is included in the measured value.

Time Difference of Arrival (TDoA) [49] is another method measuring the time of signal propagation. Unlike ToA, TDoA relates the arrival times of signals from several anchors. There are two variants: TDoA either computes the position of the



transmitter from the delay measured at several different nodes with known position or the other way around, the unknown node receives signals from several different reference nodes. The cross-correlation between received signals is calculated by Simple Cross-Correlation (SCC) or Generalized Cross-Correlation (GCC) method [50] to obtain the time difference. The reference nodes have to be perfectly synchronized to achieve appropriate accuracy. Unfortunately, this fact implies more expensive components and more complex time management, which makes other ranging methods preferable if available.

Time difference is also used in another method. However, it is not the difference between two radio signals but the difference between radio signal and ultrasonic pulse from one transmitter. The method is based on the different speed of propagation of both signals. The speed of the RF signal is almost constant close to the speed of light in vacuum but the speed of sound waves changes and it is dependent on the environment characteristic (mostly temperature). Therefore, the calibration and corrections are necessary.

It is a promising system since it avoids the necessity of time synchronization among reference nodes. The more detailed description of the method with a Cricket system implementing this method can be found in [51] and summed up in the following section.

Probably the most used and well known method is based on the fact that the signal power decreases with the distance from transmitter. The method is known as a received signal strength (RSS) method. It offers an easy implementation into a localization system, since there are no extra hardware requirements, but it suffers from high inaccuracy because of several negative effects in environment, especially indoors. Therefore, the usability of the method is limited to applications where no precise localization is necessary or a robust localization algorithm is employed to improve the accuracy. Because of the accessibility of the method and its indubitable advantages, there is a high interest to optimize the method e.g. [52], [53].

Next, a localization method called AoA (Angle of Arrival) [54] performs measurement of angles rather than distances. Despite that, it is often included in the list of localization ranging methods. AoA exploits asymmetrical pattern of antennas and either antenna rotation or antenna field, which implies hardware modification with space constraints.

In the following sections methods with high relevance to the thesis topic are described in more detail. First, a widespread method based on signal strength measurement is discussed, and then, an alternative method based on ultrasound signal propagation is briefly presented since certain works suggest it like a precise and non-expensive ranging method [57]–[58].

### 1.1.4 Received signal strength method (RSS) and radio signal propagation

A well known and broadly used method of distance estimation infers the distance from the signal strength measured at the receiver. Signal propagation models or maps are used for this purpose. There are several signal propagation models that approximate the real radio channel and allow to relate a certain received signal strength to the distance between the transmitter and the receiver. It is an inexpensive and simple method of estimation since no extra hardware is required. This fact makes the method very attractive and broadly used. However, several factors complicate the estimation and cause estimation errors. The estimation is influenced by the manufacturing process of the nodes and their radio circuits, antenna inadequacies and most importantly several phenomenons in signal propagation such as multipath propagation, shadowing, obstacles and current RF conditions [59]. Generally, the effect of negative RF phenomenons such as multiple reflections is significantly worse indoors than outdoors which often implies different approaches such as one using iso-lines [60] or fingerprints [61].

The transmission over a radio channel can be either line-of-sight or non-line-of-sight obstructed by walls, terrain shape, foliage or moving objects. Signal propagation is not a stationary process and it is influenced by several factors that can be generally attributed to reflection, diffraction and scattering. The propagation models either predict the mean of the signal strength expected at the arbitrary distance from transmitter (*large-scale models*) or characterize fast fluctuation of the received signal strength over short distances or a short time interval (*small-scale* or *fading models*). Overview of certain basic and widely used models are described further in this section as given by [62].

The signal propagation is influenced by three physical phenomenons:

- *Reflection* occurs when an EM wave hits an obstacle's surface with a dimension much larger than a wavelength of the wave. The reflection occurs from the ground, buildings and walls.
- *Diffraction* occurs when an EM wave passes the obstacle with sharp edges comparable to the wavelength of the signal. The wave is bended and reaches the space in non-line-of-sight path.
- *Scattering* occurs when a wave impinges a rough surface or small objects with dimensions smaller than the signal wavelength and number of objects is large in a volume unit. For example, foliage, street signs or heavy rain induce scattering in wireless systems [62].

### Free space propagation model

The free space model describes the signal propagation in a large scale over unobstructed signal path between a transmitter and a receiver. The model predicts the received power decay as a function of distance (similarly to other large-scale models). The power received at the receiver in the distance  $d$  from the transmitter is given by Friis free space equation as originally published in [63]:

$$P_r(d) = \frac{P_t G_t G_r \lambda^2}{(4\pi)^2 d^2 L}, \quad (1.16)$$

where  $P_t$  is the signal power transmitted,  $P_r$  is the signal power received,  $\lambda$  is a wavelength of the carrier,  $L$  stands for the system loss not related to the propagation ( $L \geq 1$ ),  $G_t$  is the transmitter antenna gain and  $G_r$  is the receiver antenna gain.

Path loss representing a signal attenuation in dB is given as the difference (in dB) between the effective transmitted power and the received power:

$$PL[\text{dB}] = 10 \log \frac{P_t}{P_r} = -10 \log \left[ \frac{G_t G_r \lambda^2}{(4\pi)^2 d^2} \right]. \quad (1.17)$$

### Ground reflection (two-ray) model

The condition of line-of-sight pathway is very limiting in real conditions, and thus, the free space model does not often give accurate predictions in practice. To enhance the prediction the second wave reflected from the ground is considered in the ground reflection model. The geometric optic of direct and ground reflected pathway is considered in this model. Path loss of the two-ray model is expressed as [62]:

$$PL[\text{dB}] = -10 \log \left[ \left( \frac{h_r h_t}{d^2} \right)^2 \left( \frac{\sin \frac{2\pi}{\lambda} \frac{h_r h_t}{d^2}}{\frac{2\pi}{\lambda} \frac{h_r h_t}{d^2}} \right) \right], \quad (1.18)$$

where  $d$  is the distance between the transmitter and the receiver,  $h_r$  is a height of the receiving antenna and  $h_t$  is a height of the transmitting antenna. If the distance between the transmitter and the receiver is larger than the product of the antenna heights  $h_r h_t$  the path loss can be simplified as

$$PL[\text{dB}] \approx -10 \log \frac{(h_r h_t)^2}{d^4}, \quad (1.19)$$

and thus, received power estimated as

$$P_r(d) = P_t G_t G_r \frac{h_r^2 h_t^2}{d^4}. \quad (1.20)$$

As previously defined  $P_t$  is the signal power transmitted,  $P_r$  is the signal power received,  $G_t$  is the transmitting antenna gain and  $G_r$  is the receiving antenna gain. Performed simulations of the channel model can be seen in Fig. 1.3

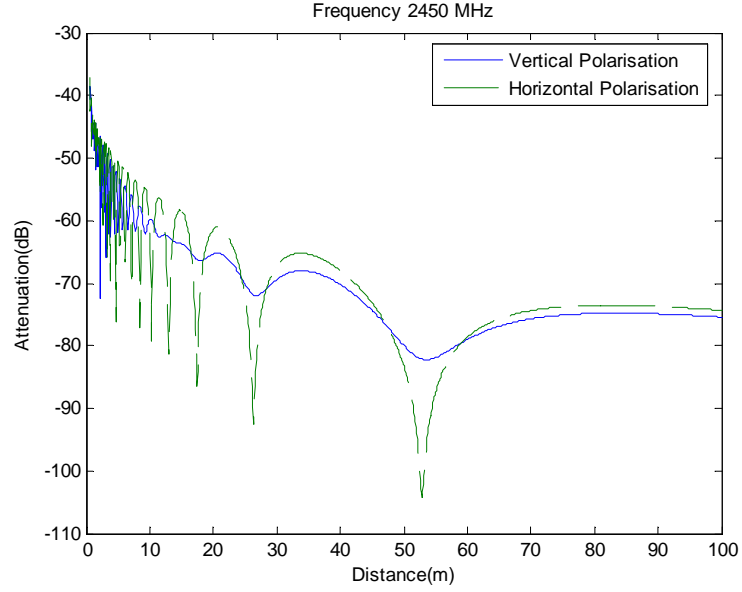


Fig. 1.3: Two-ray ground signal propagation model.

### General signal propagation model

The ground reflection model considers only two signals interfering at the receiver's antenna. However, the power level measured at the receiving node is given by the sum of all the EM waves reflected from ground, walls and other obstacles. The coefficient of reflection is called Fresnel coefficient and depends mostly on the incident angle of the signal and the surface [64].

Considering all the contribution the path power loss can be modeled according to [64] as

$$PL[\text{dB}] = -10 \log \left( \frac{\lambda}{4\pi} \right)^2 - 20 \log \left[ \frac{1}{d_0} e^{-jk d_0} + \sum_{i=1}^N \Gamma_i \sqrt{t_i} \frac{1}{r_i} e^{-jk d_i} \right], \quad (1.21)$$

where  $\lambda$  is the wavelength,  $d_0$  is the length of the direct path,  $d_i$  the length of the  $i$ -th reflected ray path,  $N$  the total number of reflections and  $k$  the wave number. The gain of the receiver antenna when transmitting depends on the direction. In order to take this into account,  $t_i$  is the normalized antenna radiation pattern and  $\Gamma_i$  is the Fresnel's reflection coefficient in the object for the  $i$ -th wave given by [64]:

$$\Gamma_i = \frac{\cos \theta_i - q \sqrt{\epsilon_c - \sin^2 \theta_i}}{\cos \theta_i + q \sqrt{\epsilon_c - \sin^2 \theta_i}}, \quad (1.22)$$

where  $\epsilon_c$  is the complex permittivity of the ground,  $\theta_i$  is the incident angle with the normal to ground and  $q$  is a polarization dependent factor;  $q = 1$  for horizontal polarization and  $q = 1/\epsilon_c$  for vertical polarization.

### Log-distance path loss model with shadowing

Many propagation models were derived from both analytical and empirical methods. Both approaches indicate that the mean received signal power decreases logarithmically with the distance. The average large-scale path loss for arbitrary distance  $d$  between a transmitter and a receiver is expressed as a function of distance with path loss exponent  $n$ :

$$\overline{PL}[\text{dB}] = \overline{PL}(d_0) + 10n \log \left( \frac{d}{d_0} \right). \quad (1.23)$$

The path loss exponent  $n$  indicates the rate at which the path loss increases with the distance and ranges from 2–4 in outdoor environments.  $d_0$  is the close reference distance and  $\overline{PL}(d_0)$  is the mean path loss at the distance  $d_0$ .

However, the actual measurement can differ significantly. It is caused by the fluctuation of the signal. It means that two measurement at the same distance  $d$  in different environments as well as two measurements at the same place can be considerably different. To express that in the formula the zero mean Gaussian distributed random variable  $X_\sigma$  (in dB) is added and the received signal power at the distance  $d$  subsequently given as

$$P_r(d) = P_0 - 10n \log \left( \frac{d}{d_0} \right) + X_\sigma, \quad (1.24)$$

where  $P_0$  is the received signal power at the reference distance  $d_0$  [62].

### Two-slope propagation model

The Two-slope path loss model is one of the most used in line-of-sight propagation (LOS) systems. Following commonly adopted two-slope path loss model was suggested in [65]:

$$P_r = \frac{C}{d^\alpha (1 + \frac{d}{g})^\rho} P_t, \quad (1.25)$$

where  $P_r$  [W] is the received signal power,  $C$  is a constant factor of path loss depending on the carrier frequency and the antenna heights,  $\alpha$  is the basic path loss exponent (ranges from 2–4) for  $d \leq g$ ,  $\rho$  is the extra path loss exponent (ranges from 2–8) for  $d \geq g$ .  $d$  is the distance between the signal transmitter and the receiver.  $P_t$  is the transmitted signal power and  $g$  is the breakpoint of the path loss

curve. The break point distance of the two-slope path loss model is the separate distance between regions with two different signal propagation properties (near and far regions relative to the signal transmitter). The breakpoint distance has been confirmed by experimental measurements in both Ultra high frequency (UHF) and Super high frequency (SHF) bands [66], [67]. The breakpoint  $g$  can be calculated as

$$g = \frac{4h_t h_r}{\lambda_c}. \quad (1.26)$$

The breakpoint distance is proportional to the product of both transmitter ( $h_t$ ) and receiver ( $h_r$ ) antenna heights and inversely proportional to the carrier wavelength  $\lambda_c$ .

### **RSS uncertainty**

The power of the received signal is influenced by several factors with deterministic and stochastic characteristic. The deterministic ones can be predicted, estimated and their influence included in the distance calculation using the appropriate channel model. Unlike these time stable factors, stochastic ones change in time and cannot be estimated before the measurement. The paper [68] analyzes the received signal strength variance from several perspectives to find any dependency in time or frequency domain. The performed experiments, however, failed in finding the regularity and repeatability of RSS signal. Also other recently published works (e.g. [69], [70]) deal with the fluctuations of the received signal strength for a stationary node.

The authors of [59] describe the RSS uncertainty as one of the four most important parameters for a propagation model proposal. Moreover, experimental studies and works consider RSS uncertainty in general and include it in the experimental system design and localization algorithms (e.g. [71]–[73]). The authors of [74], [75] proposed certain data processing methods to deal with the RSS uncertainty in practical WSN applications.

Sources of RSS uncertainty include hardware imperfections, movement of persons or any other objects in the surrounding of communicating nodes, random change of the electromagnetic field or interference with other wireless networks in the same frequency range. These factors cannot be eliminated and their influence completely avoided. It is necessary to describe and characterize RSS uncertainty and involve procedures or methods which are capable to eliminate its undesirable influence and to determine RSS value without random variations. As claimed and verified by performed measurements in a few works (e.g. [59][76]), the RSS uncertainty has normal (or log-normal in dB) distribution with the probability density function (PDF) given by the following formula:

$$PDF_{\sigma,\mu}(RSS_i) = \frac{1}{\sigma\sqrt{2\pi}} \exp\left(-\frac{(RSS_i - \overline{RSS})^2}{2\sigma^2}\right), \quad (1.27)$$

where  $\overline{RSS}$  is the expected value of the received signal,  $\sigma$  is the standard deviation and  $RSS_i$  is the variable of measured value. The authors of [76] proposed three methods for RSS value determination. Assuming we have a set of RSS measurements with  $N$  values, we have to determine one RSS value corresponding to the distance. The elementary option requires just calculation of statistical mean value by

$$\overline{RSS} = \frac{1}{N} \sum_{i=1}^N RSS_i, \quad (1.28)$$

where  $RSS_i$  represents each single measurement. Another option incorporates normal distribution and exclusion of less probable values. Gaussian distribution function is applied on the set of  $N$  values. Then, only values with probability higher then determined threshold (in [74] threshold 0.6 is used) are considered for subsequent data processing. This procedure can exclude small probability events, which could cause inaccurate determination of RSS value. The third introduced method is based on the knowledge of distance and power mean between two reference points. The distance between the unknown node and one reference node is derived from the ratio of mean powers between them.

## Coherence time

Doppler spread and coherence time are parameters describing time varying characteristic of a radio channel in a small scale region. The time disperse variation of the radio channel is caused by the varying propagation time of signal paths between the transmitter and the receiver. The time variation causes changes in frequency of the received signal, and thus, a Doppler effect. The spectrum of the received signal is wider compared to the transmitted one which is characterized by the Doppler spread. The Doppler spread can be either a result of a relative motion between the transmitter and the receiver or a consequence of a movement in the multiple signal pathway [62]. If a single harmonic signal  $f_c$  is transmitted, the receiver receives a signal in the frequency range  $< f_c - f_d; f_c + f_d >$ , where  $f_d$  is a Doppler shift. The Doppler shift is a function of the velocity and the angle between the direction of the motion and the receiver antenna.

For the multipath environments the sum of all incoming multipath signals is detected by the receiver and it can be analytically expressed using Clarke's reference model [77] as

$$S(t) = S_c(t) + jS_s(t), \quad (1.29)$$

where  $S_c(t)$  and  $S_s(t)$  are in phase and quadrature components of the complex EM signal:

$$S_c(t) = \frac{1}{\sqrt{N}} \sum_{n=1}^N \cos(\omega_d t \cos \alpha_n + \theta_n), \quad (1.30)$$

$$S_s(t) = \frac{1}{\sqrt{N}} \sum_{n=1}^N \sin(\omega_d t \cos \alpha_n + \theta_n). \quad (1.31)$$

$\omega_d$  is a Doppler frequency,  $\alpha_n$  the angle of arrival and  $\theta_n$  stands for a phase of the  $n$ -th component.

In the time domain the Doppler spread phenomenon can be expressed by the mean of coherence time  $T_c$  of the radio channel.  $T_c$  represents the time over which a radio channel is assumed to be constant.

In other words, the coherence time is a period over which the channel impulse response is invariant and so it characterizes a similarity of the channel response at different times. Within this time the two received signals have a high probability of amplitude correlation.

In modern digital communication systems the popular rule of thumb is applied to define a threshold level and the  $T_c$  is taken as [62]

$$T_c = \frac{0.423}{f_m}, \quad (1.32)$$

where  $f_m$  is a maximal Doppler shift given as

$$f_m = \frac{v}{\lambda}. \quad (1.33)$$

$v$  stands for the relative velocity of the receiver and  $\lambda$  is a carrier wavelength used.

In a nutshell, two signals with a time separation greater than  $T_c$  are affected differently by the channel. The simulation and experimental measurement results regarding the coherence time can be seen in e.g. [78] and [79].

### 1.1.5 Ultrasonic ranging method

Measurement of time duration of ultrasound signal propagation is another method of distance estimation. This method is widely used for an object detection using a sonar system where the delay of the sound wave reflected back from an object is measured.



This is used for example in robotics system where robots navigate themselves along a determined way [55][56]. One way time measurement can be used similarly to ToA method with the difference that the propagation time of the ultrasound signal is measured instead of the delay of the electromagnetic signal. Regardless the bigger delays in the sonic system, the same issue of precise nodes synchronization arises. To overcome this issue, a new system using both RF and ultrasonic (US) signal was proposed and developed under Cricket project [51]. It is based on the fact that the speed of sound in the air is approximately  $10^6$  times lower than speed of light. The transmitter sends RF signal together with the ultrasonic pulse. The receiver listens and waits for the RF signal. Because of the speed difference of the two signals, when the listener receives first several bits (which are used as a training sequence) it turns on its ultrasonic receiver. The ultrasonic pulse comes usually in a short time later. The listener then uses the time difference between the reception of RF signal and ultrasonic pulse to calculate the distance ( $d$ ) from the transmitter by

$$d = (v_{\text{radio}} - v_{\text{US}})(t_{\text{US}} - t_{\text{radio}} - t_{\text{delay}}), \quad (1.34)$$

where  $v_{\text{radio}}$  is a speed of light,  $v_{\text{US}}$  is a speed of ultrasound signal,  $t_{\text{US}}$  and  $t_{\text{radio}}$  are the arrival times and  $t_{\text{delay}}$  is the delay between transmission of radio and ultrasonic signal.

This method avoids the synchronization problem but it also has its drawbacks. The sound propagation is a complex problem and it is conditioned by its physical properties [57]. The result depends on several factors. One group of environmental factors includes temperature, humidity, movement of the air, etc. The effect of the temperature ( $t$ ) can be expressed by the following formula [57]:

$$v_{\text{US}} = (331.57 + 0.607t). \quad (1.35)$$

Other factors affecting the measurement are functional conditions. The reception can be influenced by the presence of other transmitters and sources of the sound of similar frequency or reflections from objects in the neighborhood. The reflection from an object of a certain specific shape can cause multi-echo, for example. The presence of several transmitters, often used in localization systems to improve accuracy, can be resolved by using a specific character of scheduling. The problem is that when two transmitters transmit the signal at the same time, the listener can evaluate the reception of the ultrasonic pulse incorrectly. After turning on its ultrasonic receiver when the first bits of the RF signal from a transmitter A are received, the listener waits for the ultrasonic pulse. But the ultrasonic pulse from a transmitter B can reach the listener sooner (if the transmitter B is closer than the transmitter A). Then the distance from the transmitter A is calculated erroneously. Thus, the

task of each listener is to gather the ultrasonic signals received concurrently from different transmitters, deduce and correlate them with the received RF signal and choose the transmitter's identifier. The investigation of such system with several transmitters and its performance was described in [58].

## 1.2 Energy consumption

Limitation in energy resources is one of the constraints of wireless networks (besides computational, memory and bandwidth resources) where the nodes are not supplied from the mains. WSN are the typical representatives of such networks. When a given energy is depleted nodes lose their computational and communication functionalities, become inactive, dead. With a non-uniform energy depletion in the network, some of the nodes are crucial for the whole network or its certain part and if those nodes are dead the whole dependent subnetwork (cluster) is disconnected. Therefore, to improve network reliability and prolong the network lifetime, certain techniques of communication, low-powered nodes and energy aware network topologies have to be involved in a network design.

Improvements and various energy saving techniques can be employed in the whole protocol stack. Such techniques include MAC sleeping schemes, network routing protocols, localization, security and other energy aware services and functions [80][81].

There are three main consumers of energy regarding WSN node: computing power of microcontroller (MCU), RF communication and sensing (Fig. 1.4). When we add up all those components we get an expression of entire energy consumption:

$$E = E_{\mu p} + E_{RF} + E_{\text{sensor}}. \quad (1.36)$$

$E_{\mu p}$  is the energy consumed by microprocessor,  $E_{RF}$  energy drained by transceiver circuits (transmission and reception both together) and  $E_{\text{sensor}}$  stands for the energy needed to power all the sensors required by application task.

First, regardless sensing the transceiver is the main consumer of energy because communication is much more energy demanding process than computations (typically around 35 mW [83]). Transmission of 1 bit requires the same amount of energy as execution of several thousands of instructions [82]. Therefore, computation should be preferred if possible. However, communication is a necessary part of the network. The cost of transmission, reception or listening is roughly equal, and therefore, the only way to save energy is to transit into a sleep mode as often as possible because the consumption is significantly lower (by approximately  $10^3$ ).

Considering networks with sensing capabilities, consumption of sensors is a significant burden. Some examples of typical values for commonly used sensors are listed in Tab. 1.2

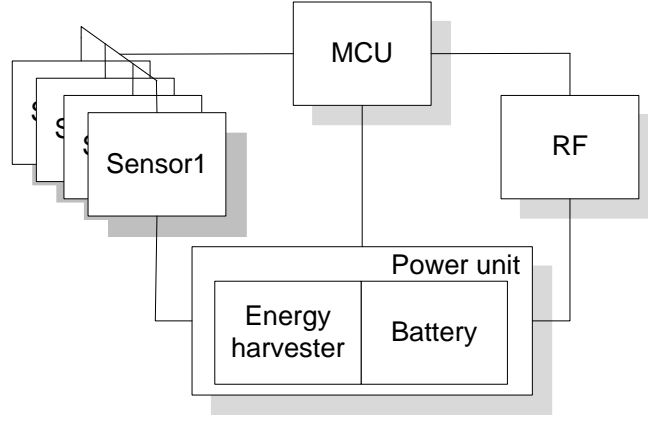


Fig. 1.4: Basic schema of a WSN node.

Sensor	Producer	Sensing	Power [mW]
STCN75	STM	Temperature	0.4
QST108KT6	STM	Touch	7
SG-LINK 1000 $\Omega$	MicroStrain	Strain gauge	9
iMEMS	ADI	Accelerometer	30
2200,2600 Series	GEMS	Pressure	50
T150	GEFRAN	Humidity	90
LUC-M10	PEPPERL+FUCHS	Level sensor	300
TDA0161	STM	Proximity	420
FCS-GL12A4-AP8X-H1141	TURCK	Flow control	1,250

Tab. 1.2: Power consumption of some COTS sensors [83].

Communication network architecture was built in a multiple layer manner. Accordingly, many energy aware techniques target specific function in a communication stack ranging from physical to application layer.

Using low-power components is a basic prerequisite of low power operation. Trading off unnecessary computational power can help to save energy for example. Other MCU related method is called dynamic voltage scaling that reduces current drain by adopting voltage and frequency of the MCU based on workload requirements [81].

Other factors that influence consumption of hardware components, especially transceiver, are modulation scheme, data rate, transmitting power, duty cycle, packet payload and header size, symbol rate, amplifier power etc.

Battery lifetime is strongly affected by the discharge rate of the current. If a high discharge rate is maintained the battery can be depleted faster. On the other side, thanks to the battery relaxation effect, if the current drained from the battery

is not constant but occasionally reduced or cut off, the battery lifetime is much longer [84]. Also dc-dc converters stabilizing the supply voltage contribute to higher current drain.

From the sensing part point of view signal sampling, physical to electrical conversion, signal conditioning and AD conversion are important factors of consumption.

To sum up, especially hardware design and choice of the components play the most important role regarding energy awareness on the physical layer.

Link layer aspects of the energy saving include idle listening on the channel, packet collision, overhead of control packets and overhearing. Therefore, the energy aware link layer protocols should efficiently deal with that and reduce packet retransmission by using an efficient method of channel utilization and error control possibly with adaptive features.

Main task of the network layer is the routing of a transmitted packet from the source to the destination. Energy aware networks feature many specifics in routing protocols because they may choose the way based on the energy available on the forwarding nodes and not the cost of the link. There have been proposed several routing protocols that can be classified as flat, hierarchical, multi-path, query, negotiation, data centric, location and quality of service [85].

Ways of energy saving available in application layer are very application specific. In WSN the sensing period and the report period (when the data are transmitted) can significantly determine the consumption of the entire network, and thus, also the lifetime.

The layer network architecture makes energy optimization difficult task for researchers. Optimization in one layer may need a cooperation of other layer or it can be contra productive in another layer despite targeting the same goal. New layer interfaces or layer merging might be helpful which is exploited in cross-layer approach of energy optimization, e.g. [86].

When designing a certain sensor network, the necessity of position accuracy should be always strictly related to the purpose of localization and to the future utilization of node position information. Not every application requires accuracy of centimeters or even meters to ensure its function. It has to be advisedly determined how much of node and network resources will be expended during a localization process. These resources include mainly time, computation and memory capacities, bandwidth and, last but not least, extra money for equipment ensuring higher precision. Apart from money invested during localization system design and implementation, all other sources have the same denominator which is energy source. All processes employed in localization need energy to be executed. In most cases it is possible to claim that the more complex and robust a localization method is, the more energy it requires.

Widely used localization technique based on GPS (Global Positioning System) technology can resolve some of the problems in getting position information. However, using GPS is quite limited to a narrow group of applications since it requires line-of-sight between receiver and satellites (not feasible for indoor applications), not speaking of high energy consumption and cost of GPS receiving modules.

## 1.3 Chapter summary

Position awareness is an important feature for many crucial functions in wireless networks or even the key information that the network provides in some applications. Therefore, localization is employed. Localization definition, formal notation and several localization approaches were presented in this chapter. A brief overview and more detailed discussion of certain localization algorithms and techniques give an introduction into problematics of localization in wireless networks.

As described, information about the distances among nodes in the network is a crucial input data for many localization algorithms. Therefore, the accuracy of the distance estimation affects directly the accuracy of the position determination. From several ranging techniques, the method based on the received signal strength is the most widely used. However, several works point out the uncertainty of the received signal strength measurement because of the environment fluctuation (e.g. [59], [68]–[70]).

However, up to my best knowledge, there is no work relating the mitigation of the uncertainty to the application requirements and energy consumption. Therefore, the objectives that follow in the next chapter are set to cover this gap in the field of wireless networks localization.

## 2 OBJECTIVES

The main objective of the thesis is a proposal of an energy-aware distance estimation method for a general use which is adaptable to predefined application accuracy requirements.

Location information is useful or even crucial information in a vast majority of wireless applications such as logistic, environmental monitoring, agriculture etc. ([4]–[6]). Therefore, several localization algorithms have been proposed in order to be able to obtain such information about each node in a network ([20]–[29]). The majority of localization algorithms use a distance between nodes as a primary and key input information to calculate the nodes' position. Based on the distance relation of the nodes, first, their relative mutual position is determined, and subsequently, their absolute position is derived. Certain algorithms use a set of nodes with a known position as reference nodes and in order to localize the other nodes, distances to the reference nodes are necessary, e.g. [23], [27]. Consequently, the accuracy of the position estimation depends highly on the accuracy of the previously estimated distance.

Because of a broad range of WSN applications (or wireless Ad-hoc networks in general) there are also considerably different requirements on the accuracy of the positioning. Some of the applications require just rough position estimation of the nodes (agriculture) but other, to the contrary, can have very strict demands (e.g. logistic and storage management applications).

Consequently, costs of the localization can also be different for each individual application. And because of energy constrains in such networks, there is an intention to save as much energy as possible and not to waste it inefficiently. Therefore, this thesis addresses the issue of the efficient use of energy resources for the distance estimation respecting specific application demands. The proposed method must also respect different environmental conditions, especially different radio channel characteristics, and must be invariant to them.

To that end, following supportive objectives were stated:

- detailed analysis of the distance estimation based on the received signal strength measurement – There are several approaches to distance estimation viable in wireless Ad-hoc networks, however, not many are well and efficiently adopted in current applications [48]. The main reason for this is mostly the additional cost of the method added to the manufacturing of nodes and the execution of the estimation in a network. The most widespread method is a method based on the received signal strength since it is relatively easy to implement at most of the commercial off-the-shelf (COTS) products. Therefore, this work

focuses on the received signal strength approach respecting the general use requirements of the primary objective. The secondary goal contains also an investigation of radio environment affecting the distance estimation method. WSNs are deployed in many various environments mostly characterized by their radio properties. This has a significant influence on the distance estimation based on the received signal strength [62]. To achieve the accomplishment of accuracy demands independently on distinct radio conditions, these conditions have to be respected. Therefore, the investigation of radio characteristics affecting the estimation method has to be conducted.

- analysis of an energy consumption and determination of an energy model used in the investigation – In order to implement energy awareness in the new method it is necessary to define and implement methods of energy consumption evaluation corresponding to energy dissipation during localization.
- proposal of a new distance estimation method – This partial objective contains a detailed proposal of the new distance estimation method and its integration into a network structure.
- verification of the proposed method – After the proposal of the new method, it has to be verified in simulations and experimental testbed to proof its benefits to wireless ad-hoc applications. For the simulations an appropriate simulation tool will be chosen. The testbed verification will be done with COTS products.

## 3 EXPERIMENTAL ANALYSIS OF LOCALIZATION

This chapter is devoted to the investigation and author's analysis of the localization in wireless networks. The basic assumption is that the localization is fully automatic and autonomous and the nodes are not equipped with any GPS receiver (except reference nodes that might have GPS receivers or some other way to obtain their position).

First, the two ranging methods (received signal strength and ultrasound measurements) are investigated in an experimental testbed and compared. Further, the method based on the received signal strength measurement is addressed and the exploration of its uncertainty presented. Regardless the ranging method, the impact of the ranging process (and erroneous distance estimation) on overall accuracy of the position estimation is discussed with the support of simulations and measurements. Moreover, the fading effect mitigation using frequency diversity is proposed and verified in this chapter.

[102]–[124] are the author's publications related to this chapter.

### 3.1 Analysis of ranging methods

Several methods for distance estimation (ranging) have been proposed and used. However, just some of them gained higher attention because of their viability in real applications. In this section, an investigation of different aspects regarding the most promising and most used ranging methods (RSS and ultrasound system) is presented and both methods are compared. First, we focus on the RSS ranging, then the ultrasound system followed by a comparison of both.

#### 3.1.1 Received signal strength method (RSS)

To investigate the RSS method of ranging, the following measurement scheme was designed. The measurement concept was proposed with the intention of general and commercial product independent investigation of localization using signal propagation. Therefore, the measurement was not affected by individual transceiver characteristics of different sensor nodes and can be repeated with any signal analyzing device. The measurement testbed was designed with respect to both indoor and outdoor scenarios.

The measurement testbed consists of two basic parts: a transmitter of a radio signal and a receiver of this signal. A microwave signal generator was used as a transmitter and the signal was received by a signal analyzer with a low-noise



amplifier connected to its input (Minicircuits ZX60-3011) to improve the receiver sensitivity. The generator transmitted the continuous harmonic signal with the frequency 2.478 GHz, zero span at the power level -20 dBm with both monopole omnidirectional antenna with ground plane (gain = 1 dB) and patched antenna (gain = 5 dB). The signal analyzer was connected via GPIB/USB interface to a PC to control, automate and process the measurements. The scheme of the measurement testbed can be seen in Fig. 3.1.

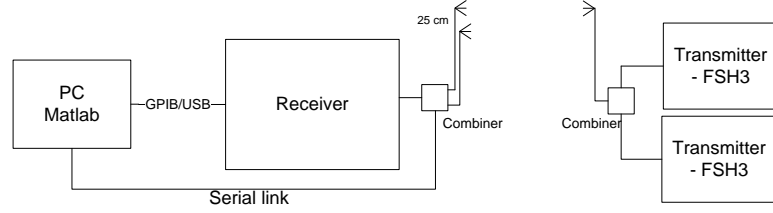


Fig. 3.1: Scheme of the experimental testbed for RSS measurements.

At the receiving side, with respect to common design of COTS products, the low noise amplifier was used to amplify the received signal before its processing. To power the amplifier 12 V power source and bias tee were used (see receiver scheme in Fig. 3.2).

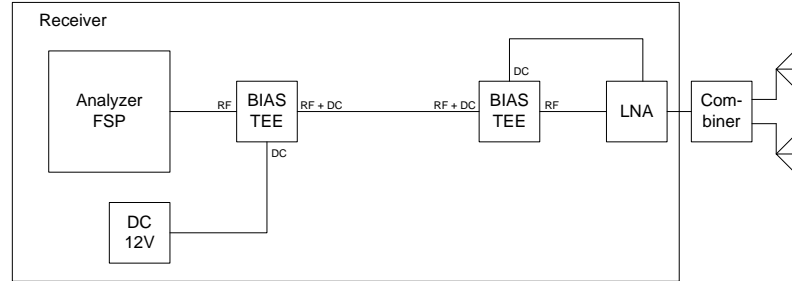


Fig. 3.2: The detailed scheme of the receiving part of the measurement testbed.

As commented in chapter 1 of this work the RSS measurement is significantly affected by uncertainty in radio channel. Thus, the measurement of the received signal power has to be performed several times at one place in order to obtain the value of power level from which the distance can be estimated. The one-place measurement consists of 10 individual measurements in a loop with a total duration of approximately 1 s.

The indoor measurement was carried out in a room with a tile flooring, plaster-board ceiling and concrete walls. The basic measurement scene consisted of measurement of the signal power level in 0.13 m steps up to 7 m since indoors we are

limited in space. Fig. 3.3 presents the results from the measurement. As commented before, at each point, ten individual measurements were performed.

Only the average value of the measurements is depicted in the figure. The regression function is calculated and displayed to show a general tendency of the received power with increasing distance. However, a significant ripple of the measurement is obvious. The decreasing tendency is caused by the path loss of the environment. The power changes observed at adjacent points of measurement are caused by fading effect and multipath signal propagation.

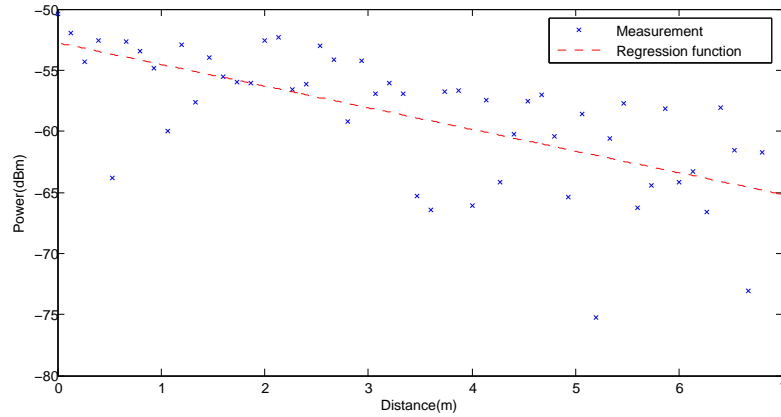


Fig. 3.3: Received signal power measurement – indoors.

The second part of the measurements was performed outdoors at the place surrounded by buildings but sufficiently faraway from their walls to avoid significant reflections. The surface was covered with small granite stones (see Fig. 3.4). The range of distances measured was larger since the distances between nodes used outdoors are longer. That is also a consequence of better signal propagation outdoors. The schema of the measurement was analogical to the previous one. The decreasing tendency of the received power is noticeable in Fig. 3.5. The ripple of the power is not so large compared to the indoor measurement. Similar to previous analysis, the regression (exponential) function was calculated and depicted.

From the presented results it can be concluded and confirmed that indoor environments are less stable and more prone to the multipath effect. Ground, walls, ceiling and other objects are sources of strong reflections and signal scattering resulting in more frequent and closely adjacent fading points.

Apart from the physical phenomena mentioned in the state of the art chapter, several system aspects have an influence on the signal propagation as well. Most of the proposed propagation models include these system parameters. For our investigation antenna heights and signal frequency were considered variable parameters of the system. First, the flat-earth signal propagation model was implemented into



Fig. 3.4: Measurement testbed.

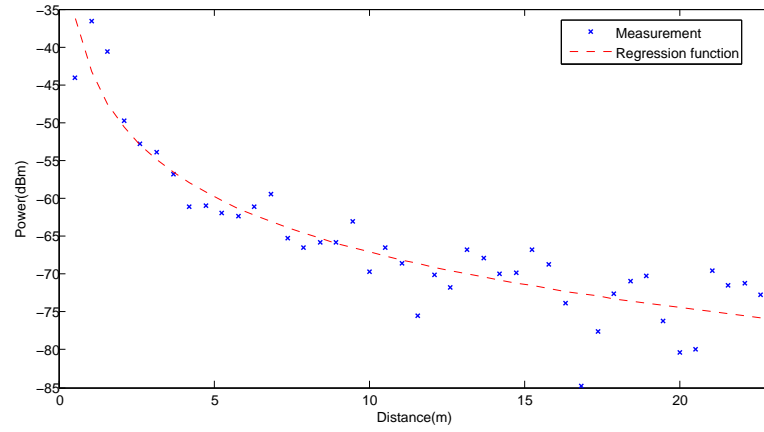


Fig. 3.5: Received signal power measurement – outdoors.

a simulation tool and then theoretical results compared with conducted measurements. The measurements were performed outdoors in previously described testbed scenario.

First, the influence of the antenna height was studied. Fig. 3.6 compares the simulated path loss on the ground reflection model using (1.19) with typical terrain characteristics at the 2.45 GHz ISM frequency band. Four antenna heights have been studied (0.15 m, 0.5 m, 1 m and 2 m) for both transmitter and receiver antennas. Only vertical polarization is considered since, in practice, dual-polarization antennas are not usually used in WSNs.

From performed simulations (Fig. 3.6), it is clear that the model works better for low antenna heights and large ranges. The number of fading points and their attenuation increase for low distances. From this point of view it is better to use low

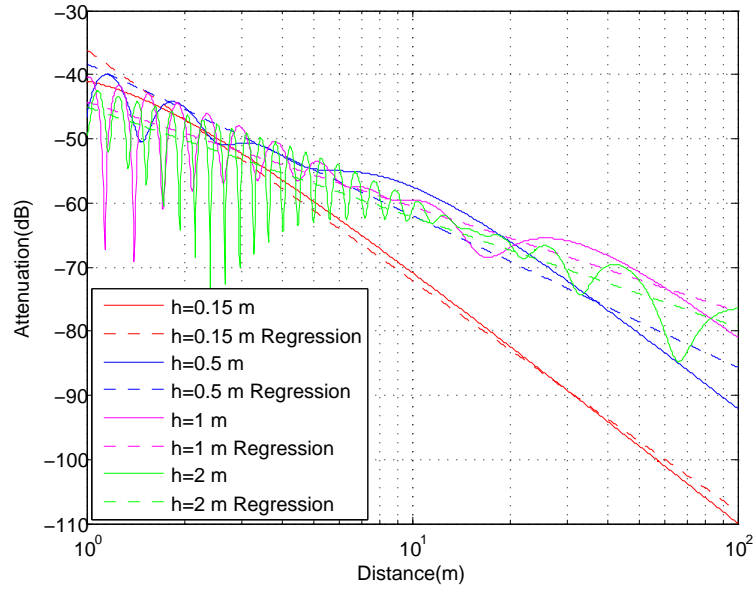


Fig. 3.6: Simulated path loss as a function of distance at 2.45 GHz with different antenna heights.

antenna heights for localization purposes which is rather typical in WSN applications. However, the attenuation increases due to partial cancellation between direct and reflected paths, thus, the received power reaches the receiver sensitivity (typically between -85 dBm to -90 dBm depending on the model and band) faster than when a higher antenna is used. Consequently, there is a compromise between the maximum range and the antenna height. Another effect of the interference between signal paths is that the positions of the fading points are separated at approximately half-wavelength for small incidence angles. Thus, the problems caused by multipath increase in the 2.45 GHz ISM band; however, this band is more interesting for communication purposes (such as ZigBee) than lower ISM bands because of the larger bandwidth available. In addition, for longer distances, more signal paths (for example reflection from walls) could explain certain large fading points that take place at about 4 m distance.

Although a flat-earth model may be suitable for outdoor systems, it is too simple for indoor systems because it does not take into account other reflections which can be significant for interference. Nevertheless, despite these limitations, the flat-earth model can help to understand some trends. In order to compare with theory, results of conducted measurements in the 2.45 GHz ISM band are presented in Fig. 3.7 for four antenna heights.

Signal wavelength is another parameter considerably influencing the signal propagation and power loss. Signal wavelength directly corresponds to frequency which

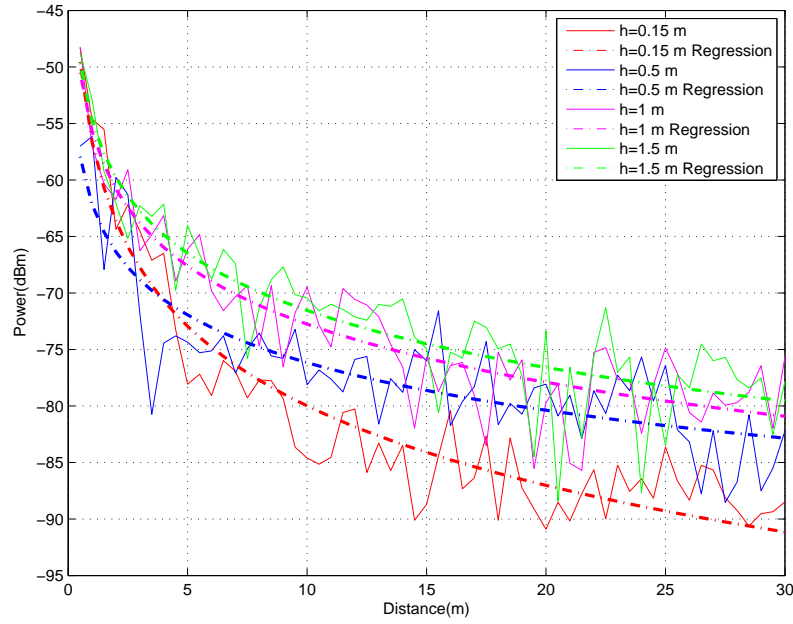


Fig. 3.7: Measured received power as a function of distance at 2.4 GHz and different antenna heights.

is for most commercial applications restricted to ISM frequency bands. A comparison of the two frequencies and their influence on the signal propagation is depicted in Fig. 3.8. Moreover, frequency 867 MHz is added for comparison with the signal propagation in another often used frequency band. One can see that propagation characteristics differ significantly comparing different frequency bands but just little within the 2.4 GHz band. Nevertheless, it is worth noticing that the fading points occur in different locations when using different frequencies even within one frequency band.

To see how these frequency differences are remarkable in reality, several measurements were conducted. The measurements took place in the same testbed and the received power was measured several times at each distance from the transmitter. The results were averaged. Measurements with several frequencies and with various antenna heights were performed. For lower antenna heights the attenuation was larger as already verified previously. The differences in used frequencies are not very obvious in Fig. 3.9 since the measurements were taken in larger steps than are the distances of fading points. However, it can be noticed that when one signal is in a local minimum (possible fading point) the other is not. This key point will be discussed further in the chapter in more detail.

Now, let me evaluate the distance estimation using the RSS method. Radio channel and its model are closely related to the particular environment and the

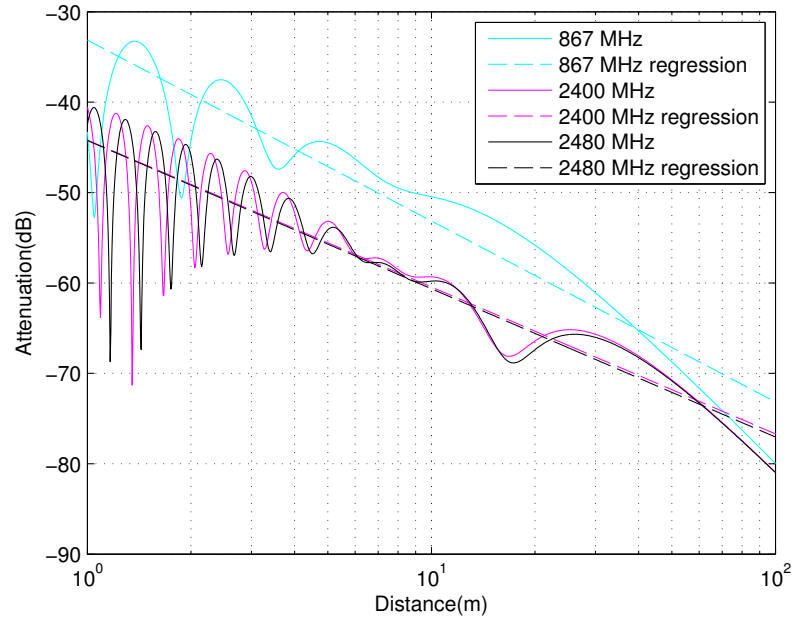


Fig. 3.8: Comparison of simulated signal propagation with different frequencies.

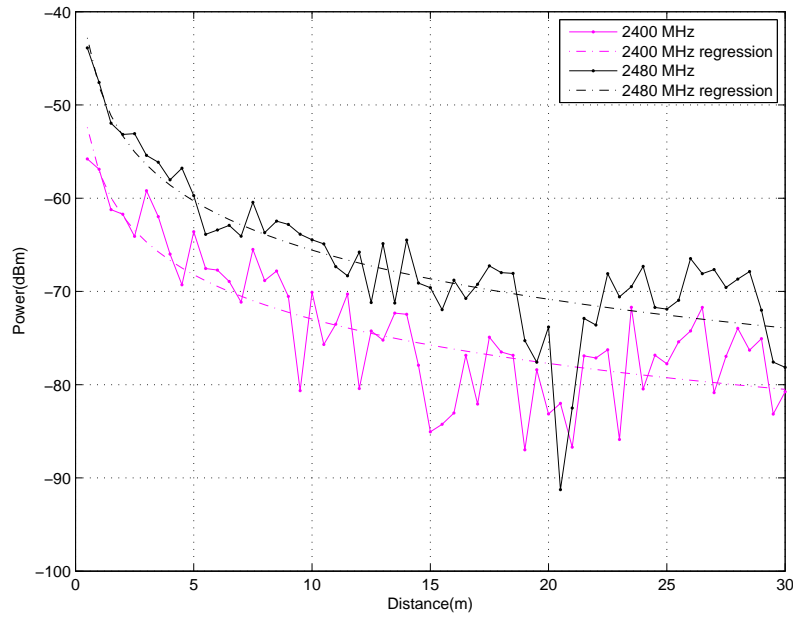


Fig. 3.9: Measured received power as a function of distance with different frequencies and antenna height 2 m.

placement of communicating nodes. In the performed experiment the flat-earth model was used and adjusted based on the values measured between two given nodes. This way we got parameters of the flat-earth model which fit best to the particular radio channel. To explore the accuracy, we conducted ten in-place mea-

measurements at each determined point between the nodes and calculated the mean value. The difference of the mean and the flat-earth model value gives the error of the estimation. For better understanding relative MAE (MAE) is used. See the results in Fig. 3.10. Most of the errors are up to 30–40 %. However, in the range from 20 to 25 m the error is reaching 100 %. At one point the measurement gives a totally wrong position. Particularly in this case the error is about 320 % and it is necessary to employ a certain procedure to eliminate this false estimation. The results confirm the experiment performed by Whitehouse et al. [94] that the RSS based estimation method can be used only up to a certain part of the radio range and not in the entire range.

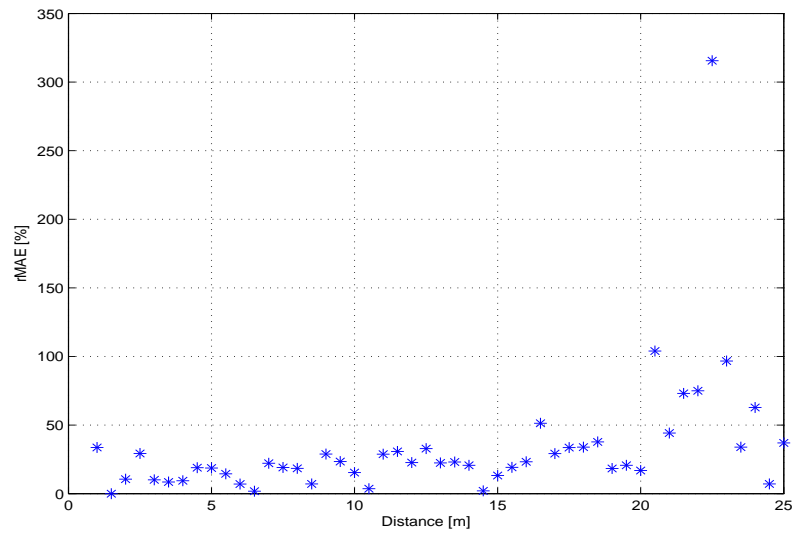


Fig. 3.10: Error of the distance estimation using RSS method in outdoor measurement.

The previous measurements were performed in order to investigate basic characteristics of a radio channel, the impact of the RSS uncertainty, the difference of the signal propagation in both indoor and outdoor environments and the influence of obstacles with relation to the possibility to use received power to estimate the distance between a transmitter and a receiver. The measurement was focused on the signal propagation without considering any influence of sensor node hardware. The next step in the research was aimed to investigate the estimation of the distance with COTS network devices. Therefore, sensor nodes were employed in a new set of measurements. The scenario consisted of two programmed nodes, one in the role of a transmitter, the second one as a permanent receiver, which represented also a gateway forwarding data to a data processing application executed on a stand-alone station. IRIS nodes from Crossbow were used for this purpose. The nodes transmit in ISM 2.4 GHz ISM frequency band with the sensitivity threshold -92 dBm. To

explore the radio channel, the receiving sensor node measured the signal power at different distances. Because of the uncertainty in the channel, the node repeated measurements several times at each distance. The algorithm implemented in the transmitter sent twenty packets at each distance consecutively. The transmitting cycle was repeated at all power levels. There are 16 RF power levels used in the AT86RF230 radio transmitter. The power detection in a sensor node is defined in IEEE 802.15.4 standard and the process is started with the reception of SFD (Start Frame Delimiter). The first experiment was conducted indoor in the building corridor with a width 2.2 m and a height 3 m. Both transmitter and receiver were placed at the axis of the corridor at the height of 0.8 m, the corridor was empty without any movable obstacles. The measured distance range is up to 40 m. The measured received signal strength for the transmitted power 3.2 dBm can be seen in Fig. 3.11.

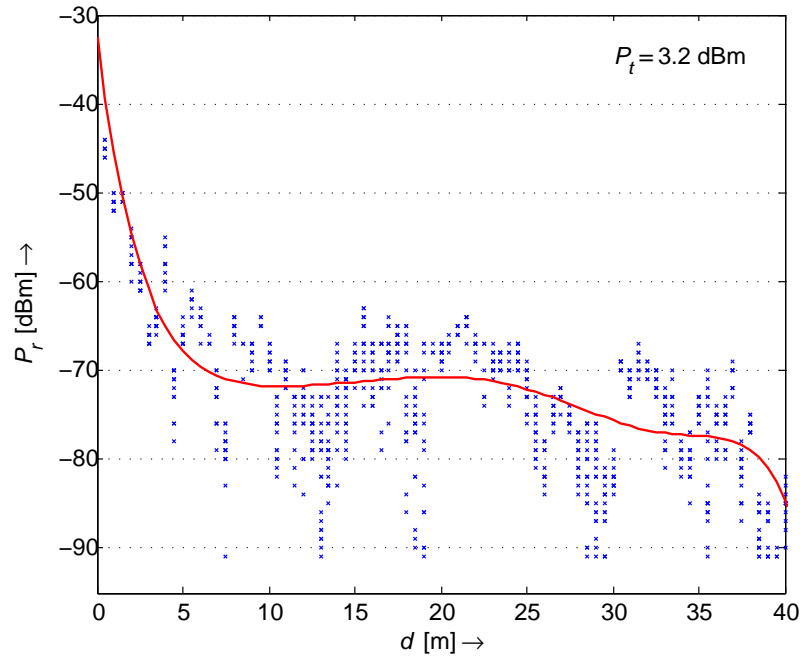


Fig. 3.11: Received signal strength indicated by receiver ( $P_t = 3.2 \text{ dBm}$ ).

The descend of the signal strength with increasing distance is obvious. The descend can be approximated as logarithmic. The fitting function is approximated based on the mean of the set of 20 measurements at each distance. From the figure, maximum indoor range can be determined. It is about 40 m with maximal transmitted power  $P_t = 3.2 \text{ dBm}$ . The coverage range decreases up to around 25 m when the lowest  $P_t$  is used ( $P_t = -17 \text{ dBm}$ ).



### 3.1.2 RSS uncertainty

The radio channel and its characteristics contribute the most to the erroneous distance estimation based on RSS. As previously presented, the channel can be approximated by a radio channel model. Unfortunately, channel modeling is very complex and mostly inaccurate due to specific environment conditions. To improve the model, it must be tuned by various parameters adjustment reflecting a particular environment. Often, a demanding channel scanning and mapping has to be conducted in advance to obtain a more accurate model. The characteristic of radio channel depends on several physical factors such as weather conditions, ground surface, obstacles and their position, material, shape etc. Those factors represent relatively stable conditions, and thus, they can be successfully modeled. On the other side, a certain variation of signal strength was observed during measurements. Those are caused by time unstable factors such as moving objects or interfering radio signals. Besides these factors, distance estimation based on received signal strength depends also on sensor node hardware (especially transceiver). Hardware imperfection or different scaling of received power can influence the investigation, therefore, the concept of the first set of measurement scenarios was proposed with the intention of general and commercial product independent investigation of radio channel for the localization purposes with general signal generator and signal analyzer. Hence, the measurements were not affected by individual transceiver characteristics of different sensor nodes, energy level of batteries and they can be repeated with any signal analyzing devices. On the other side, without any doubt, measurements of signal strength and the distance estimation are performed at COTS device, sensor mote with certain hardware characteristics. To meet the real conditions, the measurements with sensor motes were carried out as well. This section therefore addresses two basic measurement approaches; measurements performed with general signal generators and signal analyzer and measurements with IRIS sensor motes. Both measurements were done in 2.4 GHz ISM band.

For the first set of measurements, both indoor and outdoor experiments were considered. Fig. 3.12 presents the results from the indoor measurement. At each point, ten individual measurements were performed. The minimum, maximum and average value can be seen on the left in the figure. The considerable ripple along the distance is caused by large scale fading effect and multipath signal propagation. The uncertainty of the measurements at each distance can be better seen in the right side of the figure. Standard deviation (STD) of measurements is slightly increasing but it does not exceed 1 dB in most cases.

The large ripple of the measured values implies the difficulties in usability of such a measurement for the distance estimation. Although the regression of the

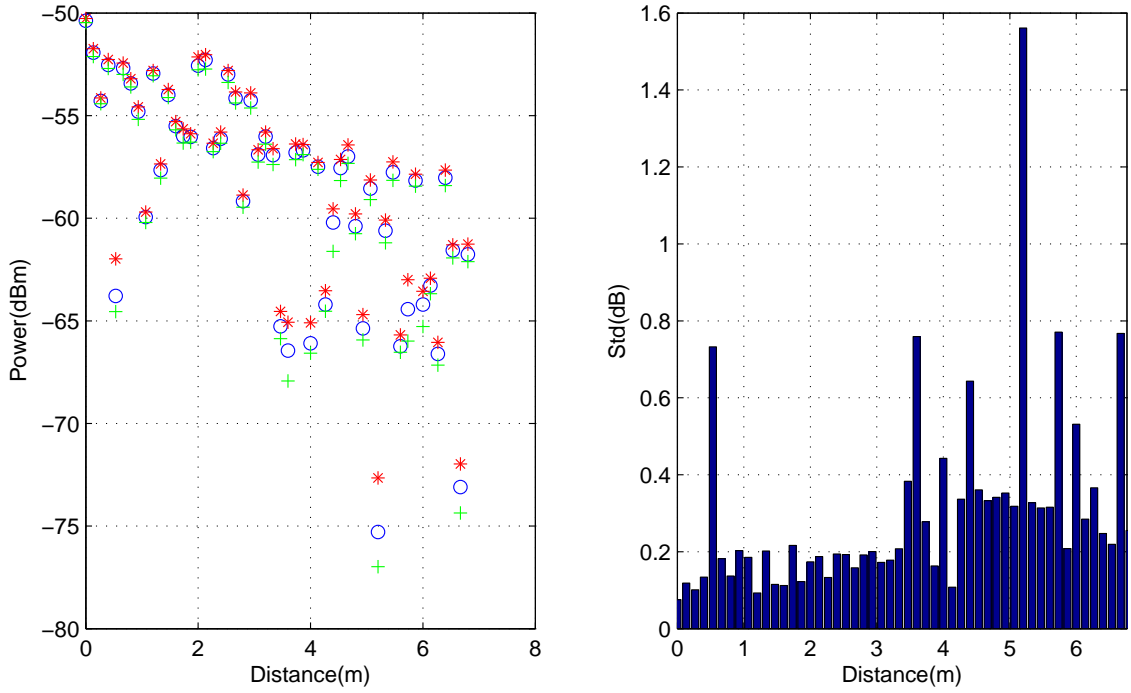


Fig. 3.12: The power levels and standard deviation of RSS indoor measurements at different distances. The minimum (green +), maximum (red \*) and average (blue o) value of each in-place measurement are depicted.

measured RSS values is slightly decreasing with the distance from the transmitter, the character of the measurement causes that a particular measured value (which can be called snapshot) cannot be used for the reliable distance determination. The standard deviation up to 1 dB is negligible in comparison with high fluctuation of adjacent measurements.

To investigate the influence of obstacles between the transmitter and the receiver, we placed wooden objects in the path of ground reflected signal. The intention was to change the radio channel and the multipath propagation. However, the results were not significantly different, and thus, the graphs are omitted.

After the indoor measurements, the experimental testbed was moved outside onto a plane ground with no obstacles between the signal source and the receiver. The received signal power with the minimum and maximum values for each in-place measurement and standard deviation of these measurements can be seen in Fig. 3.13.

There is an expected decreasing tendency of RSS without a great variance. The decrease is sharper at shorter distances whereas more gradual at larger distances. If we have a look at the figure depicting standard deviation we see its exponential increase which reaches up to 2.5 dB at distances of 20 m.

Similar observation can be done by having a look at the RSS uncertainty of the

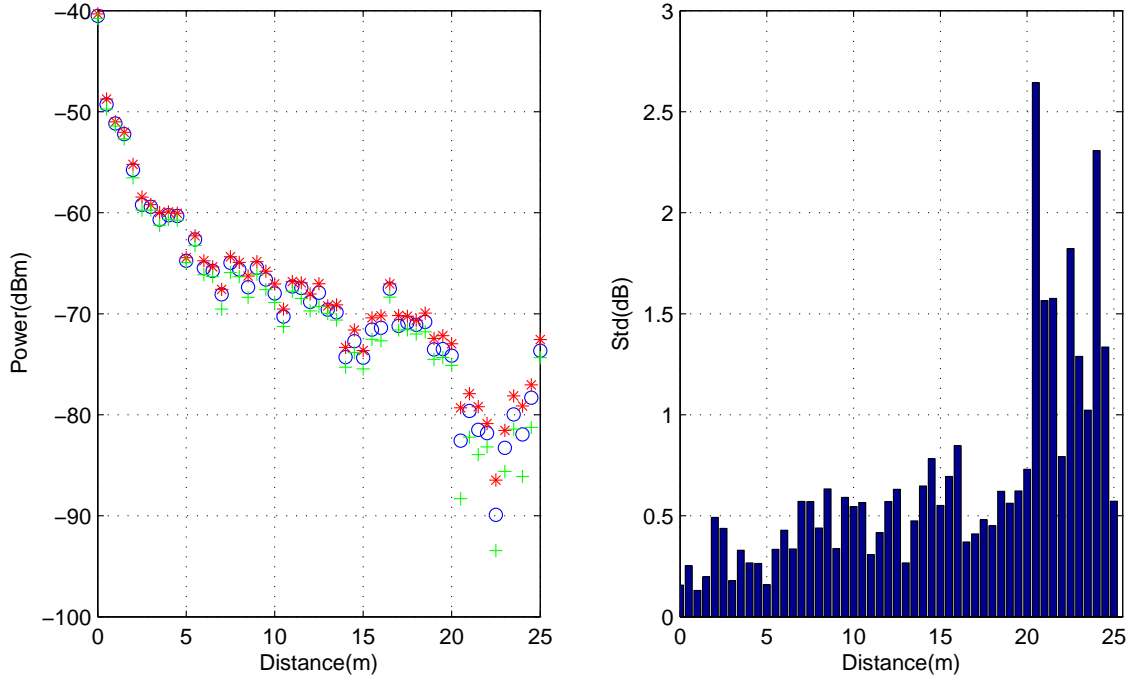


Fig. 3.13: The power levels and standard deviation of RSS outdoor measurements. The minimum (green +), maximum (red \*) and average (blue o) value of each in-place measurement are depicted in the left part of the figure.

measurement with IRIS nodes. Fig. 3.11 indicates the variance of received signal power at each distance. Twenty samples were taken consecutively in the time interval of less than 1 s. In some cases the absolute difference of minimum and maximum measured value is about 20 dB. That, off course, significantly affects the results and estimated distance. The uncertainty can be better seen in Fig. 3.14. One can notice that standard deviation, and thus, the RSS uncertainty is even higher for experiment with COTS nodes. At some distances the standard deviation of the measurement reaches almost 9 dB. The mean of standard deviations for all the measurements is almost 2 dB.

It can be concluded that both sets of measurement (generic and COTS based) show the significant variance of consecutive RSS values. The standard deviation is about up to 2.5 dB for generic and up to 9 dB for measurement with IRIS nodes. The uncertainty is more considerable outdoors than indoors. It confirms the assumption that the fast fading has more significant impact outdoors because of the higher dynamics of the electromagnetic field. The static obstacles did not have a noticeable influence on RSS variance. Variance increases with a distance in generic measurements but the same was not experienced in COTS measurements. The variance was rather unpredictable which complied with its stochastic character influenced, besides

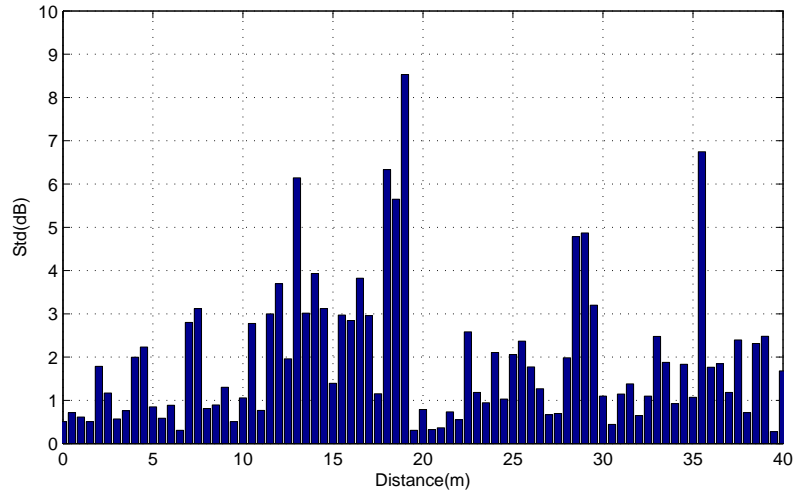


Fig. 3.14: Standard deviation of indoor measurement with IRIS nodes.

other, by the interference with other wireless communication and EM emission. The coexistence of various radio technologies is described in the following subsection in more detail.

### 3.1.3 Ultrasonic system

To compare the RSS method with another ranging technique, the method based on an ultrasonic system was chosen and investigated. In particular, a Cricket system was the tested COTS product. In fact, not only ultrasound signal is used in this system but both – electromagnetic and ultrasound signal. The system is based on the time difference measurement. However, unlike the TDOA method it is the difference between the radio signal and the ultrasonic pulse from one transmitter. The method is based on different speed of propagation of both signals. The speed of RF signal is almost constant, close to the speed of light in vacuum but the speed of sound waves changes and it is dependent on the environment characteristics (density, pressure, temperature etc.). Therefore, the calibration and corrections are necessary.

It is a promising method since it avoids the necessity of time synchronization among the nodes. The more detailed description of the system principle can be found in chapter 1.

In order to confirm accuracy (3–5 cm) and variance of measurement reported in [51], an appropriate measurement testbed was designed and several experiments carried out.

Cricket is designed to be an inexpensive device using off-the-shelf hardware parts in order to cut down the price of the units. The transmitter (called beacon in the Cricket system) is composed of a 8-bit RISC AVR processor Atmega644 running

at 10 MHz with internal flash, SRAM and EEPROM memories [87]. It uses a low power resonate-based RF transmitter and a single-chip RF receiver operating in the unlicensed band of 418 MHz [88] with amplitude modulation. Ultrasonic transmitter operates at 40 kHz.

In addition, the listener has got an ultrasonic receiver with a single-chip tone detector. It is equipped also with a TTL to RS-232 signal converter for communication with a host device, e.g laptop or camera, printer etc. Cricket is designed to be a low powered device with minimal energy consumption which is 12 mA (authors of [89] state that Cricket dissipates 15 mW during normal operation) in the active state and 0.6 mA in standby. Low consumption is achieved by changing the internal clock and reducing the power to the certain peripherals. The Cricket modules are powered by a 9 V battery.

The range of communication of Cricket nodes is determined by two main factors. First, the transmitting power of the radio signal is not adjustable, and thus, the range for the used power level is up to 12 m. The other limitation of the maximum coverage is determined by the transmitting power of the ultrasonic transmitter (up to 10 m) and the nature of boundaries for the ultrasonic signal. The natural character of the ultrasonic signal propagation limits its coverage to a bordered area since the signal is not able to overcome walls and big obstacles. On the other hand, this aspect can be advantageously used for certain applications where room granularity is the requirement [89].

The quality of the ultrasonic signal reception is highly dependent on the orientation of the ultrasonic receiver in relation to the ultrasonic transmitter. The transmitter has characteristic strong directional radiation pattern and the same applies to the receiver. The first measurements were designed to avoid this factor of positioning and we considered the ideal conditions of straight oriented nodes. The nodes – beacon and listener – were placed in line-of-sight positions and the measurement of the distances between them was conducted for different ranges. Measurements were performed in both indoor and outdoor environment without obstacles; indoor in a long corridor (the temperature about 20° Celsius) and outdoor in a free-space with surrounding temperature approximately one degree below zero. See the results in Fig. 3.15.

You can see in Fig. 3.15 that there is no big difference between indoor and outdoor measurements. The ideal case of a precise distance estimation is depicted by the dashed line. Twenty measurements were collected at each distance in order to investigate the variance of the measurement as well. As it is noticeable from Fig. 3.16 that the standard deviation (STD) of the measurement is very low and in most cases below 5 cm. Only at the distance of approximately 6 m the STD is higher because of random negative effect during the measurement. The value at the

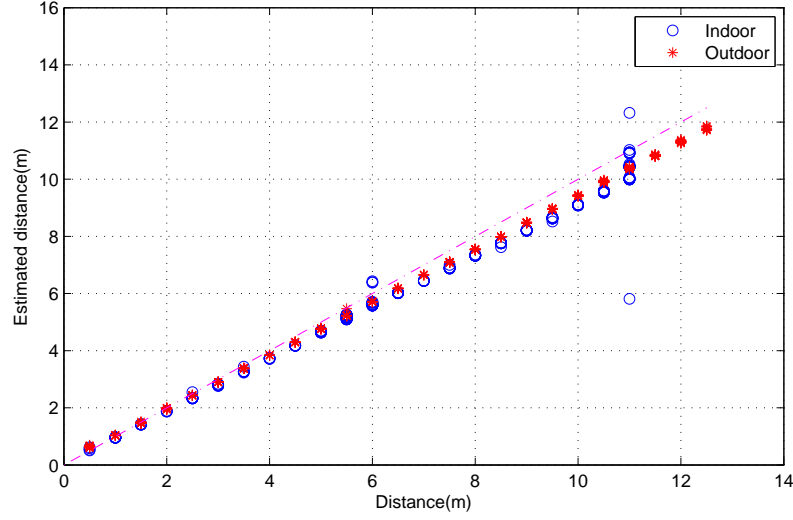


Fig. 3.15: Estimated distance for both indoor and outdoor environment.

end of the range (10 m) was omitted because of unreliable connection at the edge of the coverage range which caused loss of a lot of packets and consequently resulted in a high variance of the measured values. The difference between the outdoor and indoor case is also almost negligible omitting slightly higher values indoor at several distances.

The error of the estimated distance with the Cricket system can be expressed with the mean absolute error (MAE). MAE for each measured distance is presented in Fig. 3.17. In both cases (indoor and outdoor) the error is almost linearly increasing. We can also easily conclude that MAE indoors is in most cases higher than outdoors and reaches up to 90 cm at the distance of 10 m from the beacon (compared to an outdoor error of about 60 cm at the same distance). In other words, the measurement accuracy with the Cricket system is up to 6 % outdoors and 10 % indoors.

Now, we can evaluate and compare both methods – the ultrasonic and the RSS method. Published accuracy of the positioning stated in [51] is between 1–3 cm in the real deployment for the Cricket system. Referring to our results, this promising accuracy can be achieved only in short ranges and with a higher number of beacons. The accuracy achieved in our measurements, both indoors and outdoors in almost ideal conditions, is up to 10 %. Which means the error can reach up to 1.2 m at the edge of the coverage range outdoors, respectively 1 m indoors.

That is still a very good estimation comparing it to the RSS method where the error reaches 40 %. Therefore, we can conclude that the ultrasonic system features much better results with lower variance. However, one thing has to be highlighted. The measurements were performed under almost ideal conditions with the ultrasonic transceiver and the ultrasonic receiver oriented to each other which is the best case.

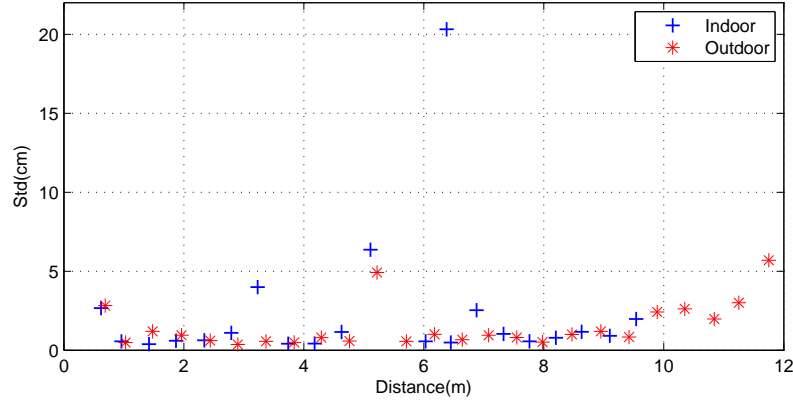


Fig. 3.16: Standard deviation of both indoor and outdoor measurement (20 values measured at each point).

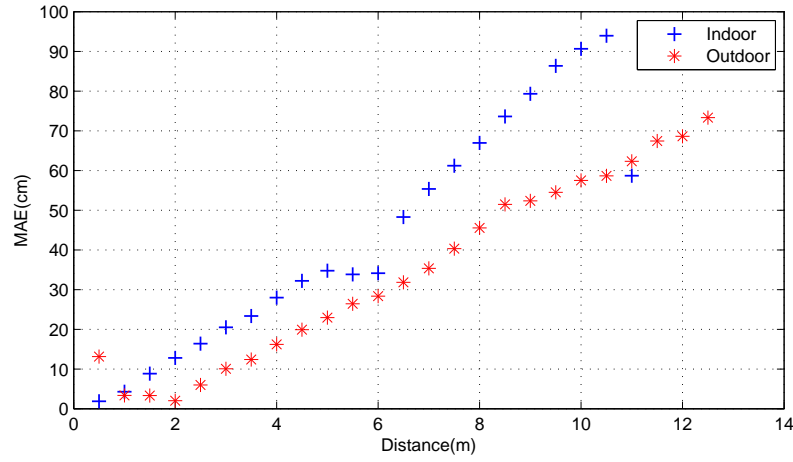


Fig. 3.17: Mean absolute error of distance estimation.

In real situation this is not always the case. The ultrasonic system is also limited to an unobstructed area or the area of one room since sound wave cannot pass through walls and big obstacles. In a nutshell, the Cricket system can achieve a good accuracy but only under certain conditions. Therefore, the usability of this system for a complex localization in wireless ad-hoc networks or localization support has to be carefully considered and further investigated.

## 3.2 Impact of ranging on position estimation

Ranging is a preliminary step to each range based localization algorithm. During the ranging phase necessary input parameters are obtained. Those are taken, processed by a certain localization algorithm and result in position estimation. This

work focuses on the distance ranging and its importance for localization. Therefore, this section presents the influence of distance estimation on the overall position calculation.

First, the impact on the lateration, one of the basic methods of range-based localization algorithms, is shown. The simulations are conducted with 400 nodes in a grid topology. For the evaluation GER and MAE error evaluation methods were used. Furthermore, the lateration was used to investigate the influence of the RSS uncertainty and its mitigation on the accuracy. For that purpose the experimental measurements were conducted.

Next, the investigation of influence of ranging inaccuracy on the complex localization algorithm is presented. The Anchor-free localization algorithm (AFL) is used for this purpose. The node deployment is random and the topology includes 300 nodes.

In the last subsection, a position estimation based on real measurements is presented. Two algorithms (Least Square algorithm and Weighted Centroid algorithm) process measurement results and estimate a position of an unknown node in the testbed scenario. Moreover, a novel method of ranging based on the frequency diversity is introduced and adapted by the two algorithms. A comparison with traditional approaches is given as well.

### 3.2.1 Position estimation using lateration

Lateration is a basic method of position estimation in range-based algorithms. It uses distances of unknown node to anchors to calculate the position. The minimum number of anchors in the range of the unknown is three to uniquely identify the most probable position. In extensions of the method, additional nodes can be considered. Then, it is referred to as a multilateration. To demonstrate the prime impact of the ranging error on the position estimation simulations in Matlab were conducted. The grid topology with 400 nodes was used. Each node in the network has a distance estimation to all the three anchors (represented by larger dots in the figure) disrupted by ranging error  $\epsilon_r$ . The topology and the result of the trilateration with  $\epsilon_r = 10\%$  are displayed in Fig. 3.18.

The left part of Fig. 3.18 represents the node deployment (black dots) and the final position estimation (red asterisks). The right part is a colored representation of the absolute position estimation error. One can notice that the error is not equally distributed but depends on the mutual arrangement of the unknown node and anchors. A more detailed study of this issue and its effect on the Map-growing algorithm was published in [107] and [108].



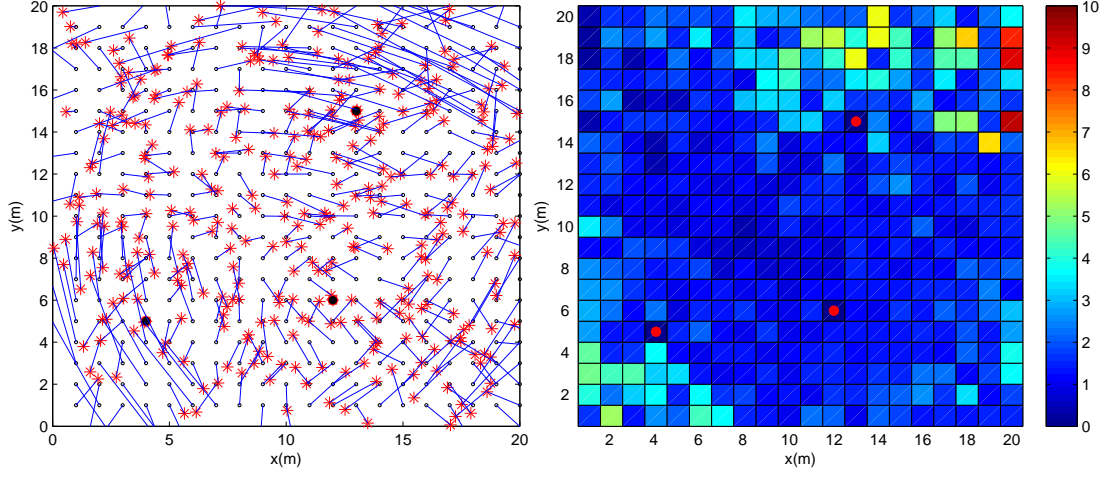


Fig. 3.18: Trilateration result with  $\epsilon_r = 10 \%$  in a field 20 x 20 m.

An investigation of the ranging error effect on the position estimation in the presented topology was conducted. The ranging error  $\epsilon_r$  is continuously increasing and the evaluation is done by means of MAE and GER. The results can be seen in Fig. 3.19

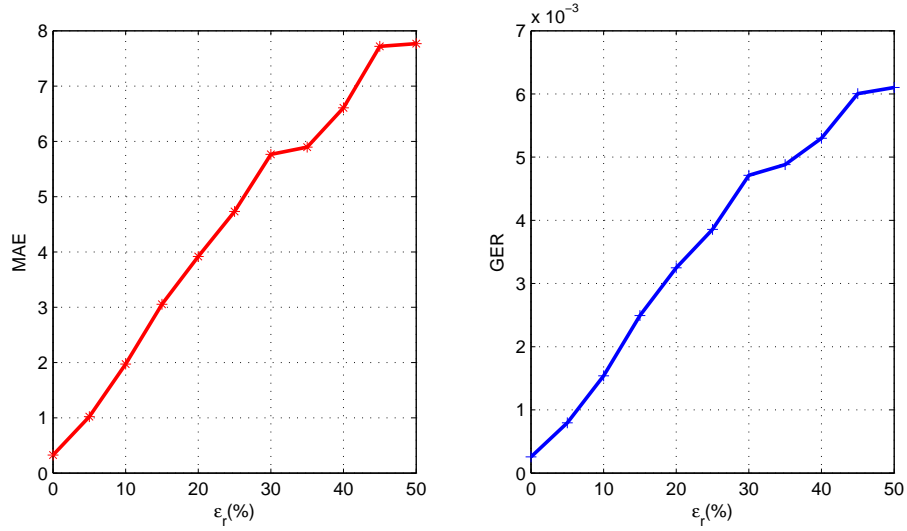


Fig. 3.19: Impact of ranging error  $\epsilon_r$  on the trilateration.

Both MAE and GER are sharply increasing with the increasing value of the ranging error. Therefore, it is highly important to minimize the error in ranging process in order to keep the position estimation error as low as possible.

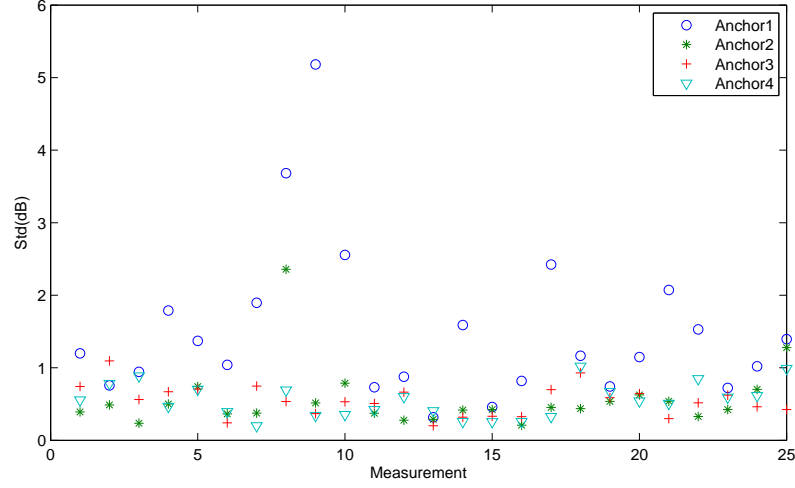


Fig. 3.20: Standard deviation of RSS measurements at 25 locations.

### 3.2.2 Experimental measurement focused on RSS uncertainty

To examine the influence of the RSS uncertainty on the accuracy of localization and to relate it to the consumed energy, the RSS value derived from a different number of sample measurements was taken and processed by a localization algorithm resulting in the position estimation. The complete work can be seen in [129]. Here, the main focus is on the impact of RSS uncertainty on the coordinate estimation.

All measurements were performed outdoor in a square area without obstacles. The presence of other wireless networks was significant. Therefore, to minimize their negative effect, the measurement frequencies not colliding with the 802.11 channels in the surroundings were chosen.

The link and environment characteristics with the path exponential loss were calculated from the initial measurements and the flat earth propagation model (see Section 1.1.4). Then, RSS measurement was performed at 25 points. At each point, 10 single values of received power were collected to calculate the mean, which is then used for distance estimation. The level of variance (expressed by standard deviation) at each point and for each anchor can be seen in Fig. 3.20. The deviation for the majority of anchors is mostly less than 1 dB. However, the radio channel for anchor 1 is worse and more prone to the effect of RSS uncertainty and that is why the level of variance is larger than in other cases.

Fig. 3.21 presents an example of three measurements performed at various points in the area. For the purposes of multilateration, distances between the receiver and the anchors were calculated from the mean of measured samples. Each point in the graph (+) represents the calculated position obtained from a different number

of samples in the dataset (indicated by the adjacent digit). The dataset ranges from 2 to 10 samples. The coordination system in the figure is set according to our experimental arrangement. The experimental testbed was placed in a field of 16x16 m with the anchor nodes located in the vertexes of the virtual square. All units in the figure are in meters. On the left side of the figure, there is the area of the experiment and circles representing the estimated distance after each measurement. The anchor nodes in the vertexes are not pictured. On the right side, the calculated position with a larger scale can be seen. Each position is the result of multilateration using a different number of measurement samples.

From the progress in position determination on the right side of Fig. 3.21 it is noticeable that with more samples the estimated position inclines to a certain position with decreasing steps. All three examples consider four anchors for multilateration. One can notice that the radio channel from one of the anchors suffers from a large uncertainty and in the example at the very bottom the power level circles are even out of the focused figure part.

Ideally, the estimated position is located in the intersection of the circles. However, because of the channel model imperfection and RSS uncertainty, the circles do not intersect at one point. Therefore, the estimated position is determined as the point with the least error to all the anchors.

Another performed experiment consists of 25 measurements at very close positions (only a few centimeters apart). Each measurement is composed of 10 samples. Fig. 3.22 combines all measurements and shows the position calculated using different number of samples (as in Fig. 3.21). As can be seen in Fig. 3.22, the calculated position converges in a smaller area with an increase in the number of samples considered (5–10). Positions determined with only two, three and four measurements are considerably far away from the position determined by measurements with more samples. Again, the figure represents a part of the experimental area.

To express the relation between measurements with different number of samples, the final estimated position is taken as the most accurate and the absolute error of each measurement is calculated in relation to the final position. The calculated absolute error is for measurements with different number of samples displayed in Fig. 3.23. The error is calculated for the mean value of performed measurements ( $N$ ). It is obvious that the error is decreasing with the number of taken samples. First, the decrease is steeper and then the error differences are smaller. Furthermore, there is also an energy consumed during the communication depicted in the figure. Obviously, the energy consumption increases according to the number of measurement samples taken.

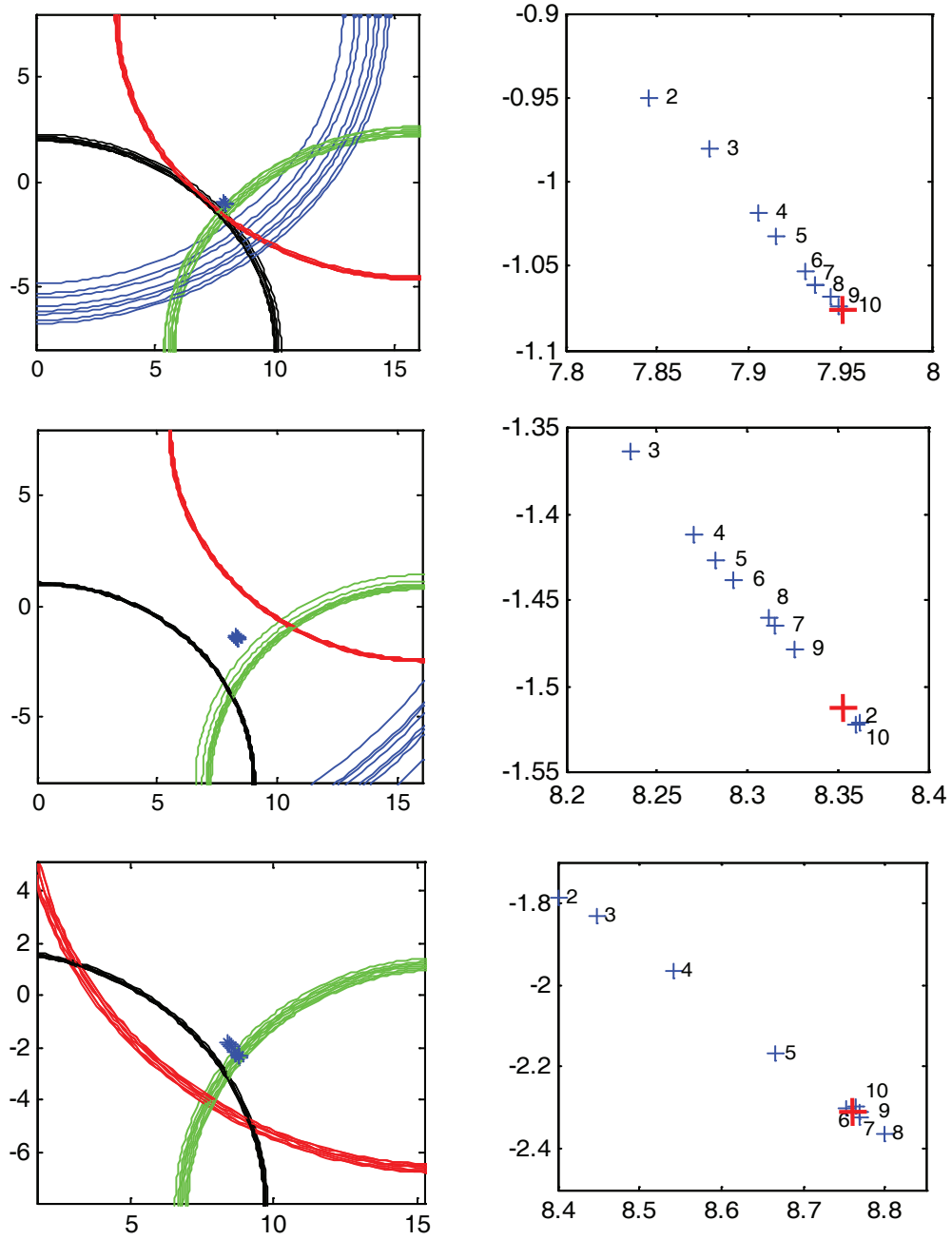


Fig. 3.21: Example of three measurements at three different points. In the left column, there are determining multilateration circles and the right side is focused on position calculation using a different number of samples. All units are in meters. The red cross shows the real position of the sensor.

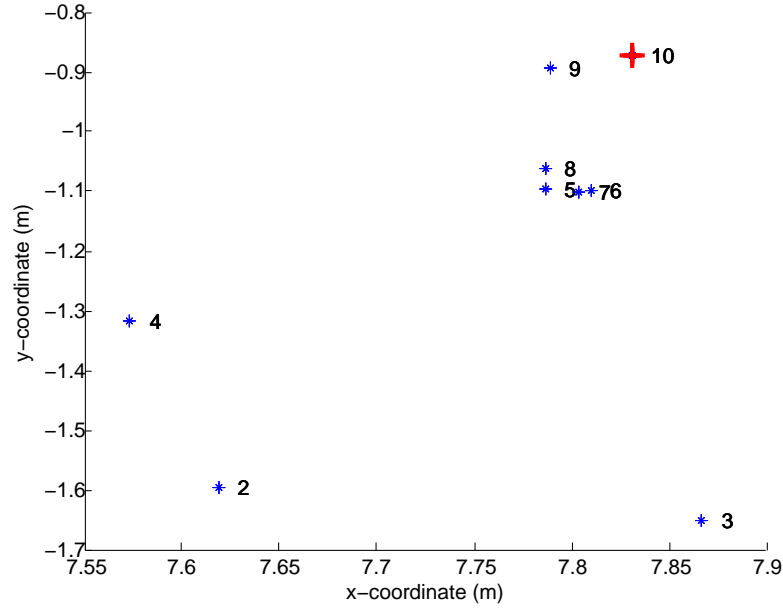


Fig. 3.22: Overall position estimation as a function of the number of samples taken at each point. The total number of measurement points was 25.

### 3.2.3 Anchor-Free Localization

For the investigation of the impact of ranging method on position estimation several localization algorithms can be used. The Anchor-free algorithm (AFL) was chosen as a representative of fully autonomous algorithms used in distributed networks without a fixed infrastructure. The AFL algorithm was implemented as described in chapter 1 based on the [24].

As mentioned in the detailed description, the AFL exploits HC (hop count) metric for distance estimation employed in the first phase of reference node selection. This metric has the advantage of having an insensitivity about the range errors but produces an inaccurate initial layout with a large GER error. To improve the accuracy of initially estimated layout the use of a widely known distance estimation method RSS in the first phase was suggested. It is further referred to as SS (Signal Strength) method. In addition, weighting procedure of SS was proposed further referred to as WSS (Weighted Signal Strength) that was compared with the two previously mentioned methods.

To investigate the distance estimation methods' performance a Matlab version of the AFL algorithm (from this point on it is referred to as AFL-M) was implemented (details can be found in [117]). For user-friendly interpretation of research results, a web-based Java Positioning Simulator for Wireless Sensor Networks was designed [92], [126]. It evaluates the performance of the the AFL-M with different distance

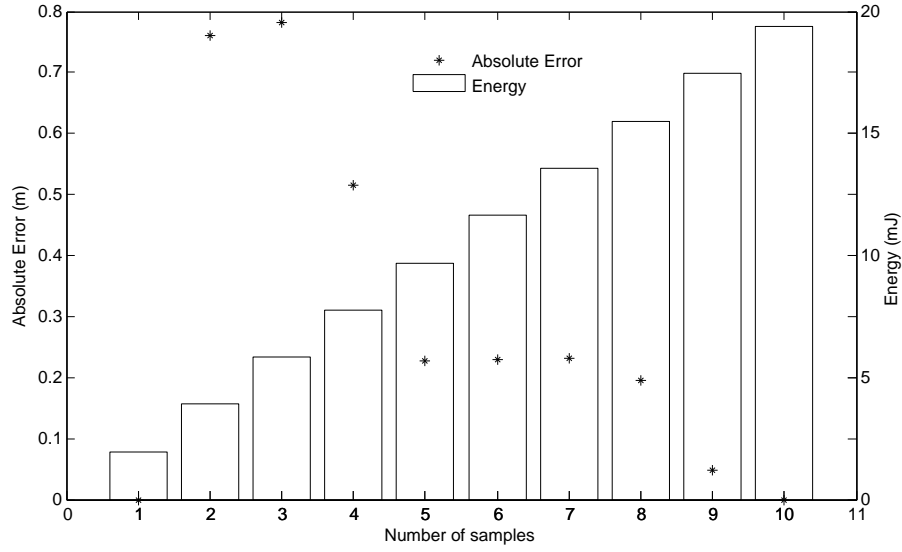


Fig. 3.23: Expended energy and mean of absolute error of estimated position with different number of samples.

estimation methods based on a localization error and energy metric. The simulator allows various simulation settings. First, a sensor node hardware specification has to be introduced. Then, the simulator incorporates a setting of noise parameter of network environment  $\varepsilon_r$ , topology definition (e.g. number of nodes, degree of nodes, general shape of the topology) and the type of the ranging method. The evaluation is expressed by global error ratio metric (GER). For envision, the GER value of the AFL algorithm introduced by [24] is 0.0006.

The influence of a ranging error was investigated to find out how the localization result is affected by a noisy environment (Fig. 3.24). Each value was obtained by averaging 100 simulation results of randomly deployed networks with the size of 300 nodes and node degree of 12. From Fig. 3.24 an important range error threshold that affects SS method performance can be obtained. Hence, if the network has  $\varepsilon_r < 12\%$  the SS method performs well and produces a layout with average GER of  $1 \times 10^{-3}$ . For more noisy environment with  $\varepsilon_r > 12\%$  the WSS method outperforms the SS method whose GER increases slightly gradually in contrast to SS whose GER progress has a rapid increasing behavior with increasing range error values. However, as the  $\varepsilon_r$  exceeds 25% the both SS and WSS methods produce less accurate results than common approach HC using the hop count metric. The GER of HC approach is  $1.5 \times 10^{-3}$ , is constant and it is depicted by dashed line. This value is exceeded with WSS approach when  $\varepsilon_r > 25\%$ .

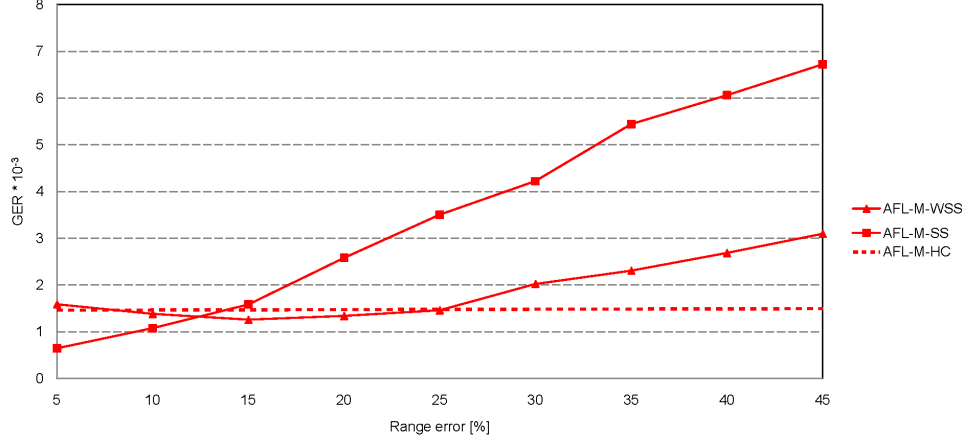


Fig. 3.24: Dependence of anchor-free localization error on the ranging error.

### 3.2.4 Frequency diversity for ranging optimization

Distance estimation based on RSS measurement has to overcome several negative phenomena as shown in the previous sections. In this subsection, the impact of ranging on the position estimation with Least Square (LS) and Centroid algorithm is shown. To improve ranging a novel method to mitigate the fading effect caused by negative interferences of the multipath signal propagation is proposed. Use of more than one measurement frequency is suggested for that purpose.

The investigation of the new method is conducted using simulations based on the a priori measurements in real outdoor environment. The measurements were used as an input for creating a radio channel model. Then, this model was used in both algorithms as a reference model to estimate distances to each anchor. The work described in more detail has been published in [123] and [124].

Since the fading amplitude is frequency dependent, the maximum and minimum positions depend on the polarization (for a given frequency band). Thus, polarization diversity can be effectively used to combat multipath channel fading as well. However, polarization diversity is not often used in WSN because of the hardware limitation. Therefore, the frequency diversity method is a method overcoming this limitation. Several frequency channels are usually available in WSN (16 channels in 2.4 GHz ISM band [93]); if the frequency spacing used for RSS measurement is larger than the coherence bandwidth of the channel, these measurements are uncorrelated [62]. The coherence bandwidth determines the correlation between two frequency components, and it is related to small-scale fading effects. However, shadowing is a large-scale fading effect, and RSS measurements are commonly averaged over to remove the effects of small-scale fading. The idea is to investigate the possibility of

using two or more frequencies to mitigate the fading effect. If the power received at one frequency falls in a minimum (fading point), then it falls in a maximum position for the second frequency. To ensure this point, the frequency spacing should be greater than the coherence bandwidth of the channel which is, in general, dependent on the utilized frequency band.

To show the effect of frequency diversity, the frequencies used in the measurement have been chosen from the beginning and the end of the 2.4 GHz ISM band (1st and 16th channel). In Fig. 3.8 the path loss is simulated for two frequencies separated by 80 MHz (2.40 and 2.48 GHz). This simulation shows that frequency diversity can successfully work for small distances; however, for larger distances, the incidence angle increases and the two paths are almost in phase with similar delays and little difference is observed in the power received at the two frequencies. This was also verified in the measurement described in the section 3.1.1. The positions of fading points between the two frequencies are different and show a certain lack of correlation between frequencies (see Fig. 3.9).

Fig. 3.25 shows the localization error as a function of the mobile node position (x,y) using four anchors located at the vertexes of a 16x16 m square. In order to evaluate these errors, several simulations were done. Since the anchors coordinates are known for a given point, the Euclidean distance to each anchor was computed. Then, the received power (RSS) was calculated interpolating the measurements at each frequency for the specific antenna height and the frequency. These measurements were done for an outdoor scenario. Then, the estimation of the position was obtained using the Least square and Centroid algorithm. Finally, the localization error was calculated as the distance between the real and the estimated position. In a single frequency case, only the RSS obtained from the measurements at this frequency were used. In case of frequency diversity, the average RSS between the two frequencies were used as an input to the localization algorithms. The procedure was repeated for each point in the analyzed area.

The lower part of Fig. 3.25 presents results obtained with Least Square and Centroid algorithms using a single frequency and an antenna height of 0.5 m. A significant improvement is obtained when the same cases are analyzed using the mean RSS computed from two frequency measurement, separated by 80 MHz within the 2.4 GHz ISM band, which is depicted in the lower part of Fig. 3.25.

The results for 0.5 m and 2 m antenna heights are summarized in Fig. 3.26. It shows the cumulative probability of the error obtained using both algorithms. The big improvement of estimation accuracy is achieved when using low antenna heights. In this case the frequency diversity helps significantly regarding both localization algorithms.

When using antenna heights of 2 m the improvement is not so large. Moreover,



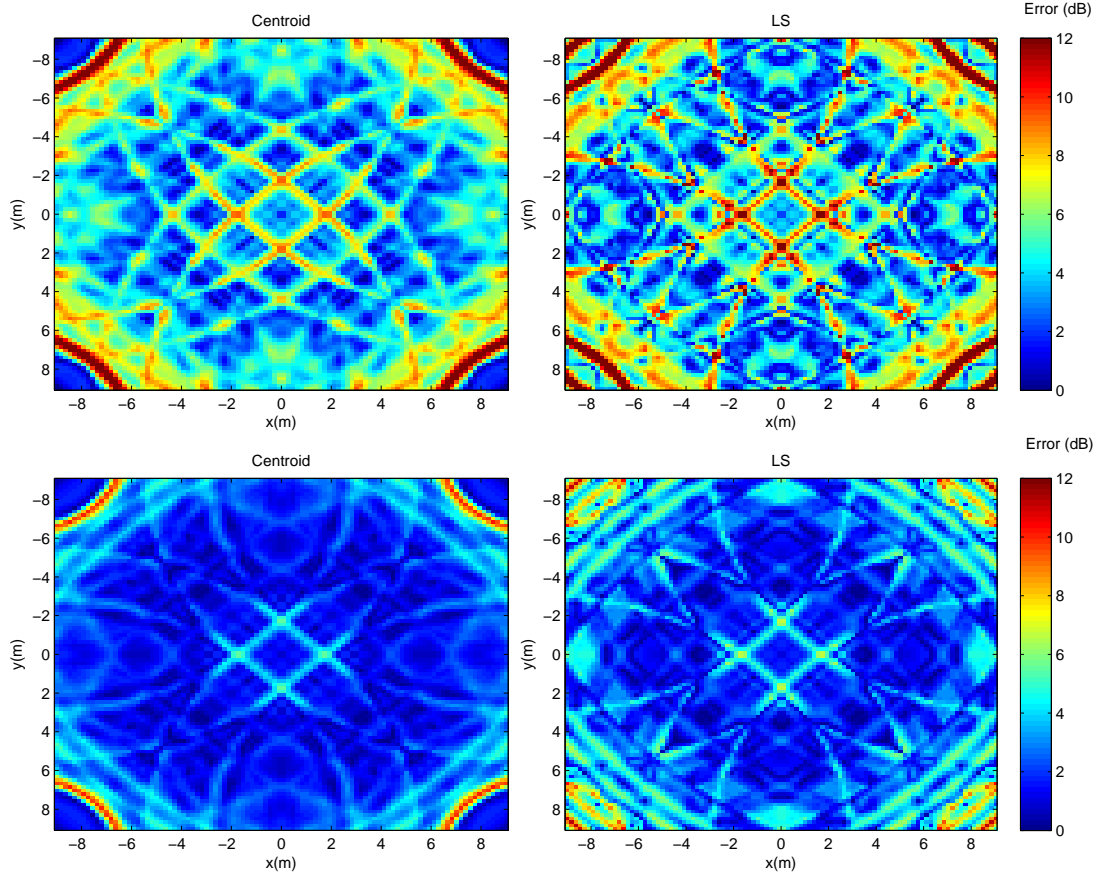


Fig. 3.25: Localization error (expressed by color) of Centroid and Least Square (LS) algorithms employing single frequency measurement (upper part) and frequency diversity (lower part).

the LS algorithm performs much worse for this antenna height in comparison to the Centroid algorithm. Regarding the Centroid algorithm, the error is up to 9 m for a single frequency and up to 7 m exploiting frequency diversity.

### 3.3 Chapter summary

This chapter focused on the localization presented the investigation of the distance estimation and the influence of its inaccuracy on the position estimation. The impact of the distance estimation error is evaluated in the simulations with three localization algorithms.

The position estimation error results to a large extent from an erroneous ranging method. The broadly used method based on the measurement of received signal strength is deeply examined in practical measurements with laboratory equipment and COTS products as well. Moreover, it is compared with another ranging method

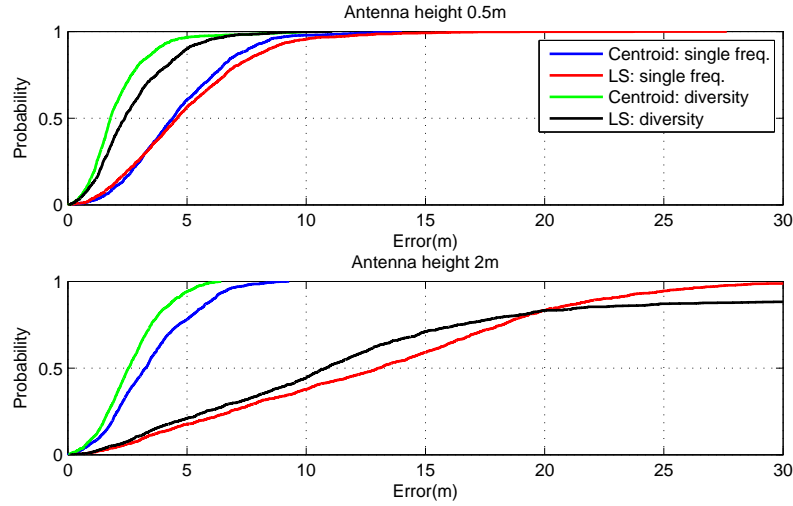


Fig. 3.26: Cumulative distribution function of the error using the least square and weighted centroid algorithms for antenna heights of 0.5 m and 2 m, with single frequency and two frequencies.

exploiting the speed difference in the propagation of radio signal and ultrasound signal. Although the ultrasound method is more accurate, concluded from the evaluation based on the estimation error, the practical use is questionable. Therefore, the signal strength measurement seems more useful for practical applications. However, we have to be aware of the inaccuracy of the method. In harsh environments, it can be even 300 % as results from the conducted measurements. The inaccuracy is caused by several aspects which basically determine the effect of slow and fast fading.

The slow fading can be partly overcome by a priori exhausting environment analysis or by a proposed method using frequency diversity. The method is based on the fact that the fading points of two signals with different frequencies do not lie in the same distance from the transmitter. This was shown using both simulations and measurement results as well. The enhancement of the novel method is presented in the chapter using simulations with two localization algorithms based on the measured data.

To conclude, it can be seen from the results that the frequency diversity can be effectively used to combat multipath channel fading for both investigated antenna heights and the typical coverage ranges in WSN. For subGHz ISM bands (867 MHz), frequency diversity is difficult to apply because of the narrow frequency band used (only one channel [93]) unlikely the ISM band 2.4 GHz that has a sufficient span to exploit the frequency diversity for distance estimations.

The fast fading features stochastic character with standard deviation up to 9 dB.

It means a difference of several meters in the distance estimation caused just by uncertainty of the measurement. This is a significant error and it is important to minimize it. Because of the stochastic character, the fast fading can not be easily overcome and multiple measurements with statistic methods have to be implemented to mitigate the inaccuracy.

## 4 EXPERIMENTAL ANALYSIS AND SIMULATION OF ENERGY CONSUMPTION

Energy is one of the crucial constraints of wireless networks with autonomous nodes. Therefore, the energy consumption has to be well investigated and considered during system design and development. Dealing with the localization, the energy aspect is taken into account in this work, too. Because the main focus lies on distance estimation based on received signal strength measurement, the communication is the most relevant consumer of the energy. Neither sensing nor heavy computational demands are considered in this work.

First in this chapter, the performed measurement of the energy consumption during communication is described. The measurement was conducted to better understand the consequences of message transmission related to energy on a certain COTS device.

Furthermore, dealing with the energy aware research, a model properly describing energy consumption based on hardware and application aspects has to be proposed and adopted. Such a model together with its implementation in network simulations is presented in the subsequent section. The simulations show the energy dissipation in a network and the lifetime accordingly. This aims to point out the importance of careful consideration of each communication in the network since it is a determining factor of the applications' lifetime.

The author's works dealing with the energy aspect of ad-hoc networks are [125]–[130].

### 4.1 Energy consumption measurement

Limited energy sources of nodes in wireless sensor networks require a careful consideration of energy consumption of all processes during the application lifetime. To analyze energy consumption and to predict the lifetime of a network, a comprehensive energy model based on commercial products is necessary. For localization, energy dissipated during RF communication and computation is determining the overall localization energy consumption. For that reason, this part is focused on the analysis of energy consumption during RF communication with particular 802.15.4 compliant nodes. The experimental testbed was designed and a scenario of node association and data transmission explored. For the measurement IRIS sensor nodes with 802.15.4/ZigBee protocol stack and shunt connection were used. For a rough estimation a datasheet could be used. However, as the results of the experiment show, more precise energy consumption cannot be calculated only from datasheet

values of current drain and length of a packet but intervals of listening and waiting between transmissions play an important role as well. The respective work was published in [125].

In order to describe precisely the energy consumption of a WSN node during its operation following specific experimental testbed was designed. The estimation of energy depleted from a battery source during node activity is based on the current powering node circuits and especially radio transceiver since it is the main source of energy consumption in the node. The focus is mostly on the operations related to communication, which means association of a node to an existing network after a node start-up and a packet transmission. Therefore, the experimental testbed consists of two communicating nodes IRIS and the current measurement setup. The simple WSN topology consists of two nodes: PAN Coordinator and end device. The Coordinator and the end device are identical from the hardware point of view but distinguished by definition of ZigBee roles. The employed IRIS nodes with XM2110CA module are based on low power Atmel Atmega1281 8bit microcontroller and Atmel AT86RF230 transceiver. The radio part is designed for the radio range 2.4 GHz ISM. These nodes originally come with XMesh protocol stack but it was replaced with Atmel's Bitcloud stack ported to IRIS motes for the experiments. The Atmel's Bitcloud stack is a full-featured certified ZigBee PRO stack. In addition, the sensor board is equipped with a turn-on switch, three LED for user visual communication, serial interface, 10-bit AD converter and other digital interfaces (I2C, SPI). The Coordinator is powered by its battery source as usual, while for powering the end node a power supply (3 V) for the experimental purpose was used. The experimental testbed schema can be seen in Fig. 4.1.

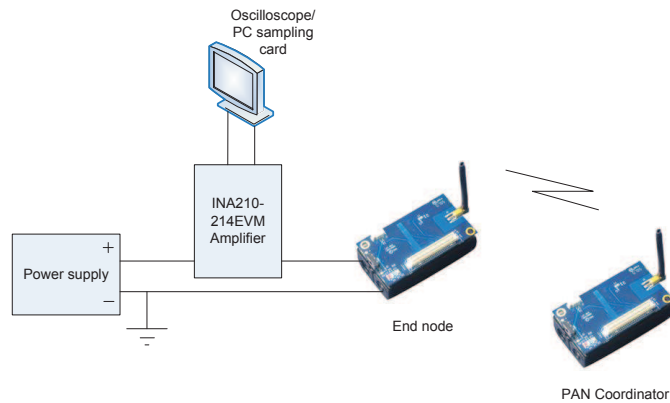


Fig. 4.1: Experimental testbed for measurement of energy consumption.

The main idea of the experiment is to measure a current drained by the end device

during communication with the PAN Coordinator. In order to precisely measure the current, a shunt resistor has to be placed in a measurement circuit. The current measurement setup contains a shunt resistor with a known value, which is placed between an energy source and a node supply pin. To minimize the impact of the shunt resistor on the node power supply, it has to be very small ( $1\ \Omega$  resistor was chosen). Because the current passing the shunt resistor is in order of mA the voltage across the shunt resistor has to be amplified for a better transparency of results. In the measurement an INA210 amplifier with the gain 100 especially conceived for current shunt monitoring was used. See the current shunt monitoring connection in Fig. 4.2.

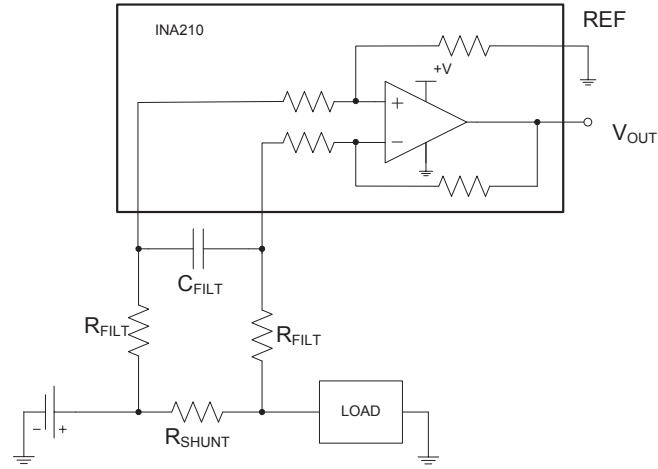


Fig. 4.2: Current measurement with a shunt resistor and low pass filter (adapted from [95]).

There is also a low-pass filter depicted in Fig. 4.1 formed by a capacitor  $C_{\text{FILT}}$  and a resistor  $R_{\text{FILT}}$ . The aim of the filter is to cut high frequency changes caused by interference and rapid current state transitions. For the filter design it has to be taken into consideration that a gain of the amplifier can be reduced by high value of  $R_{\text{FILT}}$  [95]. The gain can be expressed as

$$G_{\text{INA210}} = 100 \cdot \frac{R_{\text{INA210}}}{R_{\text{INA210}} + R_{\text{FILT}}}, \quad (4.1)$$

where  $R_{\text{INA210}}$  is an internal resistance of the amplifier which is  $5\ \text{k}\Omega$ . Another restriction requires that  $R_{\text{INA210}}$  has to be much higher than  $R_{\text{SHUNT}}$  in order to avoid a negative effect of the filter on the voltage drop. Considering both limitations  $R_{\text{FILT}} = 47\ \text{k}\Omega$  was chosen. According to the chosen value of  $R_{\text{FILT}}$ , the capacitor

$C_{\text{FILT}}$  can be calculated based on the cutoff frequency of the filter:

$$f_c = \frac{1}{2\pi \cdot (2R_{\text{FILT}}) \cdot C_{\text{FILT}}}. \quad (4.2)$$

With a value 220 nF for  $C_{\text{FILT}}$  we get a cutoff frequency 7.7 kHz which allows us to use a sampling frequency not lower than 15.4 kHz in accordance with the Nyquist theorem.

The last component of the experimental testbed is a measurement and displaying unit. Both the fast oscillator and a PC sampling card with an appropriate software tool can accomplish this function. For the testbed a PC sampling card (Humusoft AD622) and Matlab simulation tool with Simulink and real-time toolbox were chosen. A system of fast data buffering is used which allows subsequent processing (postprocessing) if needed (in case of high load). Values collected during the measurement were stored in a Matlab file and further processed in non real-time mode after the experiment.

For the experiment purposes one of the nodes was acting as a PAN Coordinator turned on before the measurement itself in order to create a network, which the end node joins after its start-up. The application executed in the end node is a simple function with a periodical packet of size 3 B transmission.

The current drained by the end node after start-up is depicted in Fig. 4.3.

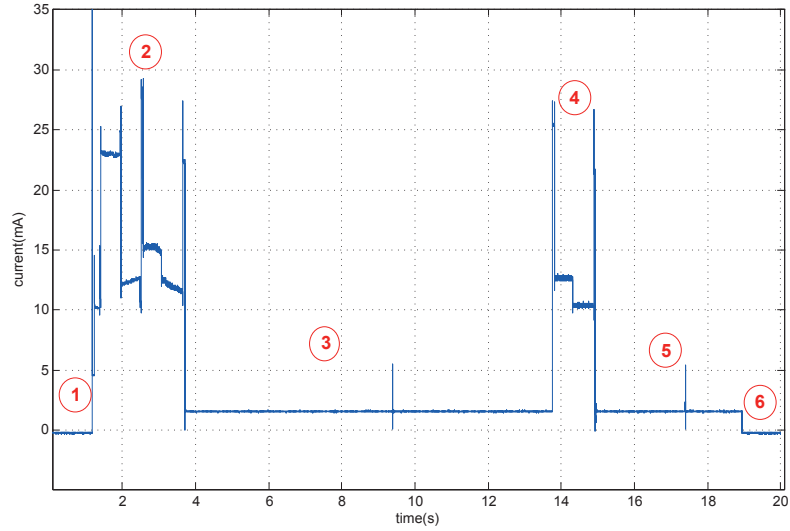


Fig. 4.3: Power consumption of IRIS node during RF communication.

In phase 1 the end node is turned off and the consumption is certainly zero. After being switch on, the sensor node performs association and binding phases exchanging information with the PAN Coordinator and initial packet transmission (phase 2). Then, following the implemented function, the end node waits in a sleep

mode (phase 3) draining a minimum of energy until periodic packet transmission takes place in phase 4. The required current in a sleep mode is 2 mA approximately which depends on the sleep mode of a microcontroller. In the deepest sleep mode the ATmega1281 requires less than  $7.5 \mu\text{A}$  [96]. Phase 5 represents a waiting for next periodic packet transmission in the sleep mode, however, the end node is turned off (phase 6).

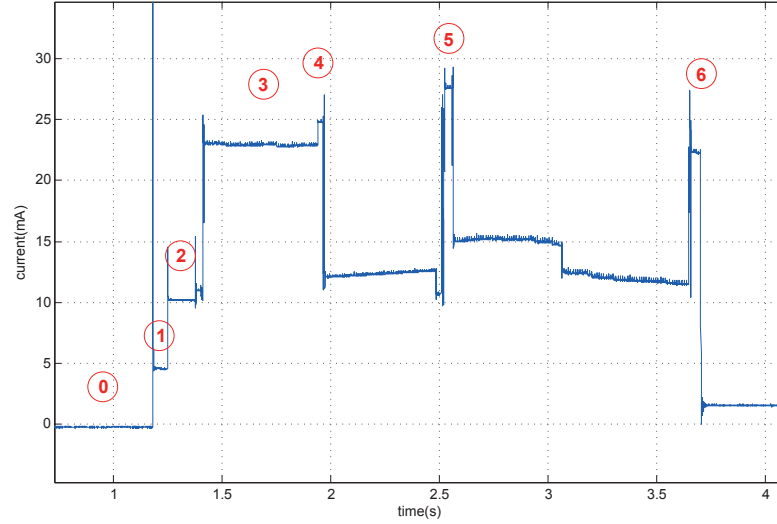


Fig. 4.4: Current drained during association and binding phase of ZigBee communication.

The next figure, Fig. 4.4, represents the turning-on process and the association phase only analyzed in more detail. During phase 0 the end node is switched off. When turned on, the current increases sharply to 50 mA for 0.5 ms. Then, in phase 1, it stays on the level 4.6 mA for approximately 70 ms when the system clock is being stabilized. Following phase and level of about 10.2 mA indicates the active state of the microprocessor (phase 2). In phase 3 the end node sends beacon request and gathers information from the PAN Coordinator. Since the communication channel (channel 15) has already been set the node then sends a rejoin request and gets an acknowledgment packet (phase 4). After 0.5 ms several packet transmissions are conducted. The end node gets rejoin response, sends the packet with its capabilities as a payload to the Coordinator (the Coordinator spreads them over the network afterwards), sends data request and then the first data packet. Each packet is followed by an acknowledgment at the link layer. It is optional in standard 802.15.4 but ZigBee strictly requires it. This is different with regards to an acknowledgment at the application layer. This ACK is optional in ZigBee communication and the user has the possibility to change it. In the experiment, the application ACK was



required and thus, after approximately one second, the end node requests application ACK, which is subsequently received (phase 6).

The end node periodically transmits a data packet after necessary data request command, which is, according to determined setting, followed by ACK at the application layer. This sequence is then repeated every ten seconds until the end node is turned off. This means a periodical energy drain, which is imposed by activating the processor and RF circuits transmitting and receiving packets. The time interval of this sequence is 1.18 s. From that period there are two time intervals of 40 ms with the 22 mA current consumption, 0.5 s of 12.5 mA and 0.6 s of 10.3 mA. The current consumption of the activities related to the sending of application data is shown in Fig. 4.5. Phase 1 is a data request with the link layer ACK reception. Then, before the data are sent in phase 3, a period of 40 ms follows (phase 2). Phase 4 represents a waiting for application ACK. Afterwards, in phase 5 a data request with application ACK is sent (both followed by link layer ACK). At the end, after about 4 ms the RF circuit is switched off.

As can be seen from all the figures, the energy consumption is mainly dependent on the active state of board circuits. It means mostly processor and RF circuits in our case. The node association takes about 1.2 s. Half of that time all the circuits consume energy which means high drain (about 23 mA). When only the processor is in the active state, the current is about 12 mA. An important fact is also that while waiting for application ACK the processor is on dissipating energy (more than 1 s). Therefore, packet transmission and MAC ACK reception itself, when the current increases to 25 mA, is actually minor consumer (takes about 40 ms) in the entire interval of communication.

Information on how much power is needed for the transmission and reception of a packet is an important input for each energy analysis. The data packet transmission, when maximal transmission power (3 dBm) is used, requires 27 mA (81 mW) and packet reception of about 25 mA (75 mW) considering IRIS node. The whole data request and transmission of 3 Bytes of payload takes about 40 ms, about the same as takes the request and the reception of application ACK. However, there is a significant interval of waiting. During the time interval of about 1 s, when the processor is on, the current consumption is 13 mA (39 mW) and 10.6 mA (31.8 mW) (see Fig. 4.5).

Despite the fact that the current drain during the packet transmission and reception is higher, due to the duration of the phases of entire data transmission process (including data request and acknowledgments), more energy is consumed just by the processor waiting for the application ACK in active state. This very important fact means that the consumption can not be calculated only from the transmission rate and number of bytes in the packet but the waiting period has to be considered,

too.

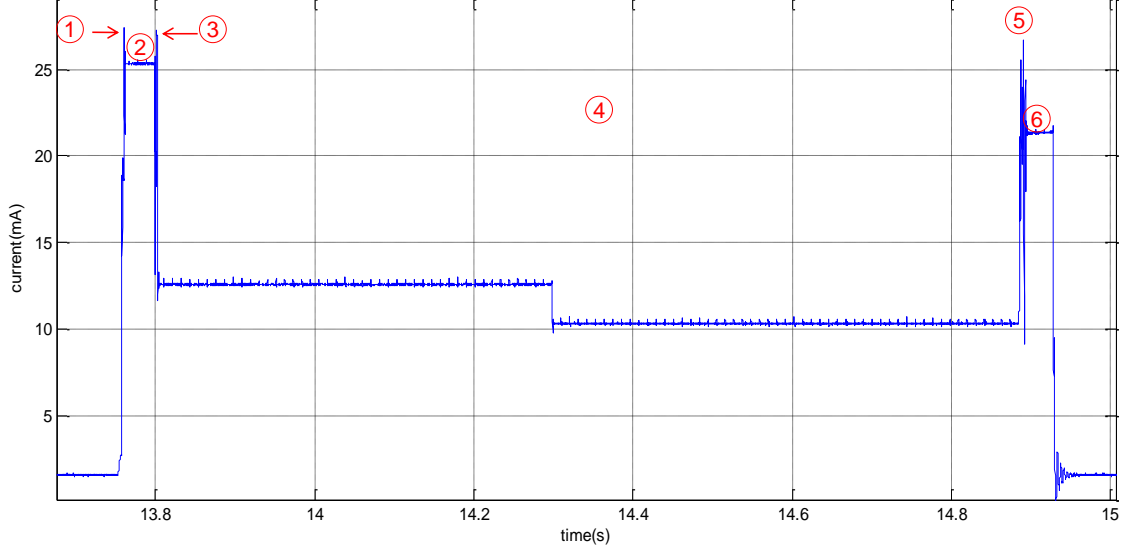


Fig. 4.5: Consumption of data transmission process in ZigBee networks with an acknowledgment at the application layer.

## 4.2 Energy model definition

Energy awareness is a key aspect in the field of energy constrained network research. Thus, this work to great extent considers energy consumption as a crucial limitation of all the processes in a network. Since the main focus lies in the localization, it omits the energy consumption of sensor regarding circuits and considers only computational and communication energy costs.

To properly include energy awareness, an appropriate energy model has to be designed and adopted in the work. Communication energy consumption is determined by the processing unit, transceiver circuits and amplifiers. In mutual communication we always consider two parts – transmitter and receiver. Therefore, energy depleted during communication is divided into energy consumed during transmission  $E_{TX}$  and during reception  $E_{RX}$  as follows:

$$E_{TX} = E_{PU} + E_{TC} + E_{PA}, \quad (4.3)$$

$$E_{RX} = E_{PU} + E_{RC} + E_{LNA}. \quad (4.4)$$

$E_{PU}$  is an energy consumed by the processing unit. It is a generalization of both the main microcontroller and RF chip. Furthermore,  $E_{TC}$ ,  $E_{RC}$  stand for energy

depleted by transmitting circuits, respectively receiving circuits.  $E_{PA}$  and  $E_{LNA}$  are energies consumed in amplifiers to amplify the signal power level. The former relates to a power amplifier amplifying the output signal to a desired level relatively to a required distance. The latter relates to a received signal level amplification.

If we sum  $E_{PU}$  and  $E_{TC}$  considering them constant and express the energy of power amplifier distance dependent, then (4.3) can be rewritten as

$$E_{TX}(d) = E_{TX0} + E_{PA}(d). \quad (4.5)$$

Analogically, we can express the reception energy as a constant based only on hardware properties:

$$E_{RX} = E_{RX0}. \quad (4.6)$$

Considering a communication between two nodes within a distance  $d$  we can express an energy necessary to send a packet as a sum of packet transmission and an acknowledgment reception. The ACK is not required in the 802.15.4 specification but many works include it. Therefore, the cost of a such simple communication scheme is

$$E(d) = E_{TX}(d) + E_{RX_{ACK}}. \quad (4.7)$$

Now, let us consider a situation when a node sends a packet to another node reaching it in several consecutive steps with multi-hop. In a network where nodes are placed in a distance  $d$  from each other reaching a goal node in a distance  $n \cdot d$  can mean a dissipation of energy  $E_{mhop}$ , which is a total energy consumed in the network:

$$\begin{aligned} E_{mhop} = & E_{TX}(d) + E_{RX_{ACK}} \\ & + (n - 1)[E_{TX}(d) + E_{RX} + E_{TX_{ACK}}(d) + E_{RX_{ACK}}] \\ & + E_{RX} + E_{TX_{ACK}}(d). \end{aligned} \quad (4.8)$$

In the previous, the straight forward path was considered during data transmission. It means that only nodes in the shortest path received the message from the initial node and retransmitted it to the next node in the path. That was a certain simplification since in real networks this is not completely true. Because of the node degree (network density) and omnidirectional antennas the transmitted signal reaches all nodes in the coverage area  $\pi R^2$ , where  $R$  is the radio range. If a node is in a listening mode it receives the packet into a buffer and partially processes it. Similarly, if the receiving node decides to forward the packet (after routing information and cyclic redundancy check) the sender will get the same packet again. This

packet is after reception discarded, despite the fact that it costs a certain amount of energy. This is called overhearing and was also studied by Basu and Redi [97].

If we want to have a more precise model of network energy consumption we have to take the overhearing into account. In the simulations published in [128] and [127] a store-and-forward mechanism was employed in the network. The nodes receive entire incoming message and after checking the header in the buffer they take a decision about further processing. Hence, the energy cost  $E_{OX}$  of the overhearing process can be equal to the  $E_{RX}$ . The initial node  $n_1$  spends energy  $E_1 = E_{TX} + E_{RX}$ . Furthermore, the relaying nodes receive message ( $E_{RX}$ ), forward message ( $E_{TX}$ ) and overhears the message sent from a downstream node ( $E_{OX}$ ). The energy dissipated by the relaying nodes equals to  $E_{rel} = E_{TX} + 2E_{RX}$ .

To express the broadcast cost, the WMA (Wireless Multicast Advantage) introduced by Wieselthier et al. [98] was employed. The WMA describes rebroadcasting process as follows: All nodes lying within the communication range of the broadcasting node can receive its transmission. Considering the broadcast transmission where all nodes represent destinations of the demanded message, the communication cost of node  $n_i$  that rebroadcasts message is affected by the presence of its own neighbors. Meaning that as node  $n_i$  receives and rebroadcasts the message while consuming  $E_{RX} + E_{TX}$ , it also subsequently overhears the communication of all neighbors. This broadcast overhearing process is referred to as a passive acknowledgment. The energy consumed by the broadcasting nodes can be expressed as:

$$E_i = E_{RX} + E_{TX} + (m_i - 1)E_{RX}. \quad (4.9)$$

The  $(m_i - 1)$  parameter represents a convention that  $n_i$  overhears the broadcast message from all nodes in  $M_i$  except the one which has sent it. The  $M_i$  stands for the set of the neighbor nodes of  $n_i$ . This communication model was used in many recent works such as [98].

### 4.3 Simulation of energy consumption

The introduced model was implemented in the Matlab environment to validate its performance. The scenario included 100 randomly deployed nodes with energy source of 1 J. The data from all nodes is sent in rounds, meaning that during one round, all nodes send data toward the base station (randomly selected node). The result of simulation is the energy colored topology and graph of the alive nodes number in dependency on the number of rounds.

The simulation ends when there is no way to route data to the base station. It means that all one-hop nodes around base station depleted their energy resources. This happens after 160 rounds in the presented scenario. The energy balance after 160 rounds can be seen in Fig. 4.6. The residual energy capacity is divided into five groups and relevant nodes are distinguished by color depending on their remaining resources. One can notice that the nodes placed close to the base station (placed on the x-axis) are loaded with an enormous network traffic since their residual energy is half in comparison to the far away nodes.

The decreasing rate of functional nodes in relation to performed communication rounds can be seen in the same figure on the right. Up to approximately 75 rounds all the nodes in the simulation have enough energy to run. Then, the first heavily exploited nodes close to the base station die because of the lack of sufficient energy. Up to approximately 160 rounds there is still a way for all the nodes to deliver a packet to the base station. Then, when the first undelivered message is detected, the simulation ends.

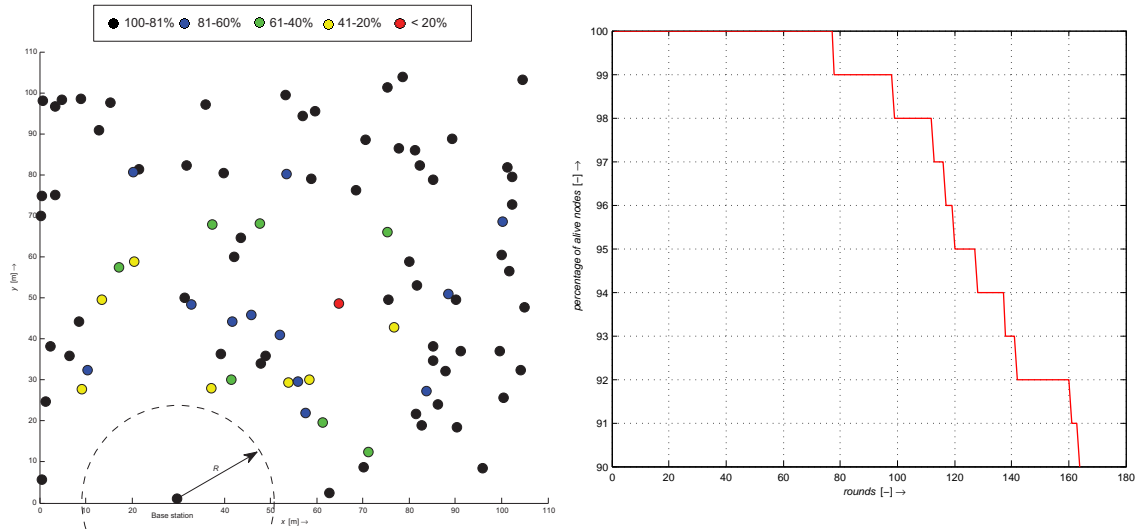


Fig. 4.6: Remaining energy resources of nodes after 160 rounds (left) and the rate of functional nodes during simulation rounds (right).

## 4.4 Chapter summary

This chapter was devoted to the analysis of energy consumption in a wireless network. To that purpose measurement and simulations were performed. It can be concluded from the conducted measurements that the communication consists of message transmission, acknowledgment reception and waiting in an active state.

The first waiting period is between data request and data transmission (40 ms) and the second waiting period (1.1 s) was observed when the node is waiting for the application ACK (ZigBee). ACK at the link layer followed data transmission in 600  $\mu$ s. Because of the waiting periods the energy consumption significantly differs in comparison to the situation without waiting. The total energy consumption is given by integration of the current drain over the period of communication including waiting in the active state.

For the simulation purposes an energy model was proposed and implemented into the simulation tool. The simulations show the influence of communication on the network performance and lifetime. With more extensive communication, nodes deplete their energy resources faster and die sooner which has a consequent effect on the rest of the network as well. Therefore, any communication has to be carefully considered and if necessary, minimize the power consumption by adaptive setting of output power and ACK usage only when advantageous.

Regarding the distance estimation based on RSS and the necessity of multiple measurement (which means multiple transmissions) it introduces the opposed requirements. On one side, the minimization of ranging errors requires several transmissions and the more the better for the accuracy. On the other side, the higher the network traffic, the shorter the application lifetime which is obviously undesirable.

The next chapter, therefore, deals with the two opposed initial requirements of distance estimation and intends to find a compromise solution. To target the issue a new distance estimation method based on the RSS method is proposed.

## 5 PROPOSAL OF NOVEL DISTANCE ESTIMATION METHOD

Distance estimation together with the energy moderation is a crucial prerequisite for localization in wireless networks with energy constraints. Depending on the application and further use of position information, the requirement of the accuracy of estimation can differ. Location information used only for geographical routing and data gathering [102]–[103] does not need to be as accurate as applications for precise object tracking or similar applications.

As concluded from chapter 3 distance estimation is negatively affected by RSS uncertainty. To overcome this issue multiple packet transmission has to be performed.

Since the wireless networks can be deployed in different environments, the radio conditions can be also significantly different. It means that in some situations we have to be aware of a high level of the RSS uncertainty while in others the RSS uncertainty is low. Moreover, the situation can change and we can experience totally different RF conditions in the same environment during a certain time period due to the stochastic character of the RSS uncertainty. To mitigate the uncertainty several repetitive measurements can be taken. However, we then collide with the prerequisite of the energy moderation. But even if we accept a higher load at the beginning of the network deployment when the nodes are localized (which is not a high portion of total communication), the same can not be acceptable in a network with mobile nodes and repetitive location update. In this case a traffic load related to localization is substantial and significantly influences the network lifetime.

A novel method of distance estimation addresses the issue by introducing an adaptive mechanism of RSS measurement control. It is a method allowing a node to control the number of RSS measurements in a response to current RF conditions and required level of RSS uncertainty mitigation.

The proposal rises from the publications [121] and [129].

### 5.1 Adaptable energy-aware distance estimation (AEDE)

The proposed novel method of ranging is called Adaptable Energy-aware Distance Estimation (AEDE) and its key feature is an energy awareness. The method allows to control energy spent by ranging while mitigating the RSS uncertainty as desired. And this is the adaptability aspect of the method. Despite keeping the energy

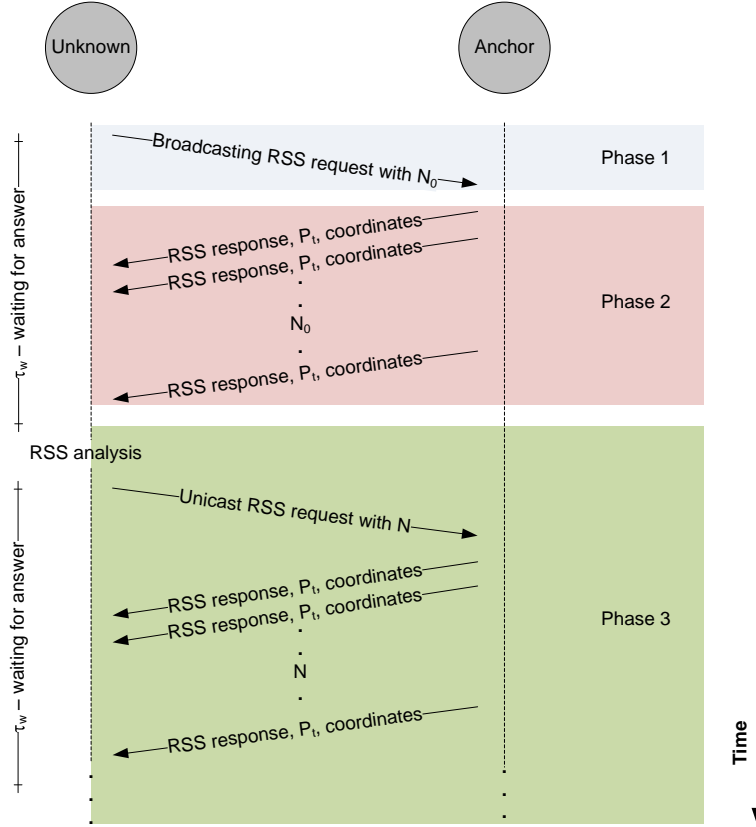


Fig. 5.1: Time diagram of AEDE method.

consumption under control, it allows to invest more energy in the case of an unstable environment and higher application accuracy needs.

The AEDE ranging method consists of three phases: RSS request, RSS response and RSS improvement (Fig. 5.1). There are certain assumptions that are considered for the method description as follows.

An initial state of a network deployment or location update in a network with mobile nodes is considered. At the beginning a node does not know either its coordinates or its neighborhood. To find its location it uses a distributive range-based localization algorithm with distances as a input. Therefore, it performs a ranging method first. Let us call this node as U node.

The AEDE method progresses in the following phases:

#### Phase 1:

The U node sends a packet RSS request with a one-hop broadcasting address in order to get to know its neighborhood and contact possible anchor nodes. The packet contains an initial number of measurements ( $N_0$ ) required for the first RSS estimation.



### Phase 2:

In the second phase all the nodes in the U node's neighborhood that have received the message and have a known position (anchor nodes) react<sup>1</sup>. They transmit  $N_0$  successive packets (RSS responses) with a time space  $RIS$  (RSS Interleaving Space). The  $RIS$  has to be larger than an interframe spacing (IFS)<sup>2</sup> or a coherence time (see 1.1.4) for the particular RF channel in order to get uncorrelated measurements:

$$RIS > Max \{IFS, Coherence\_time\}. \quad (5.1)$$

The coherence time can be also set generally for the environment. The RSS response packet contains ID of the node, transmission power level and its coordinates. The uncertainty of the location can be also part of the packet if the localization algorithm requires it.

### Phase 3:

The third phase consists of RSS analysis and RSS measurement expansion. When the U node has collected all the measurements it can perform the RSS analysis. In the RSS analysis the most probable RSS value ( $\overline{RSS}$ ) is calculated together with its uncertainty ( $u_{\overline{RSS}}$ ). These are calculated for each anchor node.  $u_{\overline{RSS}}$  represents the RSS uncertainty of the channel estimated from the standard deviation of the measurement samples collected. Based on this information and the number of samples an expected RSS estimation error  $\epsilon_{exp}$  is identified in an RSS lookup table which contains values of a statistical mean error. If the  $\epsilon_{exp}$  is larger than the required estimation error  $\epsilon_{req}$ , the U node requests another RSS responses from the particular anchor node. In other words, it sends an RSS request to a specific anchor with a required number of RSS responses ( $N_R$ ).

If there are more anchors to be asked for RSS responses, the RSS request can be cumulative. This means that the U node can create a RSS request addressing several anchors at the same time. The RSS request then contains several pairs: Anchor\_ID -  $N_R$ . The request is addressed to the entire one-hop neighborhood and the responses come only from the specified nodes.

Subsequently, the U node gets another set of RSS measurements which is processed in the RSS analysis and it updates the  $\overline{RSS}$  together with the  $u_{\overline{RSS}}$ . Then,

---

<sup>1</sup>Depending on the subsequent localization algorithm the U node can require distances to all nodes (even with unknown location) but this work considers only anchor nodes for now.

<sup>2</sup>The interframe spacing (SIFS) following after a MAC frame (MPDU) smaller than 19 Bytes is at least 192  $\mu s$  long. Longer interframe spacing LIFS is required for larger MPDU. The LIFS should exceed 640  $\mu s$ . [93]

searching in the RSS lookup table follows. This step is repeated until the required precision is reached.

All the  $\overline{RSS}$  values are used together with the signal propagation model resulting in a distance estimation processed further by a certain localization algorithm.

To make the ranging method even more efficient the link layer ACK is not transmitted since it is arbitrary in the low-power networks [93]. The reliable packet transmission is not necessary in this case. Regarding the RSS request, the recipient that does not receive the request (or the request is corrupted) is considered as inexistent. If the recipient receives the request correctly, it answers with the RSS responses.

If the RSS response is not delivered correctly the U node takes into account only the received number of RSS responses. To prevent waiting for undelivered RSS responses, the U node introduces a waiting time  $\tau_w$ , the longest time before performing the RSS analysis.

Therefore, to disable ACK, the sixth bit in the Frame Control field of the 802.15.4 frame is set to zero.

The transmission of  $N_R$  RSS responses is the most energy efficient if the transceiver is switched on only during the time necessary for the transmission and then switched off for the *RIS* period again. The burst transmission can be accomplished only if the node uses GTS (guaranteed time slot). Otherwise, the CSMA-CA method is used before each transmission which is less energy efficient. When using GTS, the superframe period has to be considered. A long period could significantly prolong the localization phase or make it even unfeasible. This issue has to be further investigated but is out of the scope of this work.

### 5.1.1 Format of localization packets

With regards to addressing, the Destination Address field is set as a broadcast address (0xffff) in the RSS request and as a specific address of the U node in the RSS response frame. It means that the request is processed by all listening nodes in the one-hop neighborhood and the response only by the U node. The differentiation between addressed nodes expecting to send RSS response is specified in the upper layer. The initial RSS request then includes an identification field with 0xffff identifying all the recipients and  $N_0$  number of requested RSS responses. In the case of a cumulative RSS request sent in the third phase the content identifying targeted nodes is given as depicted in Fig. 5.2.

$M_A$  is the number of following pairs Anchor\_ID -  $N_R$ . Apparently, for the broadcast request the  $M_A$  equals 1 and the next field is a broadcast identifier followed

Octets 2	2	2	2	2	...	2	2
$M_A$	$A_1$	$N_{r1}$	$A_2$	$N_{r2}$		$A_M$	$N_{rM}$

Fig. 5.2: Content of the RSS request packet.

by the initial number of requested measurements.

When an anchor receives the RSS request with the corresponding identifier (or broadcast request) it sends  $N_R$  RSS responses. The responses are then sent in a successive manner one by one with the  $RIS$  time spaces without waiting for ACK. The RSS responses are formatted as shown in Fig. 5.3.

Octets 1	2	1	0- $Bc$	0/4
RSS Format	ID	TX level	Coords	Coord. error

Fig. 5.3: RSS response data field.

The RSS Format field defines a format of RSS response. It identifies a type of coordinate system and a format of coordinates. Moreover, it also allows arbitrary use of location error information. There are three bits left for future use, too. The Format field is shown in Fig. 5.4.

Bits 0-3	4-6	7
Coordinates type	Reserved	Error field

Fig. 5.4: RSS response Format field.

The coordinate type and a number is given by the class code defined *a priori*. Tab. 5.1 is an example of the class code definition table. The code has a length of 4 bits, and thus, it supports up to 16 different coordination systems. The last bit in a format field determines whether a location error information is provided as well or not. Zero bit means not provided and true bit indicates that the coordinates are provided with an error information.

### ID field

ID field is an identification of the anchor node. It can be the same as the node's mac address or defined independently. Thus, each application can provide its own style of node identification. It can be either numerical code or even a string type depending on the definition.

Code	Coordinates	Length (B)
00	Cartesian 2D	8
01	Cartesian 3D	12
02	Polar	12
..	..	..

Tab. 5.1: Coordination class codes.

### TX level

This field contains an information about the transmission power level used for transmitting the RSS response. It is crucial information for the correct identification of a path loss and estimation of the distance based on the signal propagation model.

### Coords

Location information of the anchor is announced here. Coordinates are formatted according to the class code identified in the RSS Format field. Therefore, the length of this field ( $0-Bc$ ) is variable depending on the coordinate type used.

### Coord error

The last field of the RSS response is an arbitrary information about the error of the location information provided. We should be aware of the fact that anchors' coordinates can be erroneous as well. And thus, a location algorithm should be able to incorporate the location uncertainty.

## 5.1.2 Analysis of signal strength measurement

Repetitive measurements give a bigger set of data from which the RSS value for the distance estimation is calculated. Supposing a log-normal distribution of measurements (as concluded from several works, e.g. [59][76]), the larger the set we have the more precisely the mean value of the measurement can be determined. The precise mean value of the measurements is important since it represents the channel without any fast fading, and thus, also a desired output of the repetitive measurements. Fig. 5.5 presents a simulation with a different number of measurement samples in the set and the error of the estimated mean from the true value.

The simulation was conducted for several RF channels with different characteristics of RSS uncertainty. The simulation was repeated 10 thousand times and the results of this simulation were used to create a RSS lookup table which is used as a reference RSS estimation error table in the AEDE method.

It is obvious that the precision increases with a larger dataset. The increase is exponential, and thus, the precision increases the most with a lower number of samples. Additional samples have a bigger influence on a smaller dataset than on a larger one. In other words, the marginal improvement of the new measurement decreases like the total number of samples increases.

The tendency is the same for all the modeled channels but the error of the estimation is smaller for smaller RSS uncertainty. It means that the RSS estimation is more precise for a channel with less interference caused by fast fading.

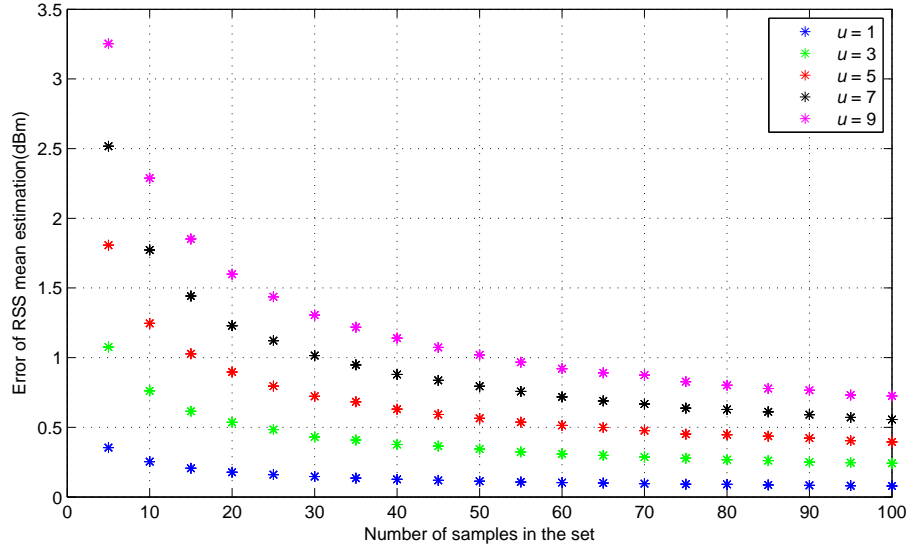


Fig. 5.5: Mean error of the RSS estimation with various number of measurement samples and under various channel uncertainty  $u$ .

It could be concluded from the simulation that the precision is given exclusively by the number of measurement samples. However, the simulation presented just an average value of the estimations. In fact, the estimation of each measurement set<sup>3</sup> with the same number of samples can be different. This can be seen in Fig. 5.6. The same number of measurement samples can result in quite a different error. It can be very precise or, on the other hand, as large as a multiple of the average value (dashed line) showed previously. Therefore, it is not possible to ensure the maximum error of the estimation based on Fig. 5.5. The values in Fig. 5.5 are the mean of the expected error with the normal distribution and a certain standard deviation. The expected error together with its standard deviation for the channel uncertainty  $u = 9$  can be seen in Fig. 5.7. It means that, if we have for example 20

<sup>3</sup>Measurement set, dataset, measurement samples refer to the set of measurements obtained from the neighbor after one RSS request

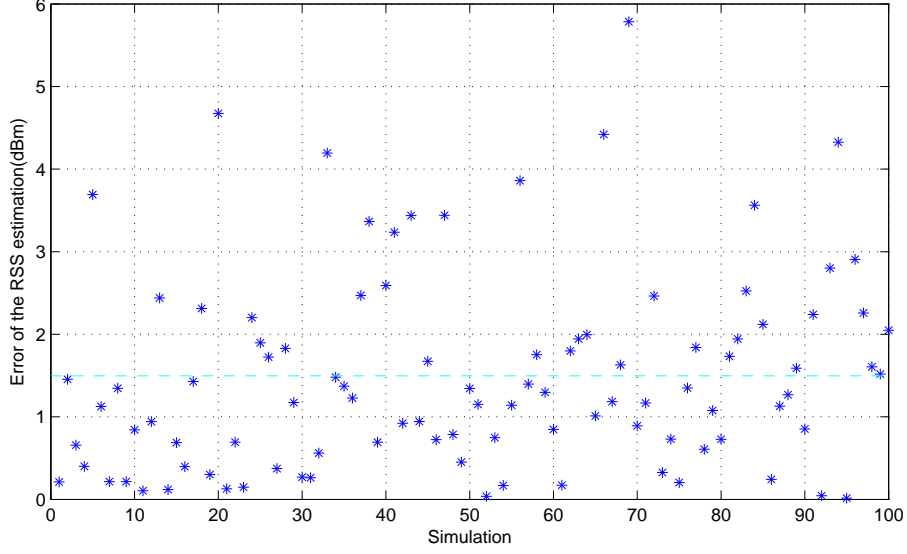


Fig. 5.6: Error of RSS estimation with 20 measurement samples.

measurements samples from the channel with  $u = 9$ , the error of the estimation will be most probably 1.6 dBm but can reach up to 2.8 dBm in some cases.

The mean calculation can be taken again to improve the RSS estimation. If we have several sets of measurements we can take their means and average them again which results in better estimation as can be seen in Fig. 5.8. The figure shows an error of the RSS estimation calculated from several sets of measurements. The measurement set of 20 measurement samples was taken as an example.

Fig. 5.8 confirms the expectation that we get a better estimation provided we repeat the measurement and we obtain a new set of measurement samples. Taking a closer look at the values in the figure one finds out that they correspond to the values in Fig. 5.5. For example, the two sets of 20 sample measurement result in the average error of 1.12 dBm which corresponds to the 40 sample measurement in Fig. 5.5. Therefore, the new set of measurements can add a certain accuracy to the estimation as expected from Fig. 5.5. However, we have to still keep in mind the standard deviation of the expected error as seen in Fig. 5.7.

In the previous simulations, the constant channel uncertainty was taken into account. However, the uncertainty can change with each measurement set. As the conditions change dynamically the channel properties can also vary and influence each measurement set. Therefore, the characteristics of actual measurement should be considered as well. Degradation of the RF channel condition can result in larger standard deviation of the measurement set and subsequently less accurate RSS estimation (see Fig. 5.5).

Therefore, in the AEDE method the actual channel properties are included into

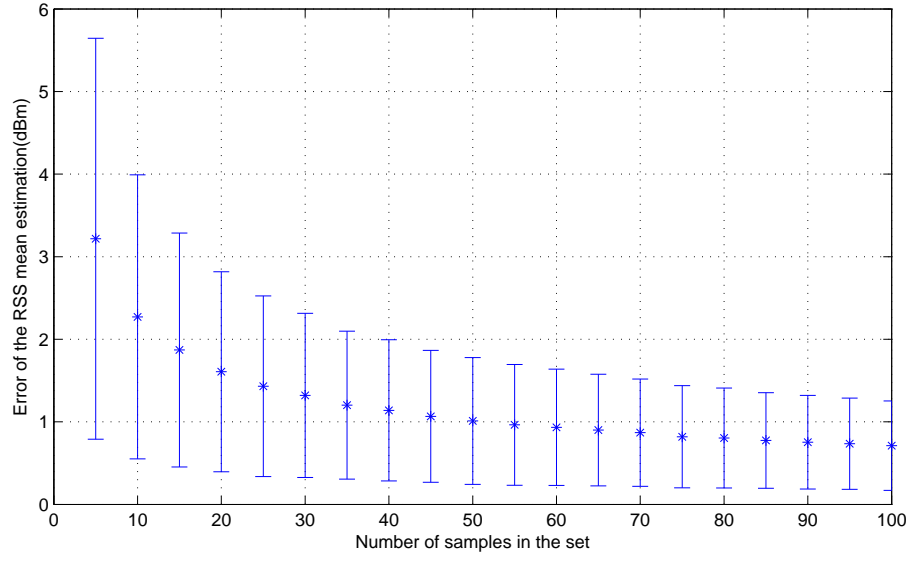


Fig. 5.7: Mean error of the RSS estimation with various number of measurement samples together with its standard deviation. Channel uncertainty  $u = 9$ .

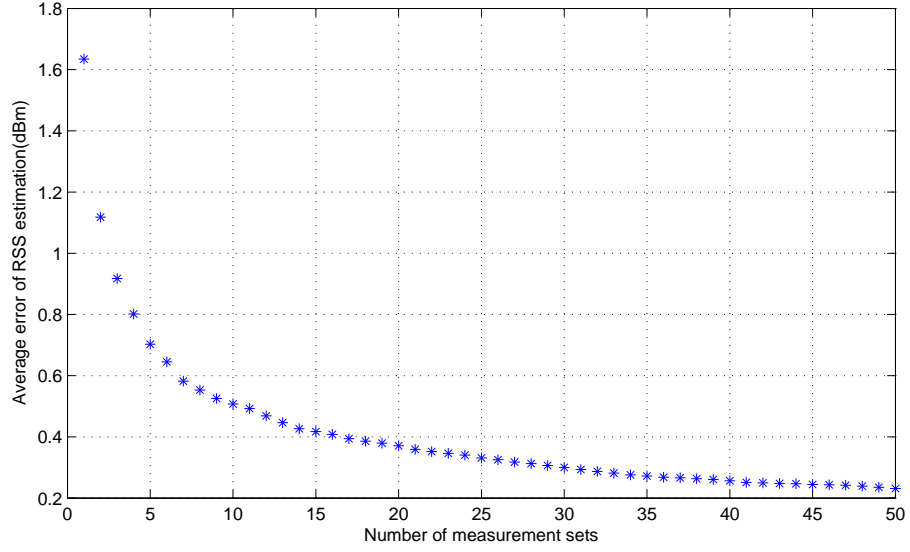


Fig. 5.8: Average error of the RSS estimation with different number of measurement sets with 20 measurement samples.

the calculation as well. Kalman filter is used for that purpose. Considering we have two sets of measurement  $\mathcal{N}(\mu_1, \sigma_1)$  and  $\mathcal{N}(\mu_2, \sigma_2)$ , we determine the new RSS estimation using Kalman filter as:

$$\overline{RSS} = \frac{\sigma_1^2 \mu_2 + \sigma_2^2 \mu_1}{\sigma_1^2 + \sigma_2^2} \quad (5.2)$$

and the update of the standard deviation is

$$\sigma = \sqrt{\frac{1}{\frac{1}{\sigma_1^2} + \frac{1}{\sigma_2^2}}}. \quad (5.3)$$

For example if we consider two datasets of 20 samples; one with  $\sigma_1 = 9$  dBm and the other with  $\sigma_2 = 3$  dBm. With the classical approach (not considering the standard deviations of the dataset) we would get an average error of approximately 0.83 dBm while with the Kalman filter we obtain a value 0.53 dBm. Further improvement could be obtained with additional datasets.

When the initial set of RSS responses ( $N_0$ ) is received at the U node, it collects all the RSS measurements and processes the RSS analysis. The purpose of the analysis is to find the most probable RSS value not affected by the time variation and its uncertainty. If the expected error is larger than a predefined threshold it requests other RSS measurements.

The initial estimation of RSS from an anchor  $i$  is given as

$$RSS_{0,i} = \overline{RSS}_i = \frac{1}{N_0} \sum_{k=1}^{N_0} RSS_{i,k} \quad (5.4)$$

with an uncertainty

$$u_{0,i} = \bar{u}_i = \sqrt{\frac{1}{N_0(N_0 - 1)} \sum_{k=1}^{N_0} (RSS_{i,k} - \overline{RSS}_i)^2}. \quad (5.5)$$

Based on the uncertainty and number of RSS packets the expected statistical mean error is looked up in the RSS lookup table for each anchor ( $\epsilon_{\text{exp},i}$ ). The RSS lookup table contains the mean error for the estimation based on the number of samples and the RSS uncertainty of the channel calculated from the standard deviation of the measurement set.

The decision whether to ask for additional RSS response packets or not is based on the condition

$$\epsilon_{\text{exp},i} > \epsilon_{\text{req}}, \quad (5.6)$$

where  $\epsilon_{\text{req}}$  is a threshold given by accuracy requirements. If the condition (5.6) is fulfilled the U node sends an RSS request to the  $i$ -anchor with  $N_{n,i}$  value indicating requested number of RSS responses. Index  $n$  indicates the  $n$ -th round of the process. The number of requested responses determines the accuracy of the new  $RSS_{n,i}$  and  $u_{n,i}$  derived from the collected measurement set.

When the new measurement set for anchor  $i$  is received and the new  $RSS_{n,i}$  and  $u_{n,i}$  are calculated (using formulas 5.4 and 5.5) the composite RSS estimation and its uncertainty are updated using Kalman filter:



$$\overline{RSS}_{n,i} = \frac{RSS_{n,i} \cdot \bar{u}_{n-1,i}^2 + \overline{RSS}_{n-1,i} \cdot u_{n,i}^2}{\bar{u}_{n-1,i}^2 + u_{n,i}^2}, \quad (5.7)$$

$$\bar{u}_{n,i} = \sqrt{\frac{1}{\frac{1}{u_{n,i}^2} + \frac{1}{\bar{u}_{n-1,i}^2}}}. \quad (5.8)$$

The total number of RSS measurement samples is updated as well:

$$N_{n,i} = N_0 + \sum_{k=1}^{n-1} N_{k,i}. \quad (5.9)$$

$N_{n,i}$  and  $\bar{u}_{n,i}$  are used as indices in the RSS lookup table and the new  $\epsilon_{\text{exp},i}$  is found. The condition 5.6 is applied again. If it is fulfilled, the whole phase repeats again. Otherwise the value  $\overline{RSS}_{n,i}$  is taken as the RSS estimation for  $i$  anchor.

## 5.2 Chapter summary

This chapter was devoted to the proposal of a novel ranging method called AEDE. First, a general description was given to understand the concept of a new approach. The AEDE method aims to reflect the actual conditions in the RF channel by adaptive RSS measurement control in order to meet the accuracy requirements of an application. The RSS estimation and exploited energy is controlled by the number of transmitted packets used for the RSS measurement. The decision making process in the AEDE is build on the statistical values of expected error provided the given number of measurements and their variance which is implemented in the RSS lookup table.

Further in the chapter, the aspects of the method regarding packet forming, timing and decision process are discussed in more detail. The method introduces RSS request and RSS response packets. The RSS request packet is used to invoke the RSS responses from anchors in the neighborhood. The reception of the RSS response packet is used to measure the RSS level and it also contains information necessary for distance and coordinates calculation.

## 6 EVALUATION OF NOVEL METHOD IN SIMULATOR

Every new algorithm, protocol or method has to be tested first in order to see if the initial assumptions were correct and the new method performs as expected before its implementation into real applications. This can be done either in an experimental testbed or in a suitable simulator. Setting an experimental testbed is often more expensive and also time consuming than simulations, therefore, simulations are preferred in the initial evaluation phases. Moreover, the basic features of the proposal can be tested better in the simplified environment where only the key aspects play a role. Experiments are more prone to failures and negative effects independent of the tested method, which complicates the evaluation. Therefore, also the novel AEDE method is first evaluated in the simulator.

For the evaluation several tools are available. Either network simulator such as NS2, Opnet, OMNet or more general simulator such as Matlab can be used. Every simulator has its particular pros and cons and it can be suitable for different purposes and in different situations. However, none of them is ideal for general use. The appropriateness of the most well known currently available tools was studied and the results are published in [131]–[134].

After a careful consideration Matlab was chosen as a suitable tool for AEDE evaluation. It offers programming environment for easy implementation of the method and a radio channel as well. Matlab is not a network simulator in general but it can be advantageously used for simulations of certain parts of the networks such as radio channel in this case.

In the next section, the description of the implementation of the AEDE method follows together with the presentation of results of preformed simulations.

### 6.1 Implementation and simulation results

The AEDE method is a method designed for a network use, however, it focuses on the node's one-hop neighborhood. The distance estimation always takes place between two nodes. And the RF channel influences the distance estimation the most. Therefore, the simulation of the AEDE method is focused on the RF channel between two neighboring nodes.

The implementation follows the proposal described in the previous chapter 5 with initial conditions set as described below.

First, and most importantly, the RF channel characterization has the biggest impact on the simulation results. The signal propagation reflecting the channel

properties can be described by a signal propagation model. As discussed in chapter 1 several models have been proposed. For the AEDE simulations the Path loss model of signal propagation (see 1.24) has been chosen and implemented since it reflects the most important path loss and fast fading. The fast fading is expressed as a log-normal random variable, which was used in the same manner in the channel model.

Then, the AEDE was implemented in phases corresponding to the logical phases of the AEDE development. The performance metric of the method consists of the final RSS estimation error and the number of packets transmitted to achieve that. The RSS estimation improves with each additional round of the AEDE while the number of packets grows accordingly.

Fig. 6.1 presents the results of the AEDE performance in comparison with the classical method using a fixed number of measurements (20 and 40 in this case) for the RSS estimation. The figure combines both metrics. The error of the RSS estimation is given on the left y-axis and the number of required packets (determining the energy consumption) on the right side. For the AEDE method both RSS request and RSS response packets were considered. For the classical approach measurement packets together with the acknowledgment packets were taken into account since the acknowledgment is a significant part of the energy consumption. In this sense, the classical approach is a method of collecting a fixed number of measurement samples regardless the ambient RF conditions or application requirements.

The simulation was performed for the distance of 15 m in the channel characterized by the Path loss model with the fast fading distribution  $\mathcal{N}(0, \sigma)$ . The  $\sigma$  is a standard deviation of the channel uncertainty determined by fast fading. The middle precision and 20 sample measurement sets were chosen in the AEDE initial setting. The maximal number of the RSS response packets was limited to 100 in total since it is a reasonable limit for most of the applications.

One can see in the figure that higher uncertainty of the channel implies also a higher consumption (given by number of transmitted packets) in order to meet the initial conditions. The smaller error is obtained with less effort for RF channel with the smaller standard deviation of the uncertainty. The error of the RSS estimation obtained from the classical approach with a constant number of measurement samples is depicted by red and green circles in the same figure. Apparently, the AEDE outperforms the classical approach with 20 measurement samples in all the cases while the consumption is even smaller than with the classical approach in the environment with  $u$  up to 5 dB of the RSS uncertainty approximately. In the rest of the cases more energy is depleted but better estimation results are achieved.

Considering the classical approach with 40 samples for RSS estimation, the AEDE has better or similar accuracy if  $u > 4$  dB. The precision of the classical

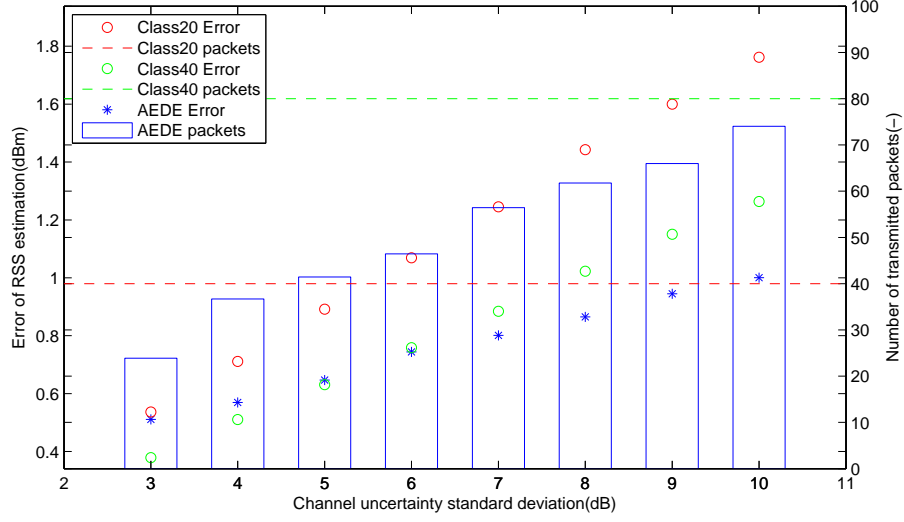


Fig. 6.1: Performance of the AEDE method together with the classical approach.

approach is better only for RF channels with a smaller uncertainty. However, the consumption is unreasonably high in that case. In all the cases the AEDE features smaller consumption although it outperforms the classical approach by approximately 30 % in the RF channel with high uncertainty.

The conducted comparison has to be seen in terms of application requirements. If an application does not require high precision the lower number of packets can be transmitted, and thus, less energy is consumed. On the other side, if the application benefits from the higher precision of the estimation and it can afford to spend more energy the AEDE allows high precision estimation even in environments with a strong fast fading effect as can be seen in Fig. 6.2.

For applications with high accuracy needs, it is possible to improve the RSS estimation by 70 % in comparison with classical approach with 20 measurement samples in highly unstable environments. In applications using the classical approach with 40 measurement samples the improvement of the AEDE is still around 55 %.

Possible performance of the AEDE method under different application requirements are depicted in Fig. 6.3. As an example, three levels of accuracy were presented – low, middle and high. Taking this as initial requirements the AEDE progresses accordingly. The RSS estimation error is depicted with markers and related to the left y-axis while the vertical bars represent the number of packets needed for the estimation which is enumerated on the right y-axis.

The figure shows that based on the application requirements the AEDE method gives different results and allows to spend less energy when low accuracy of the estimation is sufficient. If an application does not need high accuracy of the estimation, the RSS estimation error is higher but energy spent during the estimation is

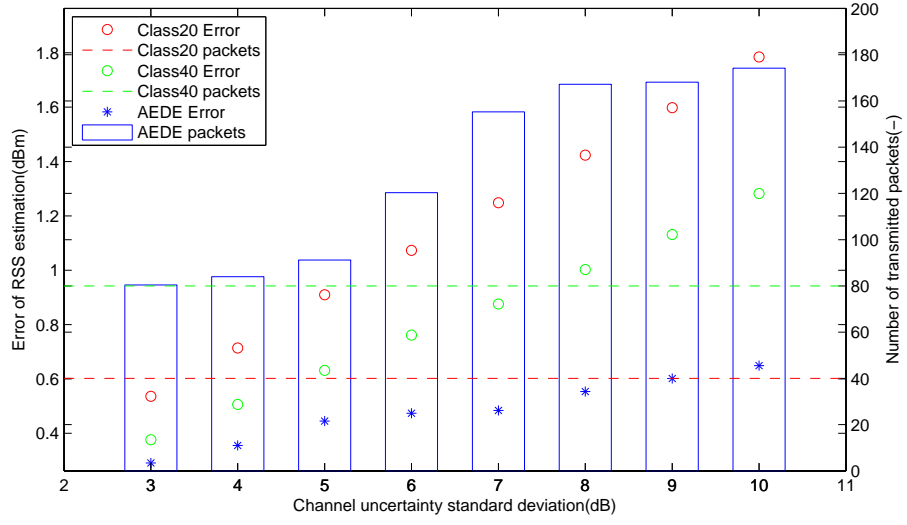


Fig. 6.2: Performance of the AEDE for applications with high accuracy needs.

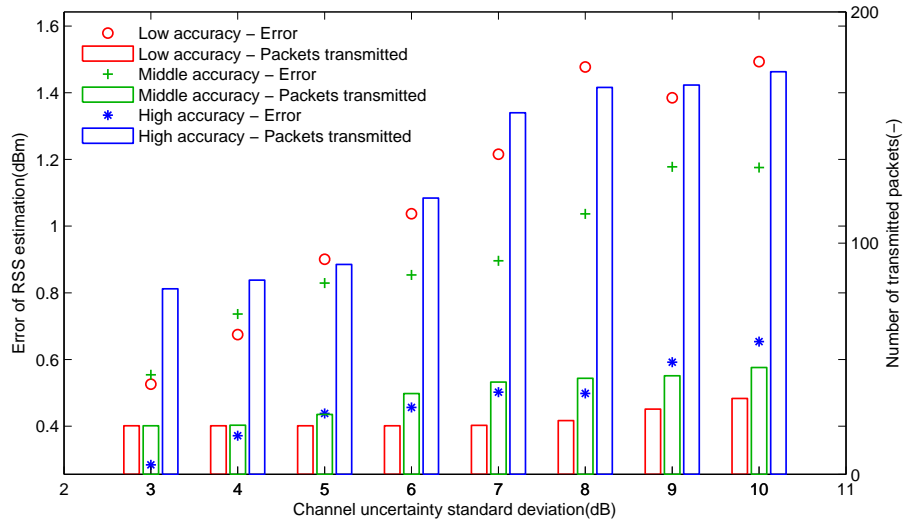


Fig. 6.3: Example of three accuracy levels of AEDE and its performance.

low. On the other hand, the accuracy can be significantly better if required which consequently results in higher energy consumption.

## 6.2 Chapter summary

For the simulation of the novel distance estimation method Matlab was chosen as the most appropriate simulation tool since it offers flexibility and all the required functionalities in a user friendly environment. First, the analysis of the uncertainty of the RSS estimation with the normal distribution was performed. The simulation resulted in the generation of a RSS lookup table, which is further used in the AEDE method.

The AEDE was implemented following the phases of the proposal (chapter 5). The simulations of the AEDE were performed in the RF channel described by the Path loss signal propagation model allowing the simulation of the random fast fading in the channel. The simulations were performed with several configurations of the AEDE, various initial requirements and channel uncertainty. For the evaluation, an error of the RSS estimation and number of transmitted packets were used as metrics. The AEDE method was compared to the classical approach with a fixed number of transmitted messages for RSS estimation (measurement sets of 20 and 40 messages were taken as an example). All the simulations were conducted 10 thousand times for the credibility of the results and the average value was depicted and used for evaluation.

There are several samples of performed simulation results presented in this chapter. For the understandability of the results and the clarity of the figures the error of the RSS estimation required by an application is classified as low, middle and high.

The simulations show that the AEDE method is able to meet the accuracy requirements of the application while taking into account the uncertainty of the channel. At the same time it respects the energy constraints of the nodes and it uses just the minimal necessary number of transmissions. One can see from the presented results that the new method outperforms the classical approach with 20 measurements by 70 % in environments with high uncertainty, provided a high accuracy of the application is required. In environments with lower uncertainty the improvement is not so enormous but it is still significant. More importantly, the AEDE reflects the lower uncertainty and reduces the number of transmitted messages while still keeping the required accuracy.

## 7 EXPERIMENTAL EVALUATION OF PROPOSED METHOD IN REAL NETWORK

After the evaluation of the AEDE method in a simulator implementation on COTS devices and testing in the network under real conditions followed. Wasmote sensor nodes<sup>1</sup> were chosen as a platform for the AEDE assessment. The AEDE was implemented as described in chapter 5 for the evaluation purposes. The testbed was composed of an unknown node, an anchor and a gateway in order to investigate the performance of the AEDE between the two standalone nodes (Fig. 7.1).

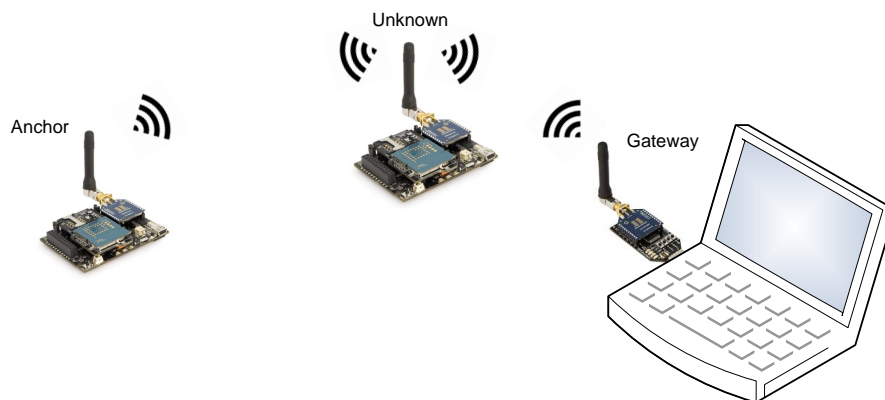


Fig. 7.1: Experimental testbed schema.

Wasmote is a low-power platform dedicated to monitor ambient environment with the capability of wireless communication. Waspomote is a modular system based on widespread ATmega1281 microcontroller with 8 kB SRAM and 4 kB EEPROM running at frequency 8 MHz. It is powered by an external battery (3.3–4.2 V) or alternative harvesting device (e.g. solar panel). It is equipped with several I/O interfaces including 7 analog, 8 digital, PWM, 2 UART, I2C and USB used for programming and debugging. A SD card (up to 2 GB) can be used for data storage. The Wasmote platform offers several modular communication interfaces such as Wifi, Bluetooth, GSM/GPRS and mainly 802.15.4/ZigBee allowing network cooperation. Wasmotes equipped with RF module Digi XBee-802.15.4 in frequency band 2.4 GHz with transmission power up to 1 mW and sensitivity -92 dBm were used in the designed testbed [99].

The Wasmote platform offers several modules that can enhance the usability of the node such as different sensor boards with specific sensors (e.g. pollution and event monitoring), GPS receiver, RFID/NFC or expansion radio board allowing to

---

<sup>1</sup>Libelium <http://libelium.com>

connect more radio interfaces. Thanks to the modular architecture Waspnotes can be customized to the various specific application needs.

Programming of Waspnotes is based on c++ programming language and for application development Wasmote IDE is provided. The code consists of two main parts – an initialization setup run just once after the program start-up and a loop part which is repeated infinitely. The novel AEDE method was implemented as an application process. The flow chart of the implementation can be seen in Fig. 7.2.

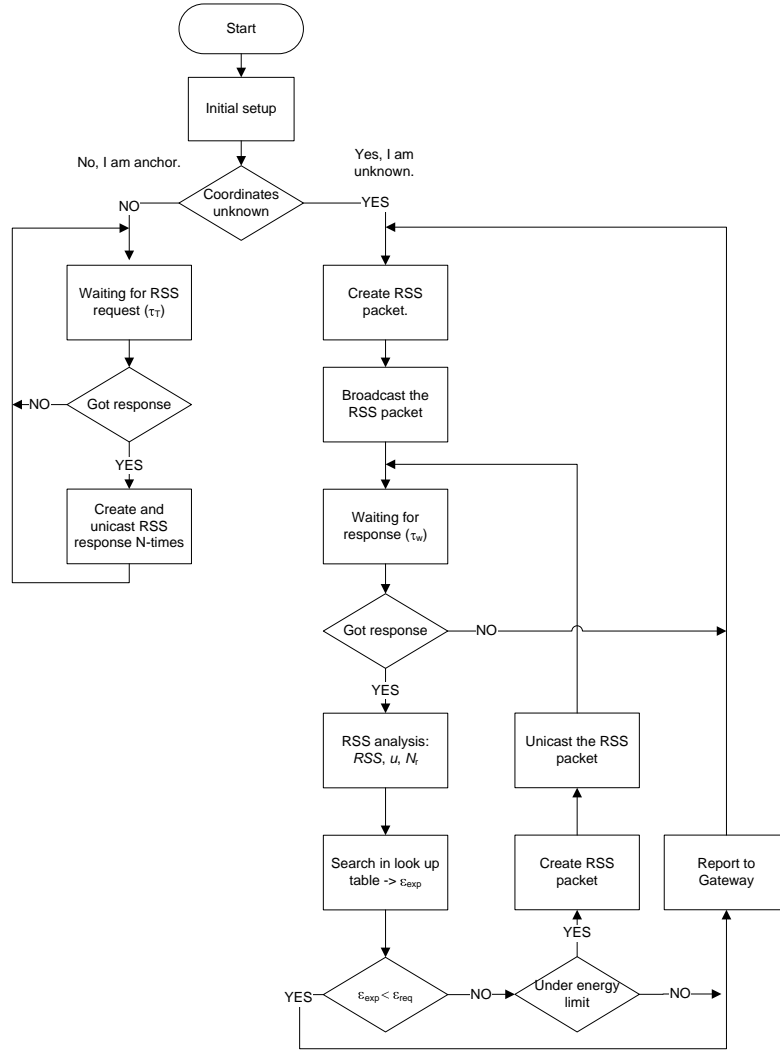


Fig. 7.2: Flow chart of the implementation of the AEDE method.

Several measurements with Waspnotes programmed with the AEDE method were conducted to evaluate the functionality of the AEDE. The testbed was deployed in a laboratory with a random movement of objects and persons. Several networks operating in the 2.4 GHz band were detected in the laboratory as well. However, their presence impacted mostly the data packet loss ratio and not RSS. The most



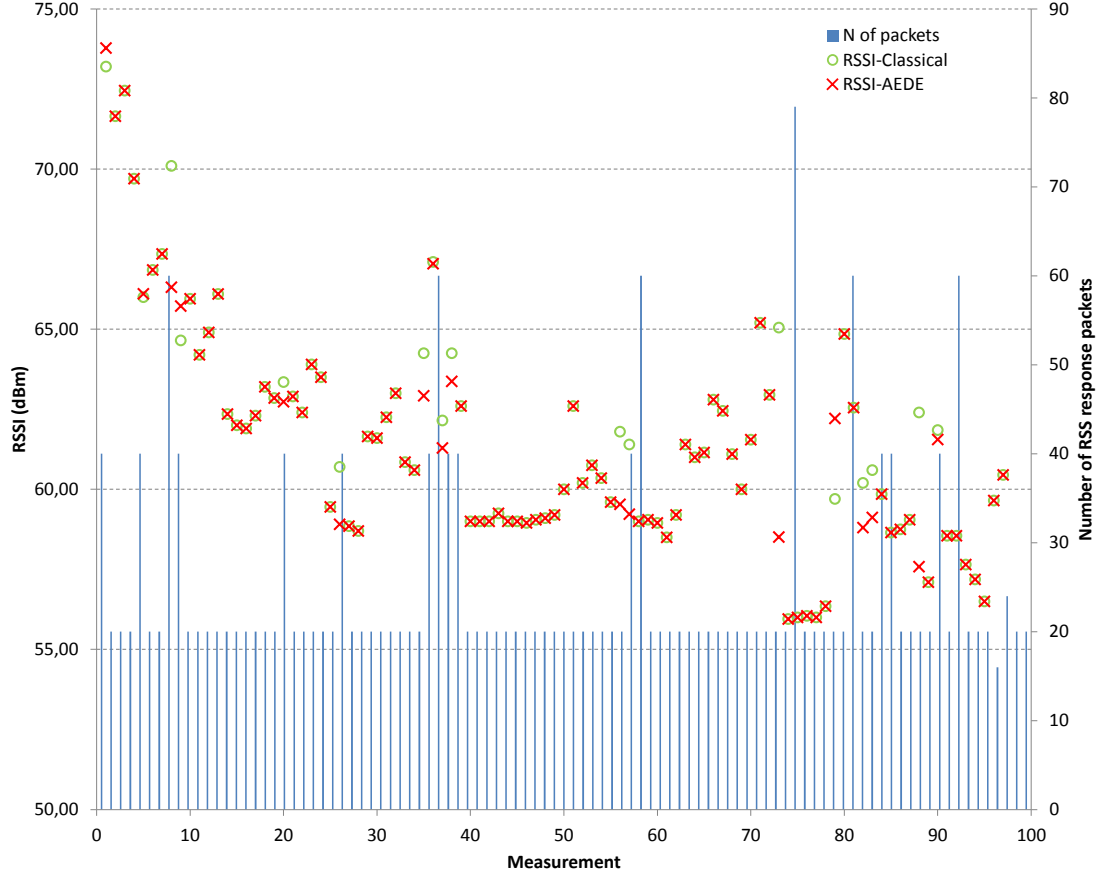


Fig. 7.3: Evaluation of the AEDE with Waspmites (detail).

significant RSS variation was observed during movement in the laboratory.

The XBee RF module provides received signal strength indicator (RSSI) parameter, which reflects the received signal strength. As the manufacturer comments the measurement is accurate from -40 dBm to the sensitivity level [99]. Therefore, the measurement was designed considering this fact and the nodes were placed in several scenarios but always keeping the distance resulting in the RSSI lower than -40 dBm. During the evaluation we should be also aware of the particular accuracy of the RSSI given by the RF module. Certain publications indicate that the RSSI measurement of 802.15.4 platforms might not be very accurate featuring even certain nonlinearities over the measurement range [100].

During the experiment the nodes in the network were set to run the AEDE process indefinitely. For comparison, the estimation of the RSSI using the classical method was conducted and reported as well. Several results of measurement are presented in Fig. 7.3. The classical method is referred to as a method collecting a fixed number of measurement samples under all conditions (20 samples in this case).

The uncertainty in the radio channel was not the same over the whole experiment.

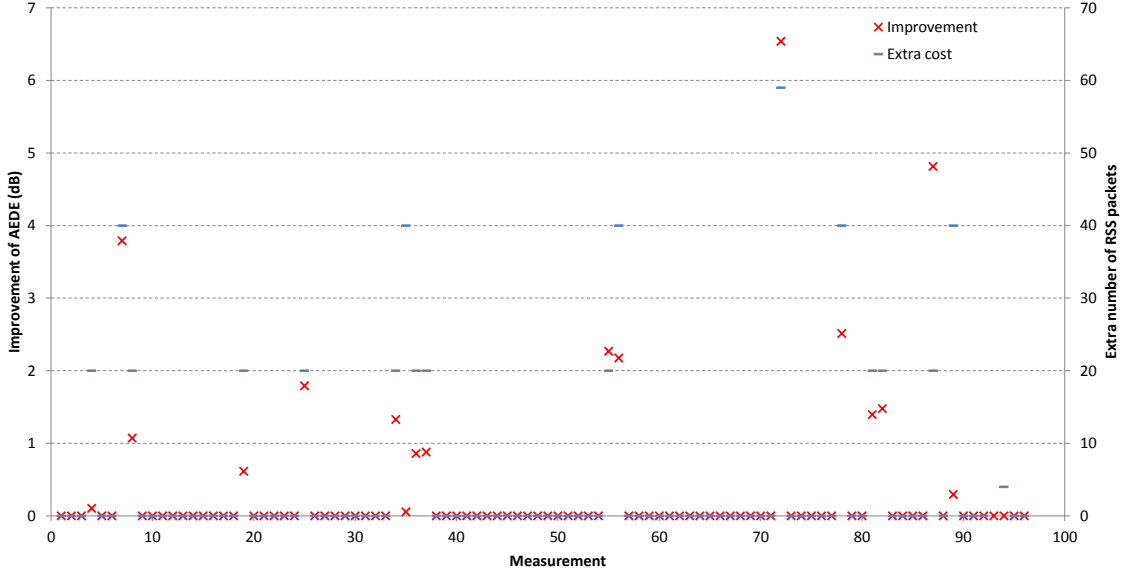


Fig. 7.4: Improvement of RSSI estimation and extra cost using AEDE.

Therefore, in some cases the AEDE method gives the same results as the classical approach. In the rest of the cases, when higher uncertainty of measured dataset was detected, the AEDE method resulted in more transmitted packets and higher accuracy. The number of transmitted packets is depicted on the right side of the figure.

The measured RSSI varies over the interval of measurement. It is a generally observed phenomenon that should be addressed by a signal propagation model. The AEDE method helps to avoid fast changes in RSSI measurement but not the slow changes of RF conditions. The improvement of the RSSI estimation in the presented measurement can be seen in Fig. 7.4. If the uncertainty of the measurement exceeds the determined threshold, the AEDE method triggers an extra measurement and the estimation of the RSSI improves. In the measurements where the uncertainty is under a given threshold the AEDE performs as a classical method without any extra energy cost. This is depicted in the figure as zero values.

It can be concluded that the AEDE method performs well also under real conditions. The proper functionality was confirmed by implementation in a network with Waspnote nodes where the AEDE was run hundreds of times. The method was implemented as an application based on the proposal from chapter 5. The nodes ran the application indefinitely, repeating the AEDE method in 10 s intervals after the initial setup of the network and application parameters. The nodes were placed in various distances respecting the accuracy range of RF modules.

The presented figures show the RSSI value resulting from both the classical method and the AEDE method for comparison. When the uncertainty of the RF

channel, and the measured dataset, is below a given threshold, the AEDE method provides the same results as the classical method without higher energy expenses. However, when the RSS uncertainty exceeds the threshold the AEDE method improves the RSSI estimation by providing more samples in the dataset. The improvement of the estimation of certain measurements can be seen in Fig. 7.4 where the AEDE method provides improvement up to almost 7 dB in some cases.

## 8 CONCLUSION

This thesis is devoted to localization in wireless networks with a focus on distance estimation since the distances between nodes are key input parameters for many localization algorithms. Thus, the accuracy of the distance estimation directly influences the accuracy of the localization. Several methods of distance estimation have been proposed but up to the author's best knowledge none of them addresses the energy consumption and adaptability as a response to ambient conditions.

Therefore, a proposal of the energy-aware distance estimation method for general use adaptable to ambient conditions and application requirements was stated as the primary objective of the thesis.

First, a brief introduction into the topic was presented in chapter 1. Several distance estimation methods together with their role and influence in the localization process were described. Because of the further focus of the thesis on the estimation method using received signal strength, the signal propagation was addressed as well.

Before the proposal of the novel method, an extensive experimental analysis of the localization method based on received signal strength and radio characteristics influencing this method was performed. Furthermore, an experimental analysis of energy consumption of commercial ZigBee devices was carried out, too. Both analyses resulted in an efficient proposal of the new method.

It was observed from the performed analysis that radio environment is not stable but stochastic and current signal propagation models are not capable to adapt to the uncertainty of the received signal strength measurement. The significant variation of the received signal strength measurement is caused by common multipath and fast fading effect of the signal propagation. The standard deviation of measurement variation observed was up to almost 9 dBm in certain cases and 2 dBm in average. It resulted subsequently in erroneous position estimation. Therefore, the uncertainty of the measurement is addressed in the new proposal.

The slow fading can be combat using proposed frequency diversity as observed during the investigation of the signal propagation. Although, it is a different approach to minimizing the ranging error, it is an important contribution that implies almost 50 % improvement of position estimation in applications operating in frequency band with sufficient frequency span (e.g. 2.4 GHz ISM band).

The main contribution of the thesis consists of the proposal of a novel method for distance estimation (AEDE) presented in chapter 5. The method is adaptable to radio channel conditions and application requirements while respecting low energy consumption during the process. The proposal includes the description of the three phases of the method, time scheme and also specific packets' formats.

The novel method was subsequently evaluated in a simulator and experimental

testbed under real conditions. Both evaluations proved the proper function of the method and its benefits in environment with radio unstable conditions as presented in chapter 6 and chapter 7.

## BIBLIOGRAPHY

- [1] HARROP, P., DAS, R. Wireless Sensor Networks 2009–2019, *IDTechEx*, Nov 2008, p. 240.
- [2] ONWORLD, ZigBee/802.15.4 Module Revenues to Approach \$1.7 Billion in 2015, *OnWorld article*, San Diego, CA, July 19, 2011 Available from URL: <<http://onworld.com/news/newszigbeenetofthings.html>>.
- [3] WIRELESS NEWS DESK, Wireless Sensor Network R&D Investment to Top \$1 Billion in 2012, *SYS-CON Media, Inc.*, January 28, 2009 Available from URL: <<http://opensource.sys-con.com/node/823199>>.
- [4] BECKER, M., WENNING, B.-L., GÖRG, C., JEDERMANN, R., TIMM-GIEL, A., Logistic applications with Wireless Sensor Networks. In: *Proc. of HotEmNets 2010*. 2010.
- [5] CORKE, P., WARK, T., JURDAK, R., WEN, H., VALENCIA, P., MOORE, D., Environmental wireless sensor networks, *Proceedings of the IEEE*, vol. 98, no. 11, pp. 1903–1917, 2010.
- [6] KWONG, K. H., WU, T., GOH, H., STEPHEN, B., GILROY, M. P., MICHIE, C., ANDONOVIC, I., Wireless sensor networks in agriculture: cattle monitoring for farming industries. *Electrical Engineering*, 2009 ,Vol. 5, pp. 31–35.
- [7] ANDERSON, B., BELHUMEUR, P., EREN, T., GOLDENBERG, D., MORSE, A., WHITELEY, W., YANG, R., Graphical properties of easily localizable sensor networks, *Wireless Networking*, vol. 15, no. 2, pp. 177–191, Feb. 2009.
- [8] HOLGER, K., ANDREAS, W., *Protocols and Architectures for Wireless Sensor Networks*, John Wiley & Sons, 2005, 526 pages, ISBN:978-0-470-09510-2.
- [9] SHAVITT, Y., TANKEL, T., On the curvature of the Internet and its usage for overlay construction and distance estimation *INFOCOM 2004 – Twenty-third Annual Joint Conference of the IEEE Computer and Communications Societies. IEEE*, 2004.
- [10] SPENCE, D., An implementation of a Coordinate based Location System, [online] Cambrigde (UK): University of Cambridge, 2003. Available from URL: <<http://www.cl.cam.ac.uk/techreports/UCAM-CL-TR-576.pdf>>.
- [11] NG, E., HUI, Z., Predicting Internet network distance with coordinates-based approaches. In *INFOCOM 2002. Twenty-First Annual Joint Conference of the*

- IEEE Computer and Communications Societies. Proceedings. IEEE*, Vol. 1, 2002.
- [12] WATTEYNE, T., SIMPLOT-RYL, D., AUGÉ-BLUM, I. DOHLER, M., On using Virtual Coordinates for Routing in the Context of Wireless Sensor Networks, Personal, Indoor and Mobile Radio Communications, *PIMRC 2007. IEEE 18th International Symposium*, pp.1–5, Sept. 2007.
  - [13] WATTEYNE, T., BARTHEL, D., DOHLER, M., AUGÉ-BLUM, I., Using virtual coordinates for wireless sensor networks: Proof-of-concept experimentation, *Testbeds and Research Infrastructures for the Development of Networks & Communities and Workshops, TridentCom 2009*, pp.1–8, April 2009.
  - [14] LIU, K., ABU-GHAZALEH, N., Aligned Virtual Coordinates for Greedy Routing in WSNs, *Mobile Adhoc and Sensor Systems (MASS)*, pp.377–386, Oct. 2006.
  - [15] HIGHTOWER, J., BORRIELLO, G., Location systems for ubiquitous computing, *Computer*, vol.34, no.8, pp.57–66, Aug 2001.
  - [16] YOUSSEF, M. Robust cooperative localization technique for wireless sensor networks. *New Technologies Mobility and Security*, pp. 1–4, 2009.
  - [17] BOON-CHONG SEET, QING ZHANG, CHUAN HENG FOH, FONG, A.C.M., GONZALEZ, A., Hybrid RF mapping and ranging based localization for wireless sensor networks, *Sensors, IEEE*, pp. 1387–1391, Oct. 2009.
  - [18] PAL, A., Localization Algorithms in Wireless Sensor Networks: Current Approaches and Future Challenges, *Macrothink Institute* , Vol 2, No 1, 2010.
  - [19] STOJMENOVIC, I., *Handbook of Sensor Networks – Algorithms and Architectures*, John Wiley & Sons, 2005.
  - [20] PRIYANTHA, N. B., CHAKRABORTY, BALAKRISHNAN, H., The Cricket Location-Support System, *Mobile Comp. and Networking*, Boston, MA, pp. 32–43, Aug. 2000.
  - [21] NICOLESCU D., NATH B., Ad-hoc positioning system, *Global Telecommunications Conference GLOBECOM '01*, IEEE, pp. 2926–2931, vol. 5, 2001.
  - [22] NICOLESCU D., NATH B., DV based positioning in ad hoc networks, *Journal of Telecommunication Systems*, 22(1/4):267–280, 2003.

- [23] DIL, B., DULMAN S. O., HAVINGA, P. J. M., Range-Based Localization in Mobile Sensor Networks. In *Proceedings of Third European Workshop on Wireless Sensor Networks*, Feb 2006.
- [24] PRIYANTHA, N. B. ,BALAKRISHNAN, H. , DEMAINE, E. D. , TELLER, S. J., Anchor-free distributed localization in sensor networks, in *SenSys*, pp. 340–341, 2003.
- [25] SHANG Y., RUML, W., FROMHERZ, M., Positioning using local maps, *Ad Hoc Networks Journal of Elsevier*, 240–253, 2006.
- [26] KANNAN, A., GUOQIANG MAO,VUCETIC, B., Simulated Annealing based Wireless Sensor Network Localization, *Journal of Computers*, Vol. 1, No. 2, pp 15–22, May 2006.
- [27] ALIPPI, C., VANINI, G., A RSSI-based and calibrated centralized localization technice for Wireless Sensor Networks, In *Proceedings of Fourth IEEE International Conference on Pervasive Computing and Communications Workshops (PERCOMW'06)* Pisa, Italy, pp. 301–305, March 2006.
- [28] LEI ZHANG, LILI DUAN, BINWEI DENG, HAO LIU, GUANGMING HUANG, S-MRL Distributed Localization Algorithm for Wireless Sensor Networks, *Wireless Communications, Networking and Mobile Computing, 2008. WiCOM '08. 4th International Conference*, pp.1–4, Oct. 2008.
- [29] HE T, Huang C, BLUM B M, et al. Range-free localization schemes for large scale sensor networks, *MobiCom2003*, San Diego, pp. 81–95, 2003.
- [30] JIZENG WANG, HONGXU JIN, Improvement on APIT Localization Algorithms for Wireless Sensor Networks, *2009 International Conference on Networks Security, Wireless Communications and Trusted Computing*, 2009.
- [31] XIAOLI LI, HONGCHI SHI, YI SHANG A map-growing localization algorithm for ad-hoc wireless sensor networks, *Parallel and Distributed Systems, ICPADS 2004*, pp. 395- 402, July 2004.
- [32] LAY, D. C., *Linear Algebra and Its Applications* (3rd ed.), Addison Wesley, August 2005,ISBN 978-0-321-28713-7.
- [33] LIU, B., LIM, K., WU, J., Analysis of hyperbolic and circular positioning algorithms using stationary signal-strength difference measurements in wireless communications, *IEEE Transactions on Vehicular Technology* 2006; 55(2), pp.499–509.



- [34] RAICHENBACH, F., TIMMERMAN, D., Indoor Localization with low complexity in Wireless Sensor Networks, In *Proceeding IEEE Int. Conf. on Industrial Informatics*, pp. 1018–1023, 2006.
- [35] JIANG, H., CAO, R., WANG, X., Apply Modified Method of Nonlinear Optimization to Improve Localization Accuracy in WSN Wireless Communications, *Networking and Mobile Computing, WiCom '09*, pp.1–6, Sept. 2009.
- [36] CHANDRASEKARAN, G., ERGIN, M.A., JIE YANG, SONG LIU, YINGYING CHEN, GRUTESER, M., MARTIN, R. P., Empirical Evaluation of the Limits on Localization Using Signal Strength Sensor, *Mesh and Ad Hoc Communications and Networks, SECON '09. 6th Annual IEEE Communications Society Conference*, pp. 1–9, June 2009.
- [37] PATWARI, N., ASH, J.N., KYPEROUNTAS, S., HERO, A.O., MOSES, R.L., CORREAL, N.S., Locating the nodes: cooperative localization in wireless sensor networks, *Signal Processing Magazine, IEEE*, vol.22, no.4, pp. 54–69, July 2005.
- [38] VAN TREES, H.L., *Detection, Estimation, and Modulation Theory, Part I*. New York: Wiley, 1968.
- [39] LARSSON, E.G., Cramer-Rao bound analysis of distributed positioning in sensor networks, *IEEE Signal Processing Letters*, Vol. 11, No. 3, pp. 334–337, March 2004.
- [40] SHEN, Y., WYMEERSCH, H., WIN, M.Z., Fundamental Limits of Wideband Cooperative Localization via Fisher Information, *In Proc. IEEE WCNC'07*, pp. 3951–3955, March 2007.
- [41] JOURDAN, D. B., DARDARI, D., WIN, M. Z., Position error bound and localization accuracy outage in dense cluttered environments, *In Proc. IEEE Int. Conf. on Ultra-Wideband*, Waltham, MA, September 2006.
- [42] ASH, J. N., MOSES, R. L., On the relative and absolute positioning errors in self-localization systems, *IEEE Trans. Signal Processing*, Vol. 56, No. 11, Nov. 2008.
- [43] ALLEN, M., BAYDERE, S., GAURA, E., KUCUK, G., *Localization Algorithms and Strategies for Wireless Sensor Networks*, IGI-Publishing, May 2009.
- [44] REICHENBACH, F., BLUMENTHAL, J., TIMMERMAN, D., Comparing the Efficiency of Localization Algorithms with the Power-Error-Product (PEP),

- Distributed Computing Systems Workshops, ICDCS '08. 28th International Conference*, pp.150–155, June 2008.
- [45] HAORAN FENG, RUIXI YUAN, CHUNDI MU, An Energy-Efficient Localization Scheme with Specified Lower Bound for Wireless Sensor Networks, *Computer and Information Technology, CIT '06. The Sixth IEEE International Conference*, pp.232–232, Sept. 2006.
  - [46] LIECKFELDT, D., JIAXI YOU, BEHNKE, R., SALZMANN, J., TIMMER-MANN, D., Assessing the Energy Efficiency of Localization in Wireless Sensor Networks, *Consumer Communications and Networking Conference, CCNC 2009. 6th IEEE*, pp.1–2, 10–13 Jan. 2009.
  - [47] ASHRAF ABDEL-KARIM HELAL ABU-EIN, Effects of Gain, Cost, and Number of Messages on Energy Efficiency Algorithm of Wireless Networking, *European Journal of Scientific Research*, Vol. 27 No. 3, pp. 426–430, 2009.
  - [48] MAO G., FIDAN, B., ANDERSON, D.O., Wireless sensor network localization techniques, *Computer Networks*, Volume 51(10), pp. 2529–2553, 2007.
  - [49] GUSTAFFSON, F., GUNNARSSON, F., Positioning using time-difference of arrival measurements, *Acoustics, Speech, and Signal Processing, 2003. IEEE International Conference*, vol.6, pp. 553–6, 2003.
  - [50] KNAPP, C., CARTER, G., The generalized correlation method for estimation of time delay. *IEEE Trans Acoust Speech Signal Process*, 24 (4), pp. 320–327, 1976.
  - [51] Cricket Project: Cricket v2 User Manual, *MIT Computer Science and Artificial Intelligence Lab*, Cambridge, MA 02139, July 2004, Available from URL: <<http://cricket.csail.mit.edu/v2man.html>>
  - [52] CAUWER, D., OVERTVELDT, V., SCHUEREN, V. D., Study of RSS-Based Localisation Methods in Wireless Sensor Networks. In *Proceedings of the Fourth European Conference on the Use of Modern Information and Communication Technologies ECUMICT 2010*, pp. 307–318, 2010.
  - [53] KUMAR, P., REDDY, L., VARMA, S., Distance measurement and error estimation scheme for RSSI based localization in Wireless Sensor Networks, *Wireless Communication and Sensor Networks (WCSN)*, pp.1–4, Dec 2009.
  - [54] RONG, P., SICHITIU, M.L., Angle of Arrival Localization for Wireless Sensor Networks, *Sensor and Ad Hoc Communications and Networks, SECON '06. 3rd Annual IEEE Communications Society*, vol.1, pp. 374–382, 2006.

- [55] WEHN, H. W., BELANGER, P. R., Ultrasound-based robot position estimation, *IEEE Trans. Robot. Autom.*, vol. 13, pp. 682—692, Oct. 1997.
- [56] KUC, R., Forward model for sonar maps produced with the Polaroid ranging module, *IEEE Trans. Robot. Autom.*, vol. 19, pp. 358—362, 2003.
- [57] SCHILLING, H. K., GIVENS, M. P., NYBORG, W. L., PIELEMEIER, W. A., THORPE, H. A., Ultrasonic Propagation in Open Air, *Acoust. Soc. Am.* 19, pp. 222, 1947.
- [58] GLEASON, C.P. PEREZ, L.C. GODDARD, S., On the Ranging Connectivity in the Cricket Localization System, *Electro/information Technology, IEEE International Conference* , pp. 619–624, 2006.
- [59] STOYANOVA, T., KERASIOTIS, F., PRAYATI, A., PAPADOPOULOS, G., A Practical RF Propagation Model for Wireless Network Sensors, *Sensor Technologies and Applications, SENSORCOMM '09*, pp. 194–199, June 2009.
- [60] TURGUT, B., MARTIN R., Localization for indoor wireless networks using minimum intersection areas of iso-RSS lines, In *Proceeding of 32nd Annual IEEE Conference on Local Computer Networks (LCN 2007)*, Oct 2007.
- [61] SWANGMUANG, N., KRISHNAMURTHY, P., Location Fingerprint Analyses Toward Efficient Indoor Positioning, *Pervasive Computing and Communications, IEEE International Conference*, pp. 100–109, 2008.
- [62] RAPPAPORT H.L., *Wireless Communications: Principles and practice*, 2nd Edition, Prentice Hall, 2001.
- [63] FRIIS, H.T., A Note on a Simple Transmission Formula. *Proceedings of the IRE*, vol. 34, p. 254. 1946.
- [64] JAKES, W.C., *Microwave Mobile Communications*, Wiley, 1974. Reprinted by IEEE Press in 1994.
- [65] HARLEY, P. Short distance attenuation measurements at 900 MHz and 1.8 GHz using low antenna heights for microcells, *IEEE J. Select. Areas Commun.*, vol. 7, no. 1, pp. 5–11, Jan. 1989.
- [66] RUSTAKO, A. J., AMITAY, N., OWEN, G. J., ROMAN, R. R., Radio propagation at microwave frequencies for line-of-sight microcellular mobile and personal communications, *IEEE Trans. Veh. Technol.*, vol. 40, no. 1, pp. 203–210, Feb. 1991.

- [67] DOMAZETOVI, A., GREENSTEIN, L. J. ,MANDAYAM, N. B., SESKAR, I., Propagation models for short-range wireless channels with predictable path geometries, *IEEE Trans. Commun.*, vol. 35, no. 7, pp. 1123–1126, Jul. 2005.
- [68] RONG-HOU WU, YAMG-HAN LEE, HSIEN-WEI TSENG, YIH-GUANG JAN, MING-HSUEH CHUANG, Study of characteristics of RSSI signal, *Industrial Technology, ICIT 2008*, pp. 1–3, April 2008.
- [69] SHIH-HAU FANG, TSUNG-NAN LIN, Accurate WLAN indoor localization based on RSS, fluctuations modeling, *Intelligent Signal Processing, WISP 2009*, pp. 27–30, Aug. 2009.
- [70] SANCHEZ, M. G., CUINAS, I., ALEJOS, A. V., Electromagnetic field level temporal variation in urban areas, *Electronics Letters*, vol. 41, no. 5, pp. 233–234, March 2005.
- [71] HALDER. S. J., TAE YOUNG CHOI, JIN HYUNG PARK, SUNG HUN KANG, SIN WOO PARK, AND JOON GOO PARK, Enhanced ranging using adaptive filter of ZIGBEE RSSI and LQI measurement. In *Proceedings of the 10th International Conference on Information Integration and Web-based Applications & Services*, ACM, November 2008.
- [72] YUNCHUN ZHANG, ZHIYI FANG, RUIXUE LI, WENPENG HU, The Design and Implementation of a RSSI-Based Localization System, *Wireless Communications, Networking and Mobile Computing, WiCom '09*, pp. 1–4, Sept. 2009.
- [73] HARA, S., DA ZHAO, YANAGIHARA, K., TAKETSUGU, J., FUKUI, K., FUKUNAGA, S., KITAYAMA, K., Propagation characteristics of IEEE 802.15.4 radio signal and their application for location estimation, *Vehicular Technology Conference*, vol.1, pp. 97–101 Vol. 1, 30 May–1 June 2005.
- [74] ZHANG JIANWU, ZHANG LU, Research on distance measurement based on RSSI of ZigBee, *Computing, Communication, Control, and Management, CCCM 2009, ISECS International Colloquium*, vol.3, pp. 210–212, Aug. 2009.
- [75] FANG ZHEN, ZHAO ZHAN, GUO PENG AND ZHANG YUGUO, Analysis of Distance Measurement Based on RSSI, *Chinese Journal of SENSORS AND ACTUATORS*, vol. 20, No. 11, pp. 2526–2530, Nov 2007.
- [76] CHO, H., KANG, M., PARK, J., PARK, B., KIM H., Performance Analysis of Location Estimation Algorithm in ZigBee Networks Using Received Signal Strength, *Advanced Information Networking and Applications Workshops, AINAW '07*, vol. 2, pp. 302–306, May 2007.

- [77] CLARKE, R.H., A Statistical Theory of Mobile radio Reception, *Bell Systems Technical Journal*, vol. 47, pp. 957–1000, 1968.
- [78] SEXTON, D., MAHONY, M., LAPINSKI, M., WERB, J., Radio Channel Quality in Industrial Wireless Sensor Networks, *Sensors for Industry Conference*, pp. 88–94, Feb. 2005.
- [79] SORRENTINO, A., FERRARA, G., MIGLIACCIO, M., Characterization of NLOS wireless propagation channels with a proper coherence time value in a continuous mode stirred Reverberating Chamber, *Wireless Technology Conference, EuWIT 2009*, pp. 168–171, Sept. 2009.
- [80] YUNBO, W., VURAN, M.C. ,GODDARD, S., Stochastic Analysis of Energy Consumption in Wireless Sensor Networks, *Sensor Mesh and Ad Hoc Communications and Networks (SECON), 2010 7th Annual IEEE Communications Society Conference*, pp.1–9, 21–25 June 2010.
- [81] ASLAM, S., FAROOQ , F., SARWAR, S. Power consumption in wireless sensor networks, In *Proceedings of the 6th International Conference on Frontiers of Information Technology*, Abbottabad, Pakistan, December 2009.
- [82] KEISER W. J., POTTIE, G. J., Wireless Integrated Network Sensors. *CACM*, vol. 43(5), pp. 51—58, 2000.
- [83] ALIPPI, C., ANASTASI, G., DI FRANCESCO, M., ROVERI, M., Energy management in wireless sensor networks with energy-hungry sensors, *Instrumentation & Measurement Magazine, IEEE* , vol. 12, no. 2, pp. 16–23, April 2009.
- [84] BENINI, L., CASTELLI, G., MACII, A., MACII, E. A Discrete-Time Battery Model for High Level Power Estimation. *DATE*. 35–39, 2000
- [85] AKKAYA, K., YOUNIS, M., A Survey on Routing Protocols for Wireless Sensor Network. *Elsevier Ad-hoc Networks*, vol. 3(3), pp. 325–349, 2003.
- [86] MADANI, S., MAHLKNECHT, S., GLASER, J., A Step towards Standardization of Wireless Sensor Networks: A Layered Protocol Architecture Perspective. *Sensor Technologies and Applications, 2007. International Conference on In Sensor Technologies and Applications, SensorComm 2007.*, pp. 82–87, 2007.
- [87] Cricket Embedded Processor: Technical Reference Manual, SOC Robotics, Inc. 2008, URL: <[http://www.soc-machines.com/pdfs/Cricket Technical Reference Manual.pdf](http://www.soc-machines.com/pdfs/Cricket%20Technical%20Reference%20Manual.pdf)>

- [88] Federal communication commission. Understanding the FCC regulations for low-power, non-licensed transmitters, Feb. 1996.
- [89] PRIYANTHA, N. B., CHAKRABORTY, A., BALAKRISHNAN, H., The Cricket location-support system. In *MobiCom Proceedings of the 6th annual international conference on Mobile computing and networking*, pp. 32–43, New York, NY, USA, 2000.
- [90] MORROW, R., *Wireless Network Coexistence*, New York:McGraw-Hill NETWORKING, 2004.
- [91] SIMEK, M., *Reference Nodes Selection for Anchor-Free Localization in Wireless Sensor Networks*, Doctoral thesis. Brno: Brno University of Technology, Faculty of Electrical Engineering and Communication, Department of Telecommunications, 2010. 105 p. Supervised by doc. Ing. Dan Komosny, Ph.D.
- [92] NOVACEK, N. A., *Simulator for wireless sensor networks positioning*, MS in Telecommunications, Supervised by Simek. M., BUT, Faculty of Electronic and Communication Technologies, Purkynova 118, Brno, 2010.
- [93] IEEE, IEEE std. 802.15.4 – 2006: Wireless Medium Access Control (MAC) and Physical Layer (PHY) specifications for Low Rate Wireless Personal Area Networks (LR-WPANs).
- [94] WHITEHOUSE, K., KARLOF, CH., CULLER, D. E., A practical evaluation of radio signal strength for ranging-based localization. *Mobile Computing and Communications Review* 11(1), pp. 41–52, 2007.
- [95] TEXAS INSTRUMENT, INA210-214EVM User’s Guide, 2008.
- [96] ATMEL, Atmel ATmega1281 datasheet, Available from URL: <[http://www.atmel.com/dyn/resources/prod\\_documents/doc2549.pdf](http://www.atmel.com/dyn/resources/prod_documents/doc2549.pdf)>.
- [97] BASU, P. REDI, J., Effect of Overhearing Transmissions on Energy Efficiency in Dense Sensor Networks, In *IPSN '04 Proceedings of the 3rd international symposium on Information processing in sensor networks*, New York, NY, USA: ACM, pp. 196—204, 2004.
- [98] WIESELTHIER, J. E. , NGUYEN, G. D. , EPHREMIDES, A., On the Construction of Energy-Efficient Broadcast and Multicast Trees in Wireless Networks, In *INFOCOM 2000. Nineteenth Annual Joint Conference of the IEEE Computer and Communications Societies. Proceedings*, IEEE, vol. 2, pp.585—594, 2000.

- [99] DIGI, Datasheet XBee RF module, Available from URL: <http://www.sparkfun.com/datasheets/Wireless/Zigbee/XBee-Datasheet.pdf>
- [100] CHEN, Y., TERZIS, A., On the Mechanisms and Effects of Calibrating RSSI Measurements for 802.15.4 Radios. In *EWSN'10: Proceedings of the 7th European Conference on Wireless Sensor Networks*, pp. 256–271, 2010.

### Author's publications

- [101] MORAVEK, P., KOMOSNY, D., JELINEK, M., SIMEK, M., Visualization of a Hierarchical Aggregation in the IPTV Network Environment, *International Journal of Computer Science and Network Security*. 8(11), pp. 210–216, 2008, ISSN 1738–7906.
- [102] MULLER, J., KOMOSNY, D., BURGET, R., MORAVEK, P., Advantage of Hierarchical Aggregation. *International Journal of Computer Science and Network Security*, 2008(8), pp. 1–7, ISSN 1738–7906.
- [103] SIMEK, M., KOMOSNY, D., BURGET, R., MORAVEK, P., SA SILVA, J., SILVA, R. Data Gathering Model for Wireless Sensor Networks Based on the Hierarchical Aggregation Algorithms for IP Networks, *International Journal of Computer Science and Network Security*, 8(11), pp. 200–208, 2008, ISSN 1738-7906.
- [104] SIMEK, M., KOMOSNY, D., MORAVEK, P., Establishment of Reference Localization System Based on Boundary Recognition of Wireless Sensor Network, *The International Conference Wireless Communication and Signal Processing*, pp. 115–120, 2010, ISBN978-1-4244-7556-8.
- [105] SIMEK, M., BOCEK, J., MORAVEK, P., Optimization of Boundary Recognition Algorithms for Wireless Sensor Network Applications, In *Proceeding of Proceeding of International Conference on Telecommunication and Signal Processing*, pp. 216–221, 2011, ISBN978-1-4577-1409-2.
- [106] SIMEK, M., KOMOSNY, D., BURGET, R., MORAVEK, P., SILVA, R., Centralized Boundary Discovery Algorithms for Anchor-Free Localization in Wireless Sensor Networks, In *Proceeding of ICUMT 2009*, St. Petersburg. 2009. pp. 220–226. ISBN978-1-4244-3941-6.
- [107] MORAVEK, P., KOMOSNY, D., SIMEK, M., Flip Ambiguity and Multilateration in Ad-hoc Networks, In *Proceeding of International Conference on*

- Research in Telecommunication Technologies*, 2011, pp. 158–162, ISBN978-80-214-4283-2.
- [108] MORAVEK, P., KOMOSNY, D., SIMEK, M., Multilateration and Flip Ambiguity Mitigation in Ad-hoc Networks, *Przeglad Electrotechniczny*, vol. 05b, pp. 91–98, 2012, ISSN 0033-2097.
  - [109] MORAVEK, P., KOMOSNY, D., SIMEK, M., SVÉDA, J., HANDL, T., Vivaldi and other localization methods, In *Proceeding of International Conference on Telecommunication and Signal Processing*, pp. 1–5, 2009, ISBN978-963-06-7716-5.
  - [110] MORAVEK, P., KOMOSNY, D., BURGET, R., HANDL, T., SVEDA, J., FOJTOVA, L., Lokalizacni metody v IP sitich – Vivaldiho algoritmu s vyskou, *Elektrorevue – Internet journal* (<http://www.elektrorevue.cz>), 2010, 2010(4), pp. 1–15, ISSN 1213–1539.
  - [111] MORAVEK, P., KOMOSNY, D., BURGET, R., HANDL, T., SVÉDA, J., FOJTOVA, L., Study and Performance of Localization Methods in IP Based Networks: Vivaldi Algorithm, *Journal of network and computer applications*, 2010, 34(1), pp. 1–17, ISSN 1084-8045.
  - [112] MORAVEK, P., KOMOSNY, D., VAJSAR, P., Synthetic Coordinate System in Wireless Sensor Networks, In *Knowledge in Telecommunication Technologies and Optics 2010*, 2010, pp. 1–6, ISBN978-80-248-2330-0.
  - [113] MORAVEK, P., KOMOSNY, D., VAJSAR, P., SVÉDA, J., HANDL, T., Study of Vivaldi Algorithm in Energy Constraint Networks, *Advances in Electrical and Electronic Engineering*, 2011, 9(4), pp. 35-42, ISSN 1336-1376.
  - [114] MORAVEK, P., Measurement of Signal Power for the Purposes of Localization, In *Student EEICT 2010*, 2010, pp. 27–31, ISBN978-80-214-4079-1.
  - [115] MORAVEK, P., GALERA, J., Investigation of Localization Based on Received Signal Strength in the 2.4 GHz ISM band, In *Proceeding of Poster 2010*, 2010, pp. 1–5, ISBN978-80-01-04544-2.
  - [116] MORAVEK, P., KOMOSNY, D., SIMEK, M., JELINEK, M., GIRBAU, D., LAZARO, A., Signal Propagation and Distance Estimation in Wireless Sensor Networks, In *The 33rd International Conference on Telecommunication and Signal Processing*, 2010, pp. 35–40, ISBN978-963-88981-0-4.



- [117] SIMEK, M., NOVACEK, A., KOMOSNY, D., MORAVEK, P., Impact of Different Distance Estimation Methods on Anchor-Free Localization Accuracy, In *The 33rd International Conference on Telecommunication and Signal Processing*, 2010, pp. 57–62.
- [118] MORAVEK, P., KOMOSNY, D., SIMEK, M., GIRBAU, D., Accuracy of Ultrasound Based Ranging Method with Cricket System, In *Proceeding of International Conference on Teleinformatics*, 2011, pp. 26–29, ISBN978-80-214-4231-3.
- [119] MORAVEK, P., KOMOSNY, D., SIMEK, M., GIRBAU, D., Measurement with the Cricket localization system, *Elektrorevue – online journal* (<http://www.elektrorevue.cz>), 2011, 9(2), pp. 13–18, ISSN 1213-1539.
- [120] MORAVEK, P., KOMOSNY, D., SIMEK, M., JELINEK, M., GIRBAU, D., LAZARO, A., Investigation of radio channel uncertainty in distance estimation in wireless sensor networks, *Telecommunication systems*, 2011, 2011(47), pp.1–10, ISSN 1018-4864.
- [121] MORAVEK, P., KOMOSNY, D., GIRBAU, D., LAZARO, A., Received Signal Strength Uncertainty in Energy-Aware Localization in Wireless Sensor Networks, In *9th International Conference on Environment and Electrical Engineering 2010*, 2010, pp. 538–541, ISBN978-1-4244-5371-9.
- [122] SIMEK, M., FUCHS, M., MRAZ, L., MORAVEK, P., BOTTA, M., Measurement of lowPAN Network Coexistence with Home Microwave Appliances in Laboratory and Home Environments, In *Proceeding of BWCCA 2011*, 2011, pp.211–219.
- [123] LAZARO, A., GIRBAU, D., MORAVEK, P., VILLARINO, R., Localization in Wireless Sensor Networks using diversity for multipath effects mitigation, In *Proceedings of the RFID SYSTECH 2010 - European Workshop on Smart Objects: Systems, Technologies and Applications*, 2010, pp. 1–6, ISBN978-3-8007-3282-1.
- [124] LAZARO, A., GIRBAU, D., MORAVEK, P., VILLARINO, R., A Study on Localization in Wireless Sensor Networks using Frequency Diversity for Mitigating Multipath Effects. *Electronic and Electrical Engineering*, ISSN 1392-1215 – to be published (No. 3(129), March of 2013).
- [125] MORAVEK, P., KOMOSNY, D., SIMEK, M., MRAZ, L., Energy demands of 802.15.4/ZigBee communication with IRIS sensor motes, In *Proceeding of 34th International Conference on Telecommunications and Signal Processing*, 2011, pp. 69–73, ISBN978-1-4577-1409-2.

- [126] SIMEK, M., MORAVEK, P., Positioning Simulator Using Global Energy Ratio Metric in Wireless Sensor Networks. *Elektrorevue - Internet journal* (<http://www.elektrorevue.cz>), 2010(104), pp. 1–8, ISSN 1213-1539.
- [127] SIMEK, M., MORAVEK, P., Analytical Simulation of Wireless Sensor Network Lifetime, In *Proceeding of International Conference on Research in Telecommunication Technologies* 2011, pp. 54–59, ISBN978-80-248-2261-7.
- [128] SIMEK, M., MORAVEK, P., Modeling of Energy Consumption of Zigbee Devices in Matlab Tool, *Elektrorevue - Internet journal* (<http://www.elektrorevue.cz>), 2011, vol. 2(3), pp. 41–46, ISSN 1213-1539.
- [129] MORAVEK, P., KOMOSNY, D., SIMEK, M., GIRBAU, D., LÁZARO, A., Energy Analysis of Received Signal Strength Localization in Wireless Sensor Networks, *Radioengineering*, 2011, vol. 10(4), pp. 937–945, ISSN 1210-2512.
- [130] MORAVEK, P.; KOMOSNY, D., Asymetrická kryptografie v bezdrátových senzorových sítích, *Access Server*, 2009, vol. 7(55), pp.1–9, ISSN 1214-9675.
- [131] MORAVEK, P., KOMOSNY, D., NS2 Simulator Capabilities in Nodes Localization in Wireless Networks, In *Student EEICT 2009*, 2009, pp. 269–273, ISBN978-80-214-3870-5.
- [132] MORAVEK, P., KOMOSNY, D., SIMEK, M., FATEMA, K., Simulations in Wireless Sensor Networks, In *Proceedings of International Conference on Teleinformatics*, 2011, pp.1–5, ISBN978-80-214-4231-3.
- [133] MORAVEK, P., KOMOSNY, D., SIMEK, M., Specifics of WSN Simulations, *Elektrorevue - Internet journal* (<http://electrorevue.cz>), 2011, 9(3), pp.19–25, ISSN 1213-1539.
- [134] SIMEK, M., MORAVEK, P., SA SILVA, J., Wireless Sensor Networking in Matlab: Step-by-Step, In *proceedings of International Conference on Teleinformatics*, 2011, pp.185–190, ISBN978-80-214-4231-3.

# LIST OF SYMBOLS, PHYSICAL CONSTANTS AND ABBREVIATIONS

WSN Wireless Sensor Network

MEMS Micro Electrical and Mechanical Systems

CRB Cramér-Rao Bound

UHF Ultra High Frequency

SHF Super High Frequency

MAE Mean Absolute Error

rMAE relative Mean Absolute Error

RF Radio Frequency

COTS Commercial Out-of-The-Shelf

RSS Received Signal Strength

ISM Industrial, Science and Medical

ITU International Telecommunication Union

SRAM Short random Access Memory

EEPROM Electrically Erasable Programmable Read-Only Memory

STD Standard Deviation

MSE Mean Square Error

DECT Digital Enhanced Cordless Telecommunications

WiFi synonym to WLAN

WLAN Wireless Local Area Network

RFID Radio-Frequency IDentification

PDR Packet Data Ratio

lowPAN low energy Personal Area Network

RISC Reduced Instruction Set Computing

AFL Anchor-Free Localization  
M-AFL Anchor-Free Localization implemented in Matlab  
M-AFL-HC M-AFL based on hop count  
M-AFL-SS M-AFL based on Signal Strength  
M-AFL-WSS M-AFL based on Weighted Signal Strength  
LS Least Square algorithm  
TTL Transistor-Transistor Logic  
EM ElectroMagnetic  
RSSI Receive Signal Strength Indication  
HC Hop Count  
GER Global Error Ratio  
SS Signal Strength  
WSS Weighted Signal Strength  
GPS Global Positioning System  
MAC Medium Access Control  
ACK Acknowledgment  
WMA Wireless Multicast Advantage  
AEDE Adaptable Energy-aware Distance Estimation  
RIS RSS Interleaving Space  
IFS InterFrame Spacing  
SIFS Short InterFrame Spacing  
LIFS Long InterFrame Spacing  
MPDU MAC Frame  
MAC Medium Access Control  
GTS Guaranteed Time Slot

LED Light-Emitting Diode

SPI Serial Peripheral Interface Bus

I2C Inter-Integrated Circuit

AD Analog Digital

WMA Wireless Multicast Advantage

CSMA-CA Carrier Sense Multiple Access-Collision Avoidance

SCC Simple Cross-Correlation

GCC Generalized Cross-Correlation

ToA Time of Arrival

AoA Angle of Arrival

TDoA Time Difference of Arrival

RTT Round-Trip Delay

SCC Simple Cross-Correlation

GCC Generalized Cross-Correlation

LOS Light of Sight

# LIST OF APPENDICES

<b>A</b>	<b>Appendix 1</b>	<b>118</b>
A.1	RSS lookup table . . . . .	118
<b>B</b>	<b>Appendix 2</b>	<b>120</b>
B.1	AEDE evaluation under real conditions – additional measurements .	120

# A APPENDIX 1

## A.1 RSS lookup table

Tab. A.1a: RSS lookup table.

		Number of samples							
Uncertainty(dB)		10	15	20	25	30	35	40	50
1		0,2532	0,2062	0,1792	0,1591	0,1478	0,1336	0,1263	0,1199
2		0,5020	0,4074	0,3554	0,3185	0,2911	0,2716	0,2514	0,2382
3		0,7500	0,6243	0,5359	0,4729	0,4358	0,4056	0,3762	0,3576
4		1,0114	0,8328	0,7138	0,6375	0,5828	0,5396	0,5062	0,4814
5		1,2736	1,0325	0,9096	0,8014	0,7316	0,6751	0,6316	0,5915
6		1,5040	1,2262	1,0728	0,9528	0,8733	0,8159	0,7611	0,7063
7		1,7886	1,4636	1,2485	1,1140	1,0222	0,9448	0,8755	0,8337
8		1,9997	1,6663	1,4233	1,2553	1,1628	1,0868	1,0023	0,9543
9		2,2724	1,8203	1,5984	1,4137	1,3061	1,2066	1,1312	1,0697
10		2,5293	2,0756	1,7848	1,6215	1,4552	1,3589	1,2824	1,1886
11		2,7862	2,2532	1,9660	1,7285	1,5957	1,4762	1,3951	1,3161
12		3,0463	2,4843	2,1621	1,9186	1,7598	1,6173	1,5069	1,4224
13		3,3216	2,6624	2,3251	2,0750	1,8968	1,7565	1,6302	1,5484
14		3,5399	2,8747	2,4877	2,2303	2,0588	1,8716	1,7515	1,6452
15		3,7608	3,1211	2,6815	2,3839	2,1638	2,0336	1,8796	1,7823
16		4,0823	3,2783	2,8904	2,5936	2,3229	2,1697	2,0117	1,9206
17		4,3441	3,5568	3,0205	2,7098	2,4549	2,2725	2,1408	2,0240
18		4,5833	3,7325	3,2002	2,8963	2,6062	2,4553	2,2674	2,1306
19		4,7742	3,8958	3,3338	3,0527	2,7181	2,5509	2,3913	2,2732
20		5,0451	4,0796	3,5637	3,2182	2,9389	2,6892	2,5346	2,3761

Tab. A.2a: RSS lookup table (continuing).

Uncertainty(dB)	Number of samples									
	55	60	65	70	75	80	85	90	95	100
1	0,1139	0,1069	0,1040	0,0997	0,0954	0,0911	0,0894	0,0868	0,0830	0,0828
2	0,2242	0,2172	0,2061	0,1990	0,1905	0,1856	0,1789	0,1733	0,1662	0,1624
3	0,3366	0,3198	0,3079	0,2958	0,2878	0,2783	0,2671	0,2602	0,2521	0,2411
4	0,4529	0,4283	0,4118	0,3953	0,3816	0,3683	0,3578	0,3451	0,3348	0,3285
5	0,5638	0,5362	0,5116	0,4953	0,4762	0,4674	0,4470	0,4334	0,4205	0,4048
6	0,6738	0,6506	0,6158	0,5940	0,5745	0,5558	0,5458	0,5165	0,5127	0,4913
7	0,7895	0,7563	0,7221	0,6953	0,6668	0,6536	0,6268	0,6113	0,5885	0,5714
8	0,9129	0,8590	0,8265	0,7956	0,7569	0,7372	0,7119	0,7012	0,6739	0,6536
9	1,0059	0,9696	0,9209	0,8798	0,8603	0,8357	0,7990	0,7727	0,7577	0,7445
10	1,1263	1,0755	1,0050	0,9892	0,9626	0,8998	0,8920	0,8614	0,8396	0,8166
11	1,2425	1,1932	1,1271	1,0915	1,0380	1,0220	0,9915	0,9497	0,9292	0,8938
12	1,3400	1,3036	1,2166	1,1857	1,1430	1,1070	1,0680	1,0472	1,0119	0,9907
13	1,4659	1,3857	1,3249	1,2906	1,2366	1,1976	1,1620	1,1381	1,0904	1,0552
14	1,5650	1,5074	1,4377	1,3907	1,3523	1,2946	1,2582	1,2064	1,1693	1,1548
15	1,6828	1,6283	1,5562	1,4728	1,4211	1,3939	1,3353	1,2994	1,2765	1,2300
16	1,7914	1,7233	1,6473	1,6128	1,5413	1,4642	1,4317	1,3840	1,3498	1,3159
17	1,9215	1,8017	1,7396	1,6798	1,6270	1,5612	1,5171	1,4708	1,4405	1,3942
18	2,0421	1,9386	1,8401	1,7703	1,7206	1,6530	1,5984	1,5532	1,5107	1,4706
19	2,1668	2,0310	1,9418	1,8618	1,8174	1,7413	1,6966	1,6384	1,5861	1,5596
20	2,2611	2,1683	2,0930	1,9773	1,8986	1,8370	1,7911	1,7242	1,6582	1,6311



## B APPENDIX 2

### B.1 AEDE evaluation under real conditions – additional measurements

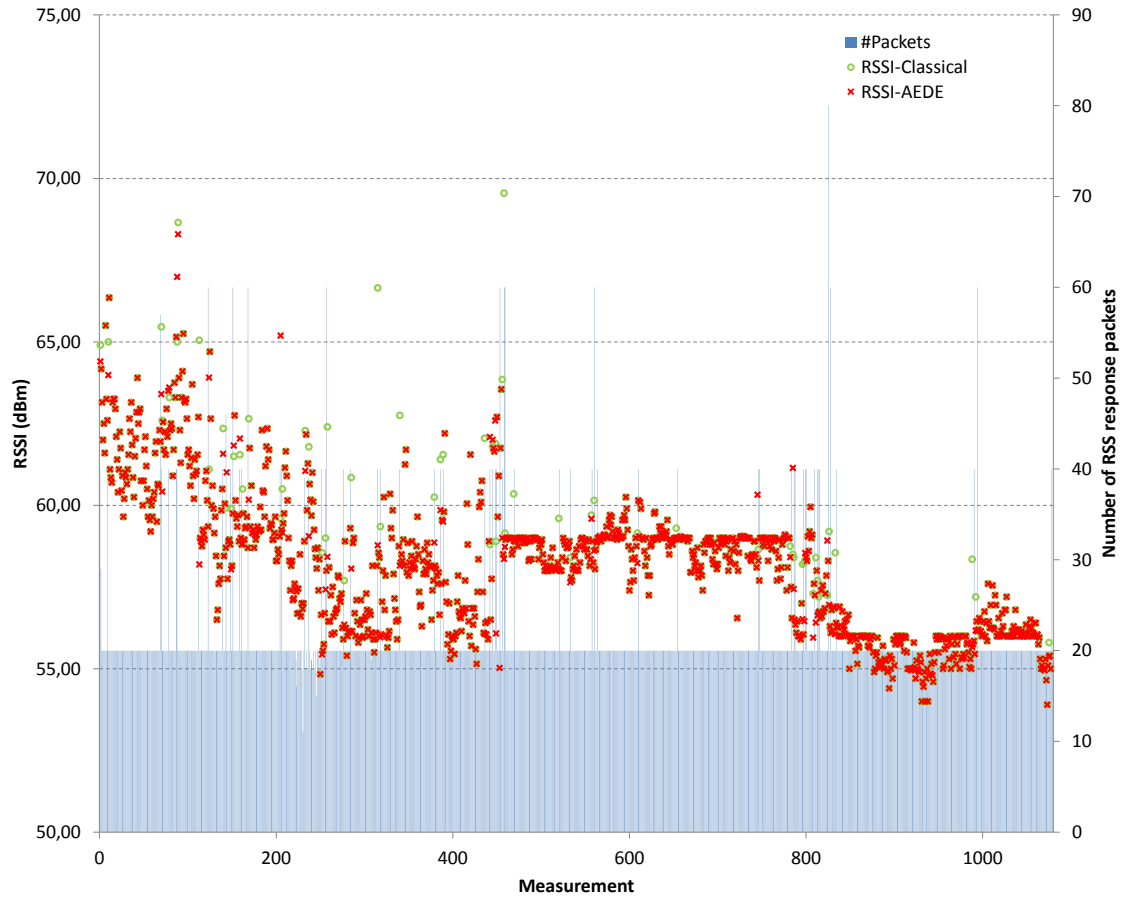


Fig. B.1: AEDE evaluation in series of RSSI measurements.

*Curriculum Vitae*

# Patrik Morávek

---

Affiliation      Brno University of Technology, Brno, Czech Republic

Contact      Zdislav 37, 53854 Luže  
moravek@phd.feec.vutbr.cz  
+420776029231

## EDUCATION

2008–2012	Department of Telecommunications Brno University of Technology, Czech Republic Doctoral program, Research on localization in wireless networks
10/2011–5/2012	Institute of Computer Engineering University of Lübeck, Germany Research on localization of moving objects
05–06/2011	Institute for Technical Informatics Graz University of Technology, Austria Research on localization algorithms simulations
2009–2010	Dep. of Electronics, Electrical, and Automatics Engineering Rovira i Virgili University, Spain Research on signal propagation for distance estimation
2006–2008	Brno University of Technology, Czech Republic Faculty of Electrical Engineering and Communication Master's program, Graduated with honors
2003–2006	Brno University of Technology, Czech Republic Faculty of Electrical Engineering and Communication Bachelor's program, Graduated with honors

## PARTICIPATION IN PROJECTS

active	FR-TI2/571: Adaptive Wireless Sensor Networks with Data Visualization for Crisis Management. Holder: prof. Vrba
active	1780/2012/F1: Implementation of security topic into a Network operation systems subject. Holder: Assoc. prof. Komosný
active	FEKT-S-11-15: Research on electronic communication systems.

	Holder: prof. Vrba
active	2056/2012/G1: Innovation of laboratory assignments addressing wireless sensor networks. Holder: Ing. Vajsar
2009–2012	CZ.1.07/2.3.00/09.0222: Educational Center for Increasing the Interest of Young People in Research into Information and Communication Technologies. Holder: Ing. Kubánek
2011	467/2011/G1: Including the topic of modern network services into a Network operation system subject. Holder: Ing. Morávek
2008–2011	MSM21630513: Electronic communication systems and technologies of novel generations (ELKOM). Holders: Prof. Z. Raida, Prof. K. Vrba, Prof. J. Jan
2010	1773/2010/F1: Extension of Cisco lab assignments. Holder: Ass. prof. Komosný

#### INVITED REVIEWS

Journal of Electromagnetic Waves and Applications  
Radioengineering journal  
Elektrorevue – internet journal  
19th European Signal Processing Conference 2011  
33–35th Int. Conf. on Telecommunications and Signal Processing  
14th Int. Conf. on Research in Telecommunication Technologies  
7th International Conference on Teleinformatics

#### RESULTS IN TOTAL

Paper reviews: **14**  
h-index according to Web of Science: **2**  
Publications: **43**  
In international journals with Impact Factor: **6**  
In proceedings of international conferences: **24**  
In other journals: **13**

#### AWARDS

2010	The best paper award at Int. Conf. on Telecommunication and Signal processing
2010	EEICT 2010 student conference and competition – 3rd prize
2009	EEICT 2009 student conference and competition – 2nd prize